UNIVERSITÀ DEGLI STUDI DI NAPOLI "FEDERICO II"

FACOLTÀ DI FARMACIA

DOTTORATO DI RICERCA IN SCIENZA DEL FARMACO
XXIV CICLO (2008-2011)

PATHOPHYSIOLOGICAL MECHANISMS AND POSSIBLE THERAPEUTIC TARGETS OF VASCULAR INJURY

Relatore
Ch.mo Prof.
ARMANDO IALENTI

Coordinatore
Ch.ma Prof.ssa
MARIA VALERIA D'AURIA

Candidato
DR. MARCELLA MADDALUNO

CONTENTS

ACKNOWLEDGEMENT

I wish to thank firstly my tutor Prof. Armando Ialenti, master and guide for my work and my person. He has always gave me precious suggestions and emotional support, since I was an undergraduate student.

My deepest gratitude to Dr. Pasquale Maffia, for his contribution to my professional growth, and to Prof. Paul Garside. They gave me the great chance to work at the Institute of Infection, Immunity and Inflammation (University of Glasgow), where I learned a lot about science and life.

Thanks also to Dr. Gianluca Grassia, my friend and co-worker. He has stirred up in me the passion for pharmacology, encouraging and supporting me in every fields.

A big thank to Dr. Maria Vittoria Di Lauro, for her friendship and help, as well as for useful discussions and criticisms.

I want to express my gratitude to all lab-mates, colleagues and friends of the Department of Experimental Pharmacology who made my lab-life happy.

I'm thankful for Dr. Astrid Parenti and her research group. They gave me the opportunity to work with them at the University of Florence and preciously collaborated to part of this thesis.

Finally I am grateful to Prof. Maria Valeria D'Auria, organizer of this PhD, for her helpful advices.

I dedicate this work to my family and my loved ones. They have sustained me in everything I have done and I have not, during my entire life. I thank them with all my heart!

SUMMARY

Percutaneous coronary intervention (PCI) is the current procedure that allows the endovascular treatment of occlusive artery disease, without the need of bypass surgery. The most problematic complication of PCI, with or without stent implantation, is the restenosis defined as the re-narrowing of the enlarged artery and characterized by an immune/inflammatory response going with a hyperplastic reaction, involving smooth muscle cell (SMC) migration/proliferation, and remodelling of the arterial wall. In an effort to improve on current therapy for restenosis we are prompted to consider new strategies for prevention and treatment, focusing on understanding of molecular mechanisms and identifying possible therapeutic targets. This thesis aims at four issues described as follows:

1. Effect of NBD peptide on injury-induced neointimal formation

The activation of nuclear factor-κB (NF-κB) is a crucial step in the arterial wall's response to injury. NF-κB essential modulator-binding domain (NBD) peptide blocks the activation of the IκB kinase complex, selectively abrogating the inflammation-induced activation of NF-κB. In this study, we investigated the effect of NBD peptide on neointimal formation using two animal models of arterial injury: rat carotid artery balloon angioplasty and wire-induced carotid injury in apolipoproteinE-deficient ($apoE^{-/-}$) mice.

Local treatment with the NBD peptide (300 μg/site) significantly reduced the number of proliferating cells in rat carotid arteries 7 days after angioplasty (by 40%; $P<0.01$) and reduced injury-induced neointimal formation (by 50%; $P<0.01$) at day 14. These effects were associated with a significant reduction of NF-κB activation and monocyte chemotactic protein-1 (MCP-1) expression in the carotid arteries of rats treated with the peptide. In addition, the NBD peptide (0.01 to 1 μM) reduced rat SMC proliferation, migration, and invasion *in vitro*, processes contributing to the injury-induced neointimal formation *in vivo*. Similar results were observed in $apoE^{-/-}$ mice in which the NBD peptide (150 μg/site) reduced wire-induced neointimal formation at day 28 (by 47%; $P<0.01$).

Our results demonstrate that the NBD peptide reduces neointimal formation and SMC proliferation/migration, both effects associated with the inhibition of NF-κB activation.

2. Use of the anti-inflammatory agent bindarit to control neointimal hyperplasia

Chemokines are a family of proteins that regulate the migration of circulating leukocytes to sites of arterial injury as well as the activation of SMCs. Many chemokine genes are under the control of NF-κB. Bindarit is an original compound with peculiar anti-inflammatory activity due to a selective inhibition of the chemokines MCP-1, MCP-3, and MCP-2. In the present study we evaluated the effect of bindarit on neointimal formation using both animal models described above.

Treatment of rats with bindarit (200 mg/kg/day) significantly reduced balloon injury-induced neointimal formation by 39% at day 14 without affecting re-endothelialisation and reduced the number of medial and neointimal proliferating cells at day 7 by 54% and 30%, respectively. These effects were associated with a significant reduction of MCP-1 levels both in sera and in injured carotid arteries of rats treated with bindarit. In addition, *in vitro* data showed that bindarit (10-300 μM) reduced rat SMC proliferation, migration, and invasion. Similar results were observed in apoE$^{-/-}$ mice in which bindarit administration resulted in a 42% reduction of the number of proliferating cells at day 7 after carotid injury and in a 47% inhibition of neointimal formation at day 28. Analysis of the cellular composition in neointimal lesions of apoE$^{-/-}$ mice treated with bindarit showed that the relative content of macrophages and the number of SMCs were reduced by 66% and 30%, respectively, compared with the control group.

This study demonstrates that bindarit is effective in reducing neointimal formation in both non-hyperlipidaemic and hyperlipidaemic animal models of vascular injury by a direct effect on SMC proliferation and migration and by reducing neointimal macrophage content. All of these data were associated with the inhibition of MCP-1 production.

3. Role of Monocyte Chemotactic Protein-3 in human coronary smooth muscle cell proliferation

Few studies have examined the role of MCP-3 in vascular pathologies such as atherosclerosis and restenosis in which SMC proliferation plays an important role. In this study, we investigated the effect of MCP-3 on human coronary artery SMC (CASMC) proliferation.

MCP-3 induced concentration-dependent CASMC proliferation with the maximum stimulatory effect at 0.3 ng/mL (about 50% vs unstimulated cells) assessed by bromodeoxyuridine (BrdU) uptake and direct cell counting. Anti-MCP-3 Ab (20 ng/mL) completely inhibited cell proliferation, demonstrating the specificity of the proliferative effect of MCP-3. Moreover, the MCP-3-induced CASMC proliferation was blocked by RS 102895 (0.06-6 μM), a specific antagonist of chemokine receptor 2 (CCR2). The mitogenic effect of MCP-3 appeared to be dependent on ERK1/2 MAPK and PI3K signalling pathway activation, as demonstrated by the reduction of MCP-3-induced CASMC proliferation observed after the treatment of cells with U0126 (1 μM) and LY-294002 (5μM), selective inhibitors of ERK 1/2 and PI3K activation, respectively. We found no relationship between MCP-3-induced CASMC proliferation and NF-κB activation. Moreover, we found that tumor necrosis factor-α (TNF-α, 30 ng/mL) and interleukin-1β (IL-1β, 1 ng/mL) both induced time-dependent increase of MCP-3 production by CASMCs, which was reduced by the anti-MCP-3 Ab (20 ng/mL), suggesting that the mitogenic effect of these stimuli is due, at least in part, to MCP-3.

Our results demonstrate that MCP-3 is produced by human CASMCs and directly induces CASMC proliferation *in vitro*, suggesting a potential role for this chemokine in vascular pathology.

4. Antigen presentation and costimulatory molecules expression by murine smooth muscle cells

The findings that SMCs express MHC II molecules during arterial response to injury suggested their active role in cellular immunity. Since it is not known if vascular SMCs can function as antigen presenting cells, in the present study we investigated the contribution of SMC in antigen presentation.

Firstly, we examined the MHC II and some costimulatory molecules expression in SMCs. The percentage of MHC II, CD54 (ICAM-1), CD44 and OX40L positive unstimulated SMCs was about 2%, 30%, 87% and 5%, respectively. The stimulation with IFN-γ (100 ng/mL)) significantly caused a 7 to 8 fold increase in the percentage of MHC II positive cells ($P<0.01$), a 2 fold increase in the percentage of ICAM-1 positive cells ($P<0.01$), while it did not affect the expression of CD44 and OX40L.

To assess the antigen presentation by SMCs we employed the Ealpha (Eα)-GFP/Y-Ae system that allows visualisation of antigen uptake, as the Eα is GFP labelled, and tracking of antigen presentation using the Y-Ae Ab to detects Eα when bound to MHC II. Treatment of SMCs with Eα for 24 h induced an increase in the percentage of GFP positive cells, both in presence or absence of IFN-γ-stimulation, without affecting the percentage of Y-Ae positive cells. Treatment with Eα of dendritic cells, used as positive control, significantly caused a 50 to 60 fold increase in the percentage of both GFP and Y-Ae positive cells. Our results show that cultured murine SMCs express MHC II molecules after stimulation with IFN-γ but are not able to present the antigen in the context of MHC II.

1. INTRODUCTION

Cardiovascular diseases (CVDs) are the leading causes of death and disability in the world, claiming 17.3 million lives a year. This fact forces us to consider new strategies for prediction, prevention, and treatment.

The prevalent type of CVDs in western societies is the coronary artery disease, in which an artery wall thickens because of the deposition of atherosclerotic plaque triggered by LDL accumulation within the artery wall. At the base of atherosclerosis there is an inflammatory process with an immune component depending on the interaction of multiple cellular populations of the peripheral blood, mainly monocytes and T lymphocytes, with cell components of the arterial wall, mostly endothelial and smooth muscle cells (SMCs), in response to multifactorial vascular injury (Hansson and Jonasson, 2009). This interaction results in the stenosis of the coronary vessels and may range from asymptomatic to angina, or to myocardial infarction.

The current procedure that allows the endovascular treatment of occlusive coronary artery disease, without the need of bypass surgery, is the percutaneous coronary intervention, commonly known as angioplasty. This procedure is executed by attaching a small balloon to a catheter. Once inflated on the stenosis, the balloon dilates the artery and improves blood flow (balloon angioplasty, Fig. 1.1).

The most problematic complication of percutaneous coronary intervention is a well known process called restenosis, defined as the re-narrowing of the artery after initial angioplastic treatment, identifiable by a lumen diameter diagnosis of <50% at follow-up (Fig 1.1).

1.1 Restenosis

The restenosis was proposed to be the arterial wall's healing response to mechanical injury consisting of platelet aggregation, inflammatory and immune cell infiltration, release of growth factors, SMC proliferation, collagen deposition and extracellular matrix (ECM) rearrangement. All these events contribute to the two major processes of restenosis following the angioplasty, intimal hyperplasia and vessel remodelling.

Between 1980s and 1990s coronary stenting strategies have been developed, in an effort to improve the outcome of angioplasty. They consist in metal mesh tubes, called stents, placed during percutaneous coronary intervention inside the artery to keep it open, thus preventing acute occlusion and restenosis (Fig. 1.1). Stents implantation initially appeared promising but after their introduction it became apparent that the late in-stent restenosis was one of the major drawbacks after successful revascularization, with restenosis rate ranging from 15% to 60% at six months depending on lesion morphology and other factors (Elezi et al., 1998) (Fig. 1.1).

The central pathogenetic events of in-stent restenosis are the recruitment of inflammatory cells to the site of injury and the migration of vascular SMCs from the tunica media through the disruption of endothelial barrier following the mechanical stretch. There, the SMCs proliferate actively giving rise to the neointima, which in turn obstructs the vessel (Costa and Simon, 2005).

In order to prevent the in-stent restenosis, recent technology has created the drug-eluting stents (DES): using a coronary stent for local delivery of drugs combines scaffolding with targeted drug action. Stents coated with any of several pharmacotherapeutic agents such as heparin, hirudin, GP IIb/IIIa inhibitors, sirolimus, and paclitaxel can be used (Whan at al., 2008). The first successful clinical trial in 2002 led to approval of the sirolimus-eluting stents. Sirolimus (rapamycin) is a macrolide antibiotic with immunosuppressive and anti-mitotic properties effective in reducing restenosis, by inhibiting the transition of cycling cells from G1 to S phase (Whan et al., 2008) and it is still now one of the most common drugs utilized in DES.

Although FDA approved the use of DES, there are reports of problems such as late stent malapposition and aneurysm formations due to the toxicity associated with this method of treatment and attributed to incomplete repair of the injured artery. Recent reports also suggest that DES may increase the risk of stent thrombosis relative to bare-metal stents (Yan et al., 2008) and, in addition, the long term effects of stents are still unknown. It is clear that the current strategies only allow us to buy time for individuals but it is too far to consider these the therapy to the restenosis. To work in this direction, the underlying molecular basis of restenosis are to be better clarified.

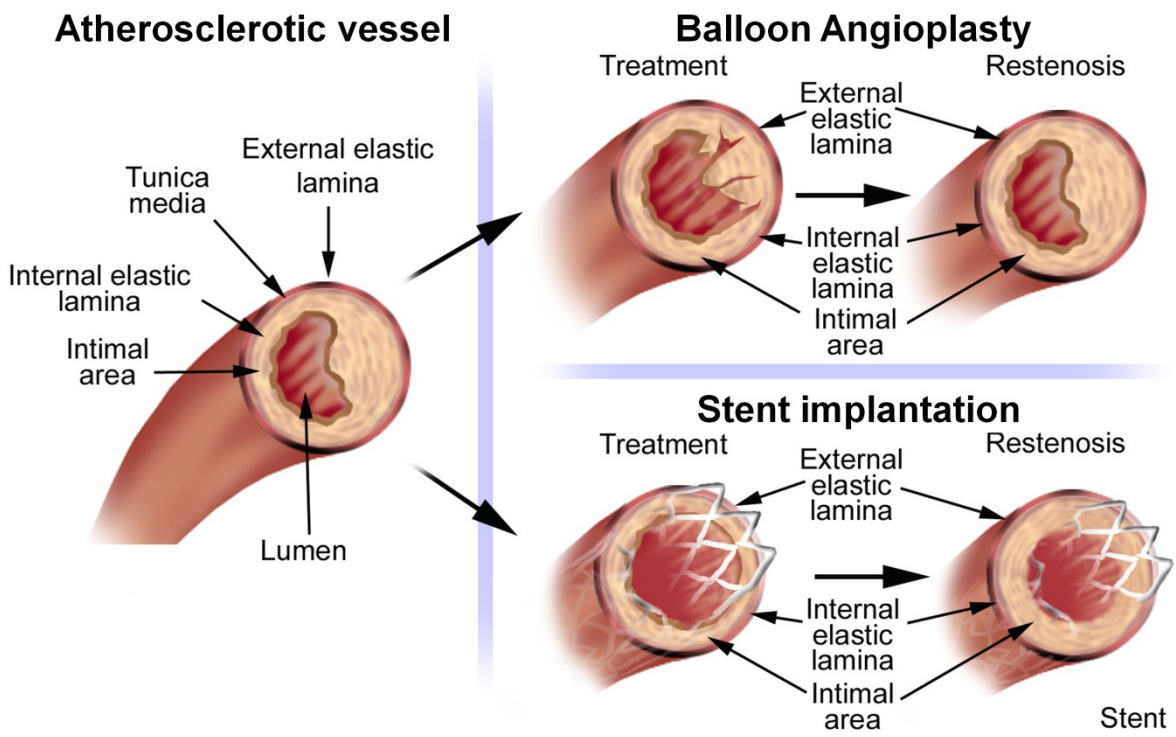

Figure 1.1

Mature atherosclerotic plaque before intervention (left). Restenosis after balloon angioplasty and stent implantation (right)

1.2 Mechanisms implicated in restenosis

The pathogenesis of restenosis is characterized by two major mechanisms: arterial remodelling and neointimal formation. Human and animal studies have shown that, in response to percutaneous coronary intervention, changes in the total arterial circumference occur (Post et al., 1997). It has been observed that the angioplasty procedure causes an actual constriction of the artery leading to the lumen-narrowing. On the other side, the endothelial denudation and the medial dissection, consequent to the intervention, induce a thrombotic response defined by platelet deposition and aggregation on the exposed sub-endothelial surface. Several growth and migratory-promoting factors, such as thrombin, platelet-derived growth factor (PDGF), interleukin (IL)-1, insulin-like growth factor-1 (IGF-1), fibroblast growth factor-2 (FGF-2), vascular endothelial cell growth factor (VEGF), and others are released from both injured vascular cells and platelets (Topol and Serruys, 1998; Lincoff et al., 1994).

The complex interactions of circulating factors and multiple vascular cell populations promote inflammatory cell infiltration and regulate SMC migration/proliferation. These processes, mediated by cell surface receptors, culminate in transcription of early response genes necessary for cells to leave their quiescent state and enter the cell cycle (Sherr and Roberts, 1999). In this context changes in matrix synthesis, such as degradation and organization, contribute to both vascular remodelling and SMC activation. Indeed, after injury caused from arterial intervention, the upregulation of matrix metalloproteinases leads to the degradation of the extracellular matrix and this allows SMCs to migrate to the intima (Galis and Khatri, 2002).

Restenosis after balloon angioplasty seems to be determined primarily by the direction and magnitude of vessel wall remodeling. In contrast, the major limitation of stent implantation is the initiation of neointimal tissue proliferation within and adjacent to the stent (Indolfi et al., 1999).

1.2.1 Vascular smooth muscle cell activation

Normally, SMCs residing in the media of the vessel are in a quiescent state, surrounded by a basement membrane and densely packed into an interstitial matrix. This differentiated condition is characterized by the expression of contractile proteins, that are useful to keep vascular tone by contraction or relaxation, and is referred to contractile phenotype. However, SMCs maintain considerable plasticity (Owens et al., 2004): during vascular injury or disease, multiple stimuli such as humoral or neuronal factors, mechanical forces or cell-cell interactions, contribute to the disruption of the normal steady state and allow to SMCs to undergo a phenotypic modulation/switching (Fig. 1.2). It is characterized by dramatic increases in the rates of proliferation, migration, and synthesis of ECM proteins, growth factors and inflammatory mediators, along with decreased expression of SMC-specific/-selective marker genes such as smooth muscle α-actin (α-SMA), smooth muscle-myosin heavy chain (SM-MHC), SM22α, h1-calponin, smoothelin, caldesmon, and telokin (Owens et al., 2004).

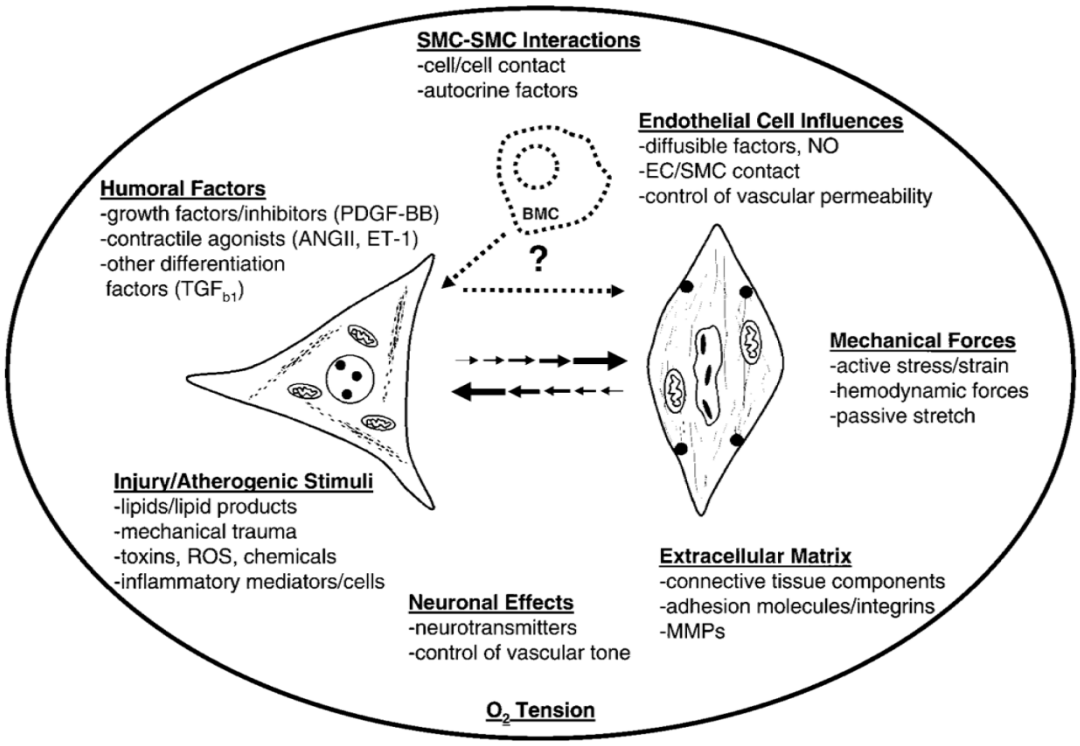

Figure 1.2

The differentiation state of SMCs is highly plastic and dependent on integration of multiple local environmental cues (Figure adapted from Owens et al., 2004).

The early markers of SMC activation, such as expression of nuclear oncogenes detectable immediately and/or several hours after angioplasty, is associated with the early G_1 events preceding DNA synthesis in SMCs.

Although the molecular mechanisms leading to SMC activation and phenotypic modulation are still unclear, injurious stimuli are known to alter the environment of the vascular wall by affecting endothelial function and inducing platelet adhesion and activation, migration of immune cells and changes in the ECM. These environmental changes subsequently induce the production of growth factors and cytokines by SMCs, which in turn activate autocrine/paracrine pathways leading to further phenotypic modulation. For example, in atherogenesis, PDGF produced by SMCs and other cell types, was shown to down regulate SMC differentiation markers such as α-SMA and SM-MHC (Owens et al., 2004); matrix degrading proteases produced by macrophages may contribute to the degradation of the basement membrane (Galis et al., 1994), and in restenosis, proteases may

also derive from the injured SMCs present in the lesion (Yoshida and Owens, 2005). This activation renders the SMCs responsive to chemoattractants and mitogens resulting in subsequent migration and proliferation, both processes contributing to neointimal hyperplasia.

1.2.2 Immune/Inflammatory response

Although SMC activation is a prominent mechanism of the intimal hyperplasia at the base of the restenosis, there is strong evidence that immune/inflammatory response plays a critical role, too. It is known that neointimal formation is increased in immune-deficient animals (Dimayuga et al., 2010) indicating a significant correlation between injury and the immune response to injury. For several decades immune modulation of neointimal formation after vascular injury has been investigated but the complexities involved continue to obscure a clear understanding of this process. However, both antigen-specific and nonspecific immune responses could occur during restenosis.

The major detrimental in innate immune responses associated to vascular injury is the macrophage infiltration. Deendothelialisation, provoked by balloon dilatation of the arterial wall, in fact, allows to a layer of platelets and fibrin to deposit at the injured site (Toutouzas et al., 2004). An interaction between platelets and leukocytes, that involves the platelet P-selectin and the β2 integrin molecule Mac-1 (CD11b/CD18), promotes a process of leukocyte recruitment and infiltration, which is critical to the inflammatory response (Welt and Rogers, 2002). Analysis of human arterial segments also suggests a critical role of inflammation during in-stent restenosis. In the initial phase, post-stent implantation, the mural thrombus formation is followed by activation and invasion of SMCs, T-lymphocytes and macrophages. After this early neointimal formation, extracellular matrix increases; growth factors, cytokines and chemokines are released from leukocytes, SMCs and endothelial cells, thus enhancing the migration of leukocytes across the platelet-fibrin layer into the tissue and inducing fibroblast proliferation and transformation to myofibroblasts (Toutouzas et al., 2004). Many chemokines such as interleukin (IL)-8, participate in the recruitment of monocytes, leukocytes and neutrophils to areas of vascular injury (Welt and Rogers, 2002). Others, like monocyte chemoattractant protein (MCP)-1, are involved in the recruitment of monocytes, basophils and T cells

(Welt and Rogers, 2002), as well as activation of SMCs (Charo and Taubman, 2004). Lately a key player in fundamental mechanisms, regulating the development of restenosis, as inflammation and proliferation, is the ubiquitin–proteasome system of intracellular protein degradation. Proteasome, in fact, is required for the activation of the transcription factor "*nuclear factor-κB*" (NF-κB) by degrading its inhibitory IκB protein. Once activated, NF-κB induces the transcription of a large number of genes codifying for cytokines and chemokines involved in inflammatory and immune responces (Hayden and Ghosh, 2008) as well as a variety of genes related to cell differentiation, apoptosis, and proliferation (Karin, 2006). Cell apoptosis or necrosis, occurring during injury, may trigger the release of intracellular material, including uric acid and heat-shock proteins that can further enhance the immune activation (Dimayuga et al., 2010).

All growth factors and proteases, described above, both contribute to neointimal formation and vessel remodeling after arterial injury (Fig. 1.3).

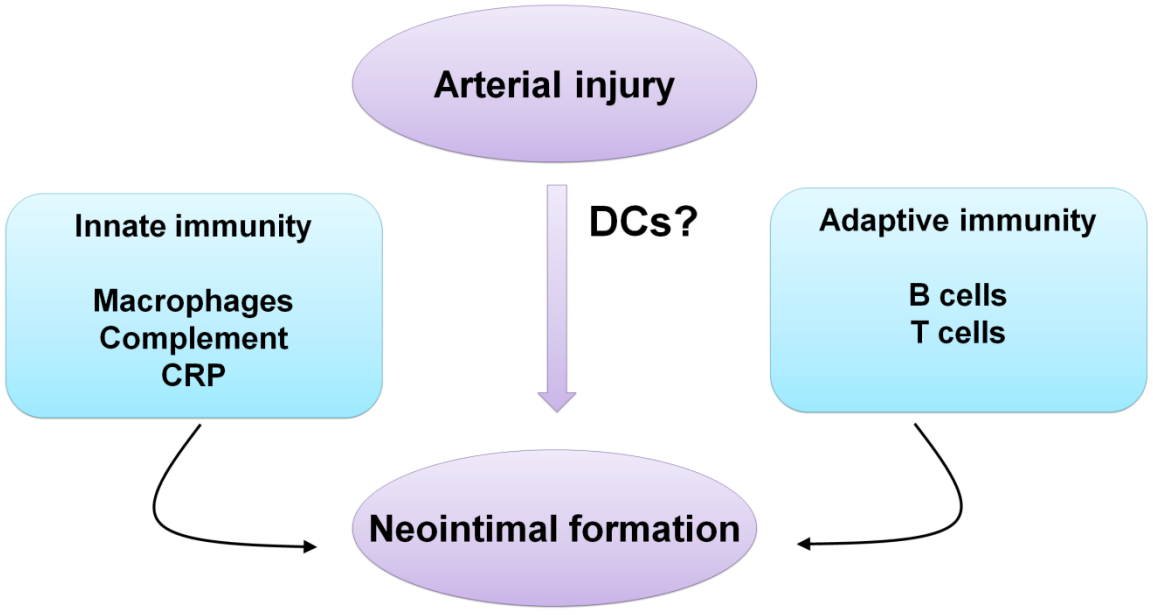

Figure 1.3

Immune response to arterial Injury

The adaptive immune response appears to be more complex. Prior studies suggest that B lymphocytes inhibit neointimal formation (Dimayuga et al., 2005),

likely through the production of immunoglobulin. Similarly, experiments based on using T-cell depletion, T-cell deficiency, or T-cell transfer indicate the inhibitory role of these cells in arterial injury (Hansson et al., 1991; Remskar et al., 2001; Dimayuga et al., 2005). It has been observed that T lymphocytes also regulate the repair processes of the vasculature to injury by inhibiting SMC proliferation (Hansson et al., 1991). Although these data suggest a protective role of immune cell activation in response to arterial injury, it has been proposed that dendritic cells, also present in neointimal lesions, may have the capacity to induce autoimmune responses in T cells (Han et al., 2008) exacerbating the inflammatory response after vascular injury (Fig. 1.3). Because the role of T lymphocyte is still unknown, few studies have been conducted to investigate the effect of drug eluting stent in spite of the use of antiproliferative/immunesuppressive drugs. One study showed a significant reduction in T lymphocyte infiltration 8 months after DES implantation; another study showed that sirolimus DES increased CD8+ central memory T cells (Dimayuga et al., 2010).

It stands to reason that the role of both innate and adaptive immunity in restenosis remains still unclear, thus further studies are needed to obtain a more comprehensive view of this growth regulatory network, also to investigate the benefit of current therapy, especially DES.

1.3 The transcription factor nuclear factor-κB

The inflammatory response at the base of restenosis involves several intracellular pathways. Among them the activation of the ubiquitous transcription factor NF-κB plays a critical role in the pathogenesis of the lesion. NF-κB is a family of transcription factors first described in 1986, now known to exist in virtually all cell types (Hayden and Ghosh, 2008) and organelles such as mitochondria (Cogswell et al., 2003). It regulates the transcription of a large number of genes involved in immune, inflammatory, and acute phase responses, as well as cell proliferation and apoptosis (Hayden and Ghosh, 2008). NF-κB family contains 5 members: p65 (RelA), c-Rel, RelB, NF-κB1 (p50 and its precursor p105), and NF-κB2 (p52 and its precursor p100), all of which have a structurally conserved N-terminal ‘rel homology’ domain responsible for dimerisation, nuclear translocation

and DNA binding, whereas only the first 3 contain a transactivation domain. The proteins can form either homodimers or heterodimers. The most widely expressed complex, often referred to as being “NF-κB”, is p65/p50 (Karin et al., 2004).

In most cells, NF-κB is sequestered in the cytoplasm and associated with members of the inhibitor of NF-κB (IκB) family, which consists of IκBα, IκBβ, IκBγ, IκBε and Bcl-3 with IκBα being the predominant. The NF-κB-IκBα interaction inhibits NF-κB-DNA binding and results in the NF-κB complex being primarily in the cytoplasm due to a stronger nuclear export signal in IκBα, compared to the import signalling on NF-κB. Thus, the complex is actually continuously shuttling between the nucleus and the cytoplasm. In contrast, the IκBβ interaction with the NF-κB complex does not undergo nucleo-cytoplasmic shuttling, keeping the complex is retained in the cytoplasm (D’Acquisto et al., 2002).

NF-κB could be activated via two pathways, a canonical pathway and an alternative pathway (Hayden and Ghosh, 2008) (Fig. 1.4). Activation of the canonical NF-κB pathway is initiated by a variety of extracellular stimuli, including cytokines such as TNF-α and IL-1β, viral products, bacterial components such as LPS, and yeast products signalling through different TLRs. These agents activate the cells through their receptors, leading to the activation of different signalling cascades, which will activate the IκB kinase (IKK) complex. This complex will phosphorylate IκB on its N-terminal serines, resulting in its ubiquitination, degradation by the 26S proteasome, and translocation of the NF-κB dimer to the nucleus, where it binds to the NF-κB consensus sequence, leading to the transcription of many genes such as cytokines, adhesion molecules and antiapoptotic genes. The phosphorylation of IκB by the IKK complex is a convergent point in the activation of this classical cascade. The IKK complex comprises several subunits, including two highly homologous catalytic kinases, IKKα and IKKβ, and an essential NF-κB modulator (NEMO; IKKγ) (D’Acquisto et al., 2002; Hayden and Ghosh, 2008; Cogswell et al., 2003; Karin et al., 2004). IKKβ is probably the most dominant kinase, whereas IKKα reveals partial redundancy for the activation of the classical NF-κB pathway (Li et al., 1999). NEMO is necessary for NF-κB activation despite lack of kinase activity (D’Acquisto et al., 2002). IKKα was shown to be responsible for an alternative NF-κB activation pathway via the processing of NF-κB2/p100 by activating lymphotoxin-β, B-cell-activating factor, CD40 ligand, and

LPS, some of which can induce the classical pathway (Strickland and Ghosh, 2006).

The relB-p52 dimers, not associated with IκB proteins, transfer to the nucleus, where they mediate transcription of genes involved in skin and skeletal development, as well as in B cell maturation (Strickland and Ghosh, 2006). IKKα knockout mice have many morphogenetic abnormalities, including shorter limbs and skull, a fused tail, and die perinatally. They exhibit a normal NF-κB activation after induction by IL-1β and TNF-α in embryonic fibroblasts. However, a recent study has revealed a new role for IKKα, which contributes to suppression of NF-κB activity and the resolution of inflammation in macrophages as a negative modulator. Inactivation of IKKα in mice enhances inflammation and bacterial clearance. Therefore, the two IKK catalytic subunits seem to have opposing but complimentary roles needed for controlling inflammation and innate immunity (Lawrence et al., 2005).

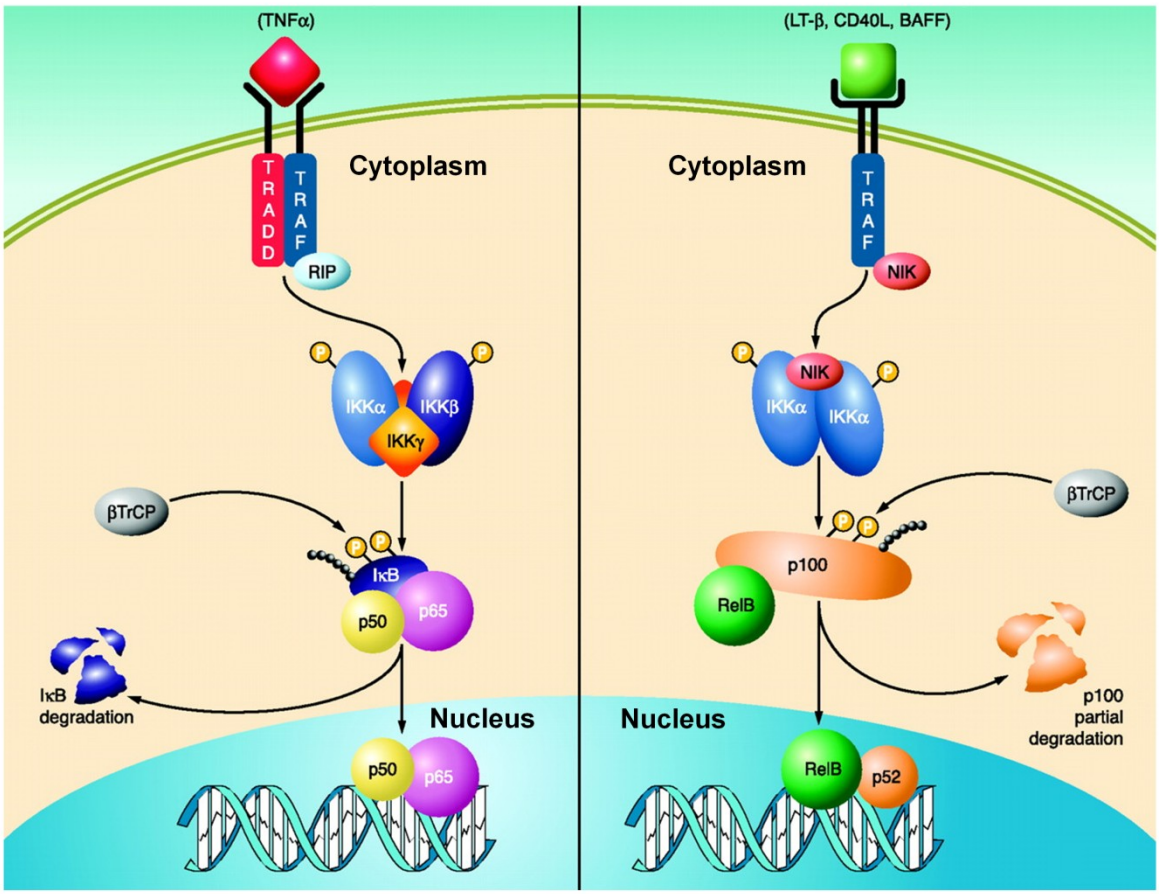

Figure 1.4

Classical and alternative NF-κB signalling pathways. The classical or canonical signalling pathway is represented using TNF-α as an activator. Signalling is initiated with the binding of TNF-α to its receptor and the subsequent sequential recruitment of the adaptors TRADD, RIP, and TRAF to the membrane. IKK complex assembly and recruitment to the cell membrane occurs between IKKα, IKKβ, and IKKγ, resulting in IKKβ phosphorylation and activation. IKKβ then phosphorylates IκBα to promote its polyubiquitination and subsequent immediate proteasomal degradation through β-TrCP. In turn, the classical p65/p50 heterodimer is freed to translocate to the nucleus and mediate transcription of NF-κB target genes, including one of its own inhibitor IκBα. Alternative NF-κB signalling is instead activated by ligands, CD40L, and lymphotoxinβ that triggers recruitment of TRAFs to the membrane-bound receptor and subsequently activates NIK. NIK then phosphorylates IKKα homodimer. Once active, IKKα phosphorylates p100, resulting in its partial proteolysis by β-TrCP to generate the p52 subunit. The resulting RelB/p52 complex then translocates to the nucleus to transcribe NF-κB target genes that may be distinct from the classical pathway.(Figure adapted from Bakkar and Guttridge, 2010)

1.3.1 NF-κB in vascular injury

NF-κB plays a critical role in the vascular response to injury (Yamasaki et al., 2003). Activated NF-κB is detected in human atherosclerotic and restenotic lesions, in SMCs, monocytes, and ECs (Brand et al., 1996). In contrast, activated NF-κB is rarely detected in normal uninjured arteries. Activation of NF-κB is a prominent response of the arterial wall upon angioplasty. After vascular injury, rapid activation of NF-κB correlates with proliferation of SMCs and induced expression of NF-κB-dependent genes (Brand et al., 1996).

Findings of *in vivo* studies about the role of NF-κB in intimal hyperplasia attain the conclusion that NF-κB was involved in neointimal hyperplasia. Using a balloon injury model in the rat carotid artery, low levels of constitutively activated NF-κB were shown in normal vessels, however, immediately after injury, levels of IκBα and IκBβ (inhibitors of NF-κB) were dramatically reduced, expression of VCAM-1 and MCP-1 was observed (Landry et al., 1997).

The results derived from *in vitro* studies consistently substantiate the notion that NF-κB signalling has a central role in regulating the inflammatory response and proliferation-apoptosis balance in the vessel wall. NF-κB regulated genes include TNF-α, IL-1β, IL-6, IL-10, VCAM-1, E selectin, COX-2 and iNOS. They are expressed in SMCs, endothelial cells and macrophages and are involved in the progression process (De Winther et al., 2005) even if some of them (e.g. IL-10, COX-2) can have anti-inflammatory roles (De Winther et al., 2005); NF-κB also mediates genes involved in proliferation and migration of SMCs such as MCP-1 (Landry et al., 1997).

These findings link the activation of NF-κB to neointimal formation and to the inflammatory response associated with injury-induced SMC proliferation/migration, thus validating NF-κB as a potential target for the control of neointimal hyperplasia.

1.3.2 NF-κB activation as a therapeutic target in neointimal formation

Consistent with the role of NF-κB in vascular injury, drugs specifically designed to target NF-κB activation, might be clinically useful for the treatment of diseases that involve inflammation and proliferation, including the neointimal hyperplasia. It is known that blocking NF-κB activation via transfection of adenoviral IκB (Breuss et al., 2002) or NF-κB “decoy” oligodeoxynucleotides, attenuate

neointimal formation after balloon injury in animal models (Ohtani et al., 2006). Recently, the first clinical use of a NF-κB decoy at the site of coronary stenting for the prevention of restenosis has been described (Suzuki et al., 2009). However, the indispensable role played by NF-κB in many biological processes has raised concern that a complete shutdown of this pathway would have significant detrimental effects on normal cellular function. Instead, drugs that selectively target only the inflammation-induced NF-κB activity would be of greater therapeutic value. In this regard, a cell-permeable peptide, namely *NEMO-binding domain* (NBD) peptide, has been shown to inhibit the NF-κB activation during inflammatory responces without completely inhibit NF-κB activity (D'Acquisto et al., 2002). It has not yet been investigated the possibility to consider the IKK inhibitor NBD as a potentially viable approach in vascular injury. The effect of this peptide on neointimal formation has been subject of this thesis (chapter 2).

1.4 Chemokines

Among NF-κB related proteins chemokines, a family of small heparin-binding proteins, play a critical role in vascular pathology. Chemokines direct the migration of circulating leukocytes to sites of inflammation or injury (Charo and Taubman, 2004) and are the major stimuli for activation of SMCs after the arterial injury (Schober, 2008), together with growth factors and cytokines.

It has been estimated that there may be as many as 40 to 50 human chemokines. Their domains are classified according to the location of cysteine residues (C) in highly conserved positions (Fig. 1.5). "CXC" chemokines represent one major chemokine family and are characterized by the presence of two cysteines, nearest the N-termini, separated by a single amino acid. The prototypical member of CXC chemokines is IL-8. The other major chemokine family is called "CC" because the two cysteines are adjacent. CC chemokines are RANTES, macrophage inflammatory protein-1α (MIP-1α) and MIP-1β and the monocyte chemotactic protein (MCP) subfamily including MCP-1, MCP-2, MCP-3, MCP-4 and MCP-5. The third family of chemokines is denoted "C" because of the lone cysteine in the N-terminal domain. Two chemokines have been described for this group and are called XCL1 (lymphotactin-α) and XCL2 (lymphotactin-ß). The last family, the

“CX3C” family, has only one known member, fractalkine (FK or CX3CL1) that consists of a soluble chemokine domain fused to a mucin-like stalk and a transmembrane domain.

Chemokines exert their cellular effects by activating seven transmembrane–domain G-protein–coupled receptors. Different cell types are characterized by different complements of chemokine receptors; this determines whether cells respond to a particular chemokine set. Chemokine binding to receptor triggers an intracellular signal transduction cascade that activates phosphatidylinositol-3 kinase, increases levels of inositol trisphosphate and intracellular calcium, activates Rho and mitogen-activated protein kinases. These events cause cell responses, including actin re-arrangement, shape change and chemotaxis. Chemokine receptors are divided into different families, CXC chemokine receptors, CC chemokine receptors, XC chemokine receptors and CX3C chemokine receptors that correspond to the four distinct families of chemokines they bind (Fig. 1.5).

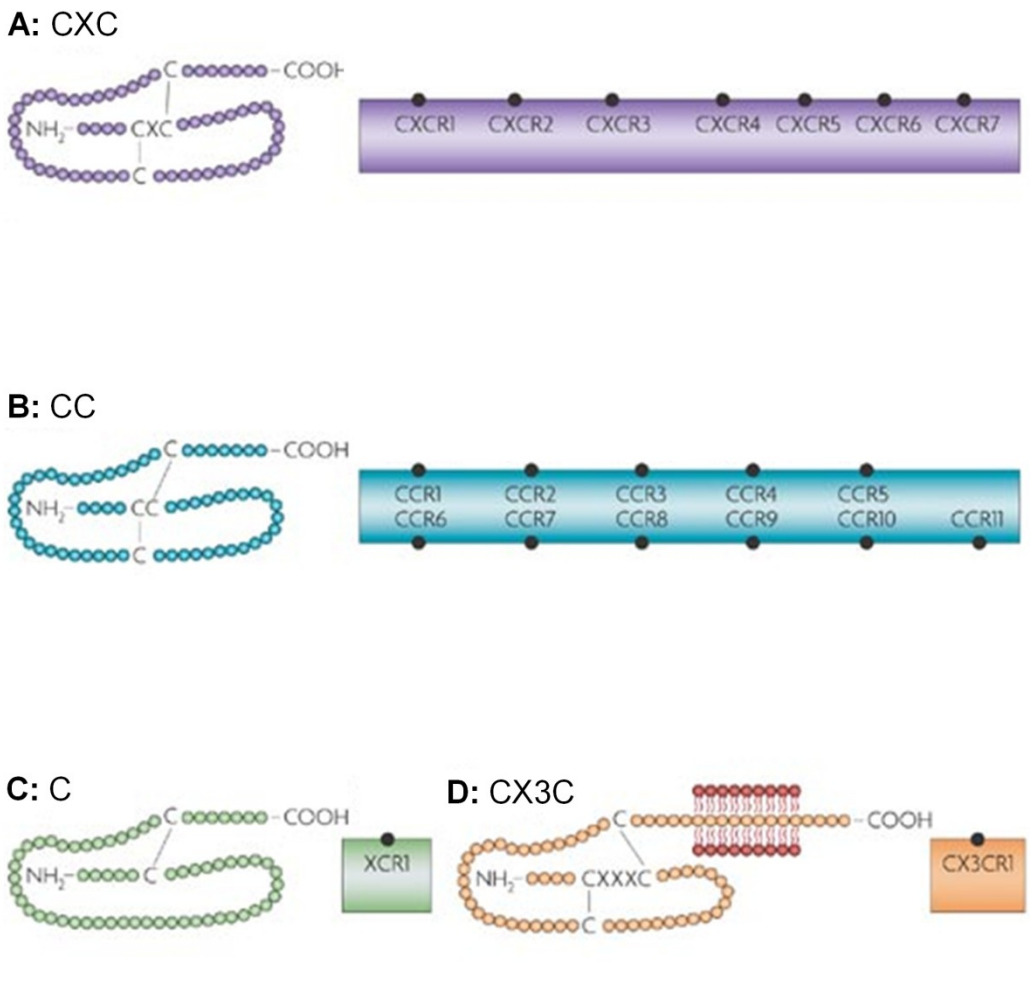

Figure 1.5

Classification of the four families of chemokines and their respective receptors (Figure adapted from Rostène et al., 2007)

1.4.1 Chemokines as therapeutic targets in vascular pathology

Chemokines and their receptors have a crucial role in initiating and progressing neointimal formation by controlling each step of the vascular remodelling in response to various noxious stimuli (Schober, 2008). Chemokines are produced by the major cells of the arterial wall, such as endothelial cells, SMCs, adventitial fibroblasts, leukocytes, as well as the circulation. They direct the leukocyte trafficking and activate the SMCs during vascular pathology (Schober, 2008). SMCs, in fact, respond to a number of chemokines involved in cell proliferation or intracellular calcium mobilization resulting in induction of tissue factor

(Charo and Taubman, 2204), a key factor in the pathogenesis of acute coronary syndromes. It is well known that MCP-1 direct the monocyte homing (Schober, 2008) as well as SMC proliferation and migration (Selzman et al., 2002; Massberg et al., 2003). RANTES induces the leukocyte recruitment through different chemokine receptors (Schober, 2008) and fractalkine induces both inflammation and SMC proliferation during neointimal formation (Schober, 2008). Eotaxin induces migration of cultured SMCs (Kodali et al., 2004).

The importance of chemokines in vascular diseases has sparked intense interest in developing broad-based inhibitors of chemokine activity as therapeutic agents. Several drugs, already in use as a treatment of vascular pathology or its risk factors, are able to modify the chemokine expression. For instance, HMG-CoA reductase inhibitors have been demonstrated to reduce, *in vitro* and *in vivo*, the expression of several markers of vascular inflammation, including chemokines (Apostolakis et al., 2006). Similar findings have been demonstrated for angiotensin converting enzyme (ACE) inhibitors, angiotensin II receptor blockade and glitazones (Apostolakis et al., 2006). Thus, some widely used anti-atherogenic drugs could mediate their beneficial actions partially through inhibition of certain chemokine pathways.

Directly blocking chemokine activation is now the goal of prevention as well as therapy of vascular disease and several preclinical studies are ongoing in this sense. It has been demonstrated that intravenous infusion of the myxoma virus M-T7, that inhibits CC and other chemokines, markedly reduced intimal hyperplasia in a rabbit model of arterial injury (Charo and Taubman, 2004). The chemokine antagonist MET-RANTES reduced neointimal formation in apolipoprotein E-deficient ($apoE^{-/-}$) mice as well as atherosclerotic plaque formation in $LDLR^{-/-}$ mice (Charo and Taubman, 2004).

Since initiation and development of atherosclerosis and intimal hyperplasia after vascular injury are regulated by MCP-1 (Boring et al., 1998; Egashira et al., 2002), MCP-1/CCR2 pathway is recently receiving increasing attention. It has been observed that eliminating the MCP-1 gene or blocking MCP-1 signalling decreases neointimal hyperplasia in several animal models of vascular injury (Furukawa et al., 1999; Egashira et al., 2007). Catheter-based adenovirus-mediated anti-monocyte chemoattractant gene therapy attenuates in-stent neointimal formation in monkeys

(Nakano et al., 2007). Up to now the possibility to use an oral inhibitor of MCP-1 pathway, has not yet been investigated. In this regard, an original indazolic compound, called bindarit, has been identified. Bindarit inhibits MCP-1 synthesis and its ability in reducing neointimal formation has been subject of this thesis (chapter 3).

In the context of MCP-1/CCR2 pathway activation during vascular injury, it is interesting to note that $CCR2^{-/-}$ mice have a ≈60% decrease in intimal hyperplasia and medial DNA synthesis in response to femoral arterial injury while $MCP\text{-}1^{-/-}$ mice show a ≈30% reduction in intimal hyperplasia, which is not associated with diminished medial DNA synthesis (Charo and Taubman, 2004). These data suggest that MCP-1 and CCR2 deficiencies have distinct and separate effects on arterial injury; therefore, it is possible that the results obtained with $CCR2^{-/-}$ mice may not be solely mediated by MCP-1 but also by other chemokines acting on the same receptor. It is known that CCR2 is shared with MCP-3 and that this chemokine acts through interaction with not only CCR2 but also CCR1 and CCR3, all expressed on vascular SMCs. The role of MCP-3 in vascular pathology is not well known; in this thesis its effect on SMC proliferation has been evaluated (chapter 4).

Although in the past few years we have witnessed a rapid increase in our understanding of the role of chemokines and their receptors in cardiovascular pathologies, all investigators agree on the fact that the precise mechanism of the chemokine pathways involved in the response of the arterial wall to vascular injury is not fully elucidated. Much more information is needed before chemokine-based therapies can be applied in clinical practice.

1.5 Specific aims

In an effort to improve on current therapy for restenosis we are prompted to consider new strategies for prevention and treatment. In this regard, the objective of the thesis was to identify molecular mechanisms and possible therapeutic targets in the context of immunity/inflammatory response and SMC proliferation, both contributing to vascular pathology in humans. Our specific aims were:

- to investigate the effect of two different agents, the NF-κB inhibitor NBD peptide and the anti-inflammatory drug bindarit, on neointimal formation *in vivo*, and on SMC proliferation/migration *in vitro*;
- to evaluate the influence of MCP-3 on human coronary SMC proliferation and to analyse the intracellular signalling pathways involved;
- to investigate the contribution of SMCs in antigen presentation, to better understand their role in vascular immunity (this part of the thesis was carried out in the Institute of Infection, Immunity and Inflammation, University of Glasgow, UK).

2. NBD PEPTIDE INHIBITS INJURY-INDUCED NEOINTIMAL FORMATION

NF-κB plays a critical role in the pathophysiological processes leading to neointimal formation (Collins and Cybulsky, 2001) and it is well established that blocking NF-κB activation attenuates the responses to vascular injury. Activation of the IKK complex represents an essential regulatory step in all pathways leading to NF-κB activation. The "core" complex containing the two catalytic subunits, IKKα and IKKβ, and the regulatory subunit known as NEMO or IKKγ, is an indispensable component of all proinflammatory signalling pathways to NF-κB. A very small region in the COOH-terminus of IKKα (L738–L743) and IKKβ (L737–L742) is essential for stable interaction with NEMO, and for the assembly of the heteromeric IKK-NEMO complex. This region is known as the "*NEMO binding domain*" (NBD) (Strickland and Ghosh, 2006). The small size of the NBD permitted the design of a peptide that can disrupt the interaction of NEMO with the IKKs. To make this peptide cell permeable NBD peptide was conjugated to a sequence from the *Drosophila antennapedia* protein, called penetratin, that facilitates cellular uptake (May et al., 2000) (Fig. 2.1)

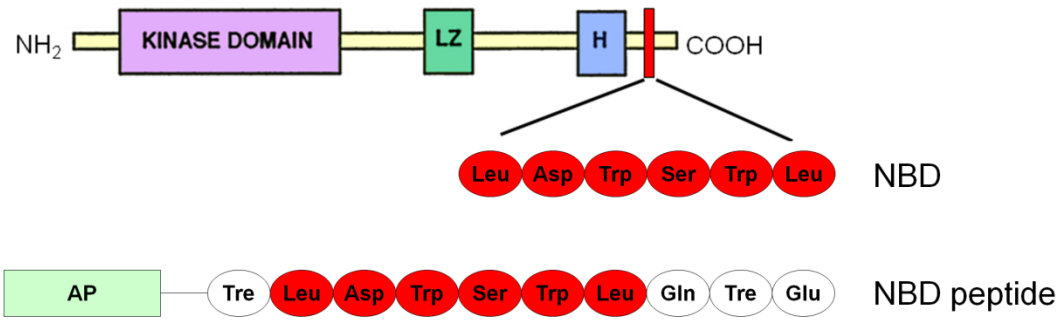

Figure 2.1

The NBD region, in the COOH-terminus of IKKα and IKKβ, and the NBD peptide. AP=Penetratin

NBD peptide, blocking the association of NEMO with IKKα and with IKKβ, inhibited TNF-α-induced NF-κB activation in HeLa cells, E-selectin expression in

human umbilical vein endothelia cells (HUVEC), NO production in macrophages (May et al., 2000). The potential of this peptide to function as a potent anti-inflammatory agent has been demonstrated *in vivo* in various animal models including phorbol ester–induced ear edema and zymosan induced peritononitis (May et al., 2000), as well as LPS-induced septic shock (D'Acquisto et al., 2002), carrageenan-induced paw swelling (D'Acquisto et al., 2002), spontaneously occurring chronic murine colitis (Davé et al., 2007) and in a mouse model of rheumatoid arthritis, namely collagen-induced arthritis (CIA) (Strickland and Ghosh, 2206). However, the effects of a highly selective pharmacological inhibition of the proinflammatory IKK activity have not yet been investigated in vascular injury, thus blocking IKK through NBD peptide strategy could be interesting in this sense.

The aim of the present study was to investigate the effect of the NBD peptide on neointimal formation *in vivo* using two well-known animal models of arterial injury: the rat carotid artery balloon angioplasty and the wire-induced carotid injury in apoE$^{-/-}$ mice. In addition, the effects of the NBD peptide on SMC proliferation and migration *in vitro* were also examined.

2.1 Methods

2.1.1 Cell culture

Primary aortic SMCs were isolated from the thoracic aorta of male Wistar rats as previously described (Parenti et al., 2004) and grown in Dulbecco's modified Eagle medium (DMEM; Cambrex Bio Sciences) supplemented with L-glutamine, 10% fetal bovine serum (FBS; Cambrex Bio Sciences), 100 U/mL penicillin, and 100 µg/mL streptomycin in a humidified incubator at 37°C in 5% CO_2. Before initiation of the assays, the SMCs were starved into DMEM supplemented with 0.1% FBS for 48 h. Studies were performed with cells at passages 3-6.

2.1.2 Cell proliferation study

SMC proliferation was quantified by the total cell number as previously reported (Parenti, et al., 2004). Briefly, $5x10^3$ cells were seeded onto 48-multiwell plates and allowed to adhere overnight. Starved cells were stimulated with TNF-α (5

ng/mL; R&D Systems), PDGF-BB (10 ng/mL; R&D Systems) or FGF-2 (10 ng/mL; R&D Systems) in the presence or absence of the NBD peptide (0.01-1 μM; Genosphere Biotech). After 72 h, cells were fixed with methanol and stained with Diff-Quik. Proliferation was evaluated as cell duplication by counting the number of cells in ten random fields of each well at 200X magnification (TNF-α experiment) or 400X magnification (PDGF-BB and FGF-2 experiments) with the aid of a 21 mm^2 ocular grid. These experiments were performed in collaboration with Dr. Astrid Parenti, University of Florence.

2.1.3 Chemotactic migration and invasion

The modified Boyden chamber (48-multiwell plates; Neuroprobe) was used for chemotaxis studies. Polyvinyl-pyrrolidone-free polycarbonate filters, 8 μm pore size, were coated with 100 μg/mL collagen type I and 10 μg/mL fibronectin. Biocoat Matrigel invasion chambers (24-multiwell plates with 8.0 μm pore size filter; Becton Dickinson) were used according to the manufacturer's instructions for invasion studies. TNF-α (5 ng/mL), PDGF-BB (10 ng/mL) or FGF-2 (10 ng/mL) were added to the lower wells, while starved cells ($12x10^3$ for migration assay and $3x10^4$ for invasion assay) were seeded into the upper wells of the chamber, and incubated at 37°C. The NBD peptide (0.01-1 μM) was added to the cell suspension 60 min before seeding. After 4h for migration assay or 48h for invasion assay, the migrated cells were fixed and stained with haematoxylin. Cell migration was measured by microscopic evaluation of the number of cells moved across the filter, in ten random fields for the migration assay and in the entire filter for the invasion assay. Part of these experiments was performed in collaboration with Dr. Astrid Parenti, University of Florence.

2.1.4 Flow cytometry

Apoptosis was quantified by flow cytometry, using a commercially available Annexin V- Alexa Fluor® 488 apoptosis detection kit following the manufacturer's guidelines (Molecular Probes™). Starved SMCs were stimulated for 24h with TNF-α (5 ng/mL) then washed twice in PBS, trypsinized, and collected. To evaluate the effect of the NBD peptide, SMCs were pretreated for 1h with the peptide (1 μM) before the TNF-α stimulation. Cells were centrifuged, the supernatant discarded,

and the cell pellet resuspended in the kit's binding buffer. The cells were centrifuged again, the supernatant discarded, and the pellet resuspended in the kit's buffer containing Alexa Fluor® 488 Annexin V solution and MitoTracker® Red dye. Samples were incubated in the dark for 10 minutes and analysed using an Epics XL flow cytometer (Beckman Coulter) equipped with a 488-nm Argon laser. Apoptotic cells showed green fluorescence with decreased red fluorescence and live cells showed very little green fluorescence and bright red fluorescence. Isotype-matched antibodies (Abs) were used as a negative control. These experiments were performed in collaboration with Dr. Astrid Parenti, University of Florence.

2.1.5 Gelatin zymography

Cells were cultured in 96-well culture plates in 10% FBS medium until 90% confluence was achieved. Starved cells were stimulated with TNF-A-α (5 ng/mL) in the presence or absence of the NBD peptide (1 μM). After 24h the media were collected, clarified by centrifugation and subjected to electrophoresis in 8% SDS-PAGE containing 1 mg/mL gelatin under non-denaturing conditions. After electrophoresis the gels were washed with 2.5% Triton X-100 to remove SDS and incubated for 24 h at 37°C in 50 mM Tris buffer containing 200 mM NaCl and 20 mM $CaCl_2$, pH 7.4. The gels were stained with 0.5% Coomassie brilliant blue R-250 in 10% acetic acid and 45% methanol and destained with 10% acetic acid and 45% methanol. Bands of gelatinase activity appeared as transparent areas against a blue background. Gelatinase activity was then evaluated by quantitative densitometry. These experiments were performed in collaboration with Dr. Astrid Parenti, University of Florence.

2.1.6 Enzyme-Linked Immunosorbent Assay (ELISA)

Cells were used after the induction of quiescence in 24-well plastic culture plates at a density of 2×10^4 cells/well. The cells were stimulated with TNF-α (5 ng/mL) in the presence or absence of the NBD peptide (0.01-1 μM). After 24 h media were collected, centrifuged at 2000xg for 15 min at 4°C and supernatants were used for ELISA to detect MCP-1 (OptEIA™, Biosciences).

2.1.7 Cytosolic and nuclear extracts

Cells (1×10^5) suspended in 10% FBS medium were seeded in 6-multiwell plates and allowed to adhere overnight. Cells were kept in starving conditions for 48 h. The medium was then removed and replaced with fresh medium containing TNF-α (5 ng/mL) or PDGF-BB (10 ng/mL) in the presence or absence of the NBD peptide (0.01-1 μM) or the mut-NBD peptide (1 μM). The NBD peptides used in this study were described previously (Di Meglio et al., 2005).

The cell pellet was resuspended in 100 μL of ice-cold hypotonic lysis buffer (10 mM Hepes, 10 mM KCl, 0.5 mM phenylmethylsulphonyfluoride, 1.5 μg/mL soybean trypsin inhibitor, 7 μg/mL pepstatinA, 5 μg/mL leupeptin, 0.1 mM benzamidine, 0.5 mM dithiothreitol) and incubated on ice for 15 min. The cells were lysed by rapid passage through a syringe needle five times and centrifuged for 10 min at 13.000×g. The supernatant containing the cytosolic fraction was removed and stored at -80°C. The nuclear pellet was resuspended in 30 μL of high salt extraction buffer (20 mM Hepes pH 7.9, 10 mM NaCl, 0.2 mM EDTA, 25% v/v glycerol, 0.5 mM phenylmethylsulphonyfluoride, 1.5 μg/mL soybean trypsin inhibitor, 7 μg/mL pepstatin A, 5 μg/mL leupeptin, 0.1 mM benzamidine, 0.5 mM dithiothreitol) and incubated at 4°C for 30 min with constant agitation. The nuclear extract was then centrifuged for 10 min at 6000×g with the supernatant aliquoted and stored at -80°C. Protein concentration was determined by the Bio-Rad protein assay kit (Bio-Rad).

2.1.8 Western blot analysis

Immunoblotting analysis of phospho-IκBα (Ser32/36) was performed on cytosolic extracts. The samples were mixed with gel loading buffer (50 mM Tris, 10% SDS, 10% glycerol, 10% 2-mercaptoethanol, 2 mg/mL of bromophenol) in a ratio of 1:1, boiled for 3 min and centrifuged at 1000×g for 5 min. An equivalent protein amount (30 μg) of each sample was electrophoresed in a 10% discontinuous polyacrylamide gel. The proteins were transferred onto nitro-cellulose membranes, according to the manufacturer's instructions (Bio-Rad). The membranes were saturated by incubation for 2 h with 10% milk buffer and then incubated with the primary Ab (mouse anti-phospho-IκBα, 1:1000; Cell Signaling) at 4°C overnight. The membranes were washed three times with 0.01% Tween20 in

PBS and then incubated with anti-rabbit or anti-mouse immunoglobulins coupled to peroxidase (1:1000; DAKO). The immunocomplexes were visualized using the ECL chemiluminescence method.

2.1.9 Electrophoretic mobility shift assay (EMSA)

Double stranded NF-κB consensus oligonucleotide probe (5' AGC TTC AGA GGG GAC TTT CCG AGA GG 3') was end-labelled with [^{32}P]γ-ATP. Nuclear extracts (10 μg protein from each sample) were incubated for 20 min with radiolabelled oligonucleotides (2.5-5.0x10^4 cpm) in 20 μL reaction buffer containing 2 μg poly dI-dC, 10 mM Tris-HCl (pH 7.5), 100 mM NaCl, 1 mM EDTA, 1 mM dithiothreitol, 1 μg/μL bovine serum albumin, 10% (v/v) glycerol. Nuclear protein-oligonucleotide complexes were resolved by electrophoresis on a 5% non-denaturing polyacrylamide gel in 0.5 x Tris-borate/EDTA at 150 V for 2 h at 4°C. The gels were dried and autoradiographed with intensifying screen at -80°C for 24h.

2.1.10 Animals

Male Wistar rats (Harlan Laboratories) weighing 250 g and 8-week-old female apoE$^{-/-}$ mice (Charles River) were used. Animals were housed at the Department of Experimental Pharmacology, University of Naples Federico II. All procedures were performed according to Italian ministerial authorization (DL 116/92) and European regulations on the protection of animals used for experimental and other scientific purposes.

2.1.11 Rat carotid balloon angioplasty

Rats were anesthetized with an intraperitoneal injection of ketamine (100 mg/kg) (Gellini International) and xylazine (5 mg/kg) (Sigma). Endothelial denudation of the left carotid artery was performed with a balloon embolectomy catheter (2F, Fogarty, Edwards Lifesciences) according to the procedure validated in our laboratories (Maffia et al., 2006). Immediately after endothelial denudation, 300 μg of the NBD peptide or 300 μg of the mut-NBD peptide in 100 μL of pluronic gel (pH 7.2) was applied to the adventitia (Ianaro et al., 2003). The control group received pluronic gel only. Some animals were subjected to anesthesia and surgical

procedure without balloon injury (sham-operated group). Rats were euthanized 7 and 14 days after angioplasty. Carotid arteries were collected and processed as described below.

2.1.12 Atherogenic murine model of vascular injury

ApoE$^{-/-}$ mice were fed an atherogenic diet (21% fat, 0.15% cholesterol, 19.5% casein, wt/wt, TD88137, Mucedola) from 1 week before until 4 weeks after carotid injury performed as described previously (Lindner et al., 1993), with minor modification. Briefly, mice were anaesthetized as described above, and endothelial injury of the left common carotid artery was performed with a 0.35 mm diameter flexible nylon wire introduced through the left external carotid artery and advanced to the aortic arch. The endothelium was damaged by passing the wire through the lumen of the artery three times. Immediately after endothelial denudation, 150 μg of the NBD peptide or 150 μg of the mut-NBD peptide in 50 μL of pluronic gel was applied to the adventitia. Carotid arteries were collected 28 days after wire injury and processed as described below.

2.1.13 Evaluation of neointimal formation

Carotid arteries were fixed by perfusion with phosphate-buffered saline (PBS; pH 7.2) followed by PBS containing 4% formaldehyde through a cannula placed in the left ventricle. Paraffin-embedded sections were cut (6 μm thick) from the approximate middle portion of the artery and stained with haematoxylin and eosin to demarcate cell types. Ten sections from each carotid artery were reviewed and scored under blind conditions. The cross-sectional areas of tunica media and neointima were determined by a computerized analysis system (LAS, Leica).

2.1.14 Proliferating Cell Nuclear Antigen Analysis

Proliferating cell nuclear antigen (PCNA) analysis was used to quantify the proliferative activity of cells at the balloon injury sites, and was performed using monoclonal mouse anti-PCNA Ab (1:250, PC10, Sigma) and biotinylated anti-mouse secondary Ab (1:400, DakoCytomation). Slides were treated with streptavidin-HRP (DakoCytomation) and exposed to diaminobenzidine chromogen

(DakoCytomation) with hematoxylin counterstain. Six sections from each carotid artery and 10 fields per section were reviewed and scored under blind conditions. Data are represented as percentage of cells positive for PCNA 7 days after angioplasty.

2.1.15 Immunohistochemical localization of the NBD peptide

Localization of the biotinylated (bio)-NBD peptide in rat carotid arteries was performed by immunofluorescence in order to determine the temporal and spatial distribution of the peptide delivered to the adventitia. Briefly, 300 μg of the bio-NBD peptide (Genosphere Biotech, Paris, France) in 100 μl of pluronic gel were applied on the carotid artery immediately after the injury. Immunohistochemical analysis was performed on 5 μm frozen sections of rat carotid artery, 3, 7 and 14 days after injury. The biotinylated peptide was detected by texas red-conjugated streptavidin (1:100; DakoCytomation). For the identification of the SMCs a monoclonal anti-α-SMA FITC (1:250, clone 1A4, Sigma) was used. DAPI was used to identify nuclei.

2.1.16 Preparation of Total Extracts of rat carotid arteries

All the extraction procedures were performed on ice with ice-cold reagents as described above. Briefly, liquid nitrogen frozen pooled carotid arteries (n=2) were crushed into powder and resuspended in an adequate volume of hypotonic lysis buffer and then centrifuged for 15 minutes at 6000xg with the supernatant being placed in aliquots, and stored at -80°C. Protein concentration was determined by the Bio-Rad protein assay kit. Total extracts were used to evaluate MCP-1 production and NF-κB activity by ELISA and EMSA respectively.

2.1.17 Statistical analysis

Results are expressed as mean±SEM of n animals for *in vivo* experiments and mean±SEM of multiple experiments for *in vitro* assays. Student's *t* test was used to compare 2 groups or ANOVA (Two-Tail *P* value) was used with the Dunnett's *post hoc* test for multiple groups using Graph Pad Instat 3 software (San Diego). Non parametric Mann Whitney test was used for evaluation of neointimal formation. The level of statistical significance was 0.05 per test.

2.2 Results

2.2.1 Effect of the NBD peptide on NF-κB activation in SMCs

Thirty minutes of stimulation with TNF-α (5 ng/mL) caused a significant IκBα phosphorylation at Ser32 (Fig. 2.2A). Consistent with its mechanism of action, treatment with the NBD peptide reduced the phosphorylation of IκBα in a concentration-dependent manner. Treatment with the mut-NBD peptide (1 μM) did not affect IκBα phosphorylation (Fig. 2.2A). To further confirm the inhibitory effect of the NBD peptide on NF-κB activation, we examined the NF-κB/DNA binding 4h after TNF-α stimulation. As shown in Figure 2.2B, the NBD peptide (0.01-1 μM) inhibited TNF-α-induced NF-κB activation. The relative densitometric analysis showed a concentration-dependent inhibition, significant at all concentrations studied (Fig. 2.2B).

2.2.2 Effect of the NBD peptide on SMC proliferation and apoptosis

Initiation and maintenance of SMC proliferation is a critical event in the pathogenesis of neointimal formation. As shown in Figure 2.3A, the NBD peptide (0.01-1 μM) significantly inhibited TNF-α-induced SMC proliferation by 15% (P<0.05, n=3), 20% (P<0.001, n=3), and 30% (P<0.001, n=3) respectively. This effect of the NBD peptide was not due to induction of cell apoptosis as demonstrated by flow cytometry analysis of Annexin V-labelled cells. The NBD peptide (1 μM) neither alone nor in presence of TNF-α (5 ng/mL) stimulated cell apoptosis (Fig. 2.3B). Similarly, the NBD peptide (1 μM) significantly inhibited PDGF-BB (10 ng/mL)-induced SMC proliferation by 27% (P<0.05, n=3) but was without effect when the stimulant was FGF-2 (10 ng/mL) (Fig. 2.4A).

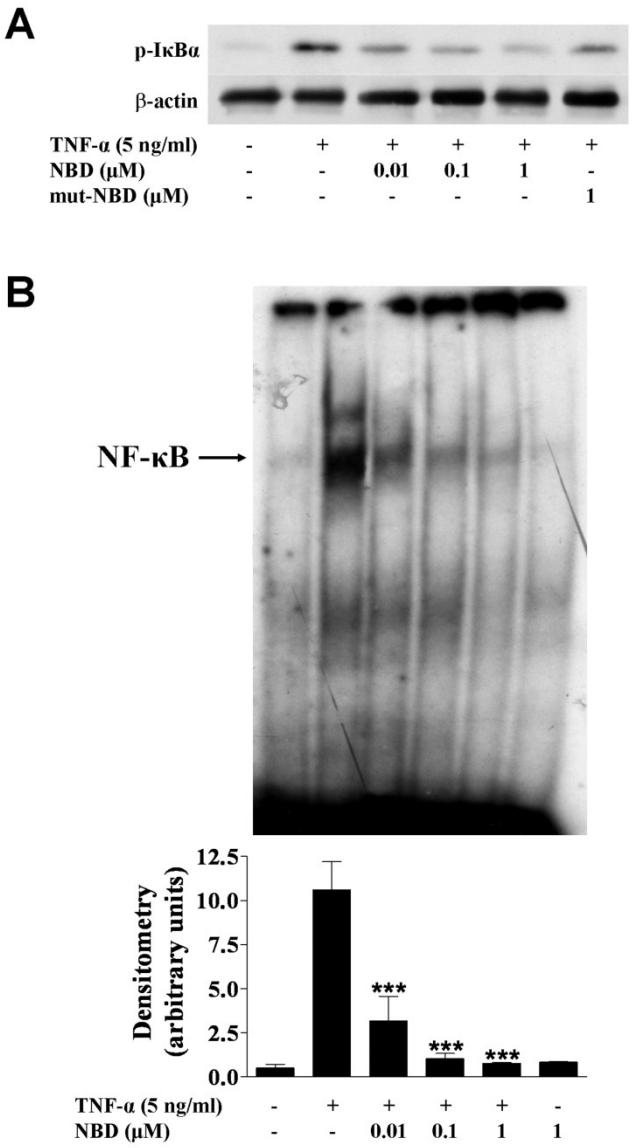

Figure 2.2

(A) Representative Western blot showing the effect of the NBD peptide (0.01 to 1 μM) or the mut-NBD peptide (1μM) on rat SMC IkBα phosphorylation induced by TNF-α (5 ng/mL). (B) Representative EMSA and relative densitometric analysis showing the effect of the NBD peptide (0.01 to 1 μM) on TNF-α (5 ng/mL)-induced NF-kB activation in rat SMCs. Results are expressed as mean±SEM of 3 separate experiments. ***P<0.001 *vs* TNF-α-stimulated cells.

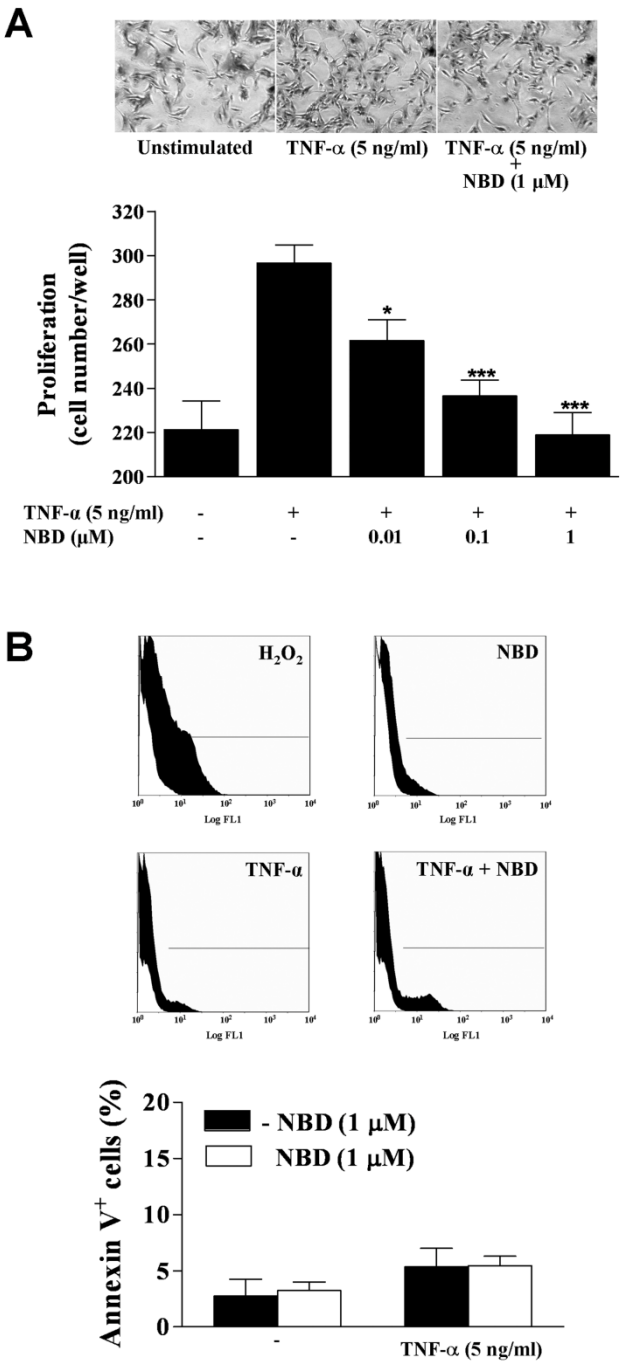

Figure 2.3

(A) Upper panel: representative photomicrographs showing the inhibition of TNF-α-induced proliferation by the NBD peptide. In the lower panel the graph shows the effect of the NBD peptide (0.01-1 μM) on SMC proliferation induced by TNF-α (5 ng/mL). Results are expressed as mean±SEM of 4 experiments run in triplicate. **P*<0.05; ****P*<0.001 *vs* TNF-α-stimulated cells. (B) Upper panel: representative histograms of apoptotic cells (black) stimulated for 24h with TNF-α (5 ng/mL), and the NBD peptide (1 μM) with or without TNF-α. Positive control: 1mM H_2O_2 for 4h. Isotype-matched Abs were used as negative control (white). In the lower panel the graph shows the effect of the NBD peptide (1 μM) with or without TNF-α on cell apoptosis. Mean ± SEM of 4 experiments.

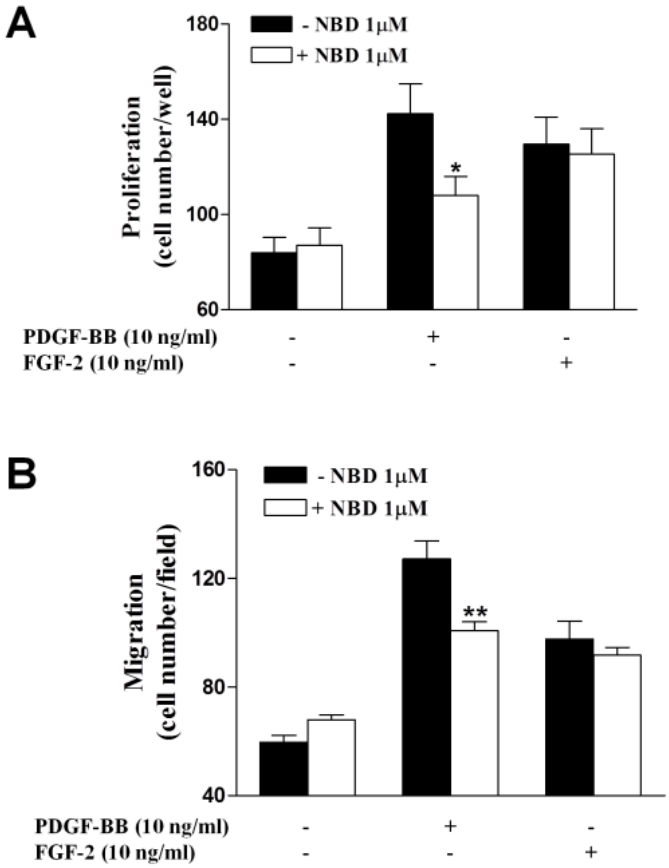

Figure 2.4

(A) Graph showing the effect of the NBD peptide (1 μM) on SMC proliferation induced by PDGF-BB (10 ng/mL) or FGF-2 (10 ng/mL). Results are expressed as mean ± SEM of 4 experiments run in triplicate. **P*<0.05 *vs* PDGF-BB-stimulated cells without peptide. (B) Graph showing the effect of the NBD peptide (1 μM) on SMC migration induced by PDGFBB (10 ng/mL) or FGF-2 (10 ng/mL). Results are expressed as mean ± SEM of 3 experiments run in triplicate. ***P*<0.01 *vs* PDGF-BB-stimulated cells without peptide.

2.2.3 Effect of the NBD peptide on SMC migration

We also evaluated the effects of the NBD peptide on TNF-α-induced SMC chemotaxis. The NBD peptide significantly inhibited chemotactic migration by 15% (*P*<0.05, n=3) at 0.01 μM, and about 20% (*P*<0.001, n=3) at both 0.1 μM and 1 μM (Fig. 2.5A). The NBD peptide reduced PDGF-BB-, but not FGF-2-induced SMC migration (Fig. 2.4B). Moreover, the NBD peptide (1 μM) significantly reduced TNF-α-induced SMC invasion (by 70%, *P*<0.001, n=3) through the Matrigel^{TM} barrier which mimics the extracellular matrix (Fig. 2.5B).

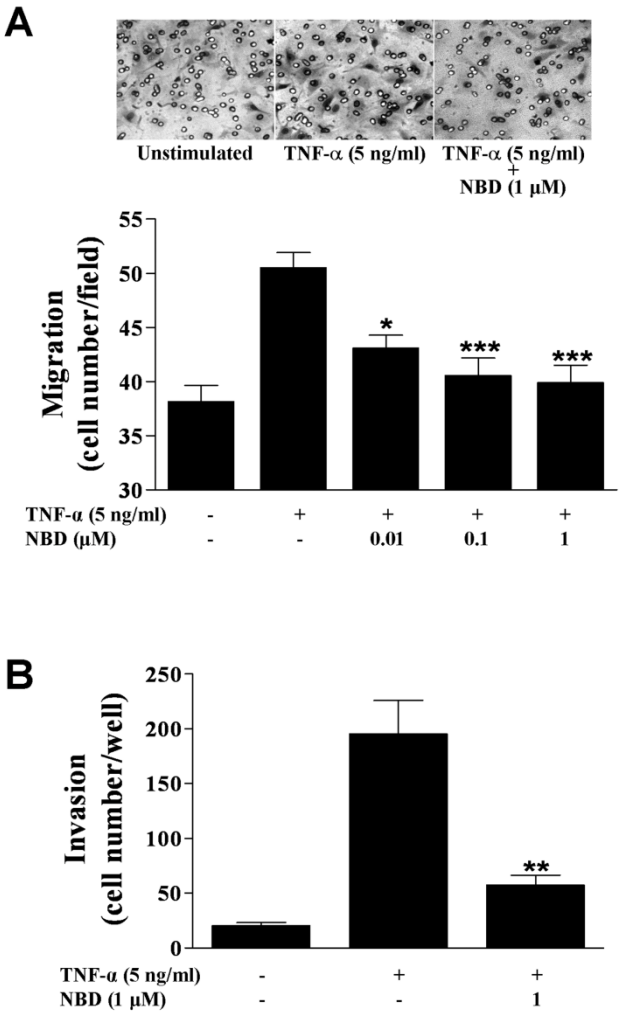

Figure 2.5

(A) Representative photomicrographs showing the inhibition of TNF-α-induced migration by the NBD peptide. In the lower panel the graph shows the effect of the NBD peptide (0.01-1 μM) on SMC migration induced by TNF-α (5 ng/mL). Results are expressed as mean±SEM of 3 experiments run in triplicate. **P*<0.05; ****P*<0.001 *vs* TNF-α-stimulated cells. (B) Effect of the NBD peptide on SMC invasion through a matrigel™ barrier induced by TNF-α. Results are expressed as mean±SEM of 3 experiments run in triplicate. ***P*<0.01 *vs* TNF-α-stimulated cells.

2.2.4 Effect of the NBD peptide on MMP2 and MMP9 activity

Subconfluent cultures of SMCs were exposed to TNF-α (5 ng/mL) for 24h in the presence or absence of the NBD peptide (1 μM) to assess gelatinase production. Gelatin zymography of control supernatants showed the constitutive release of the latent forms of MMP-2, visualized as a band at 72 and 68 kDa. TNF-α stimulated the release of MMP-2 and induced its activation as revealed by the appearance of the 62 kDa form (Fig. 2.6A). The NBD peptide significantly (*P*<0.05)

inhibited the latent form of MMP-2 without affecting the activated form and slightly decreased, although not significantly, the TNF-α-induced MMP-9 gelatinase active form production (92 kDa) (Fig. 2.6A,B).

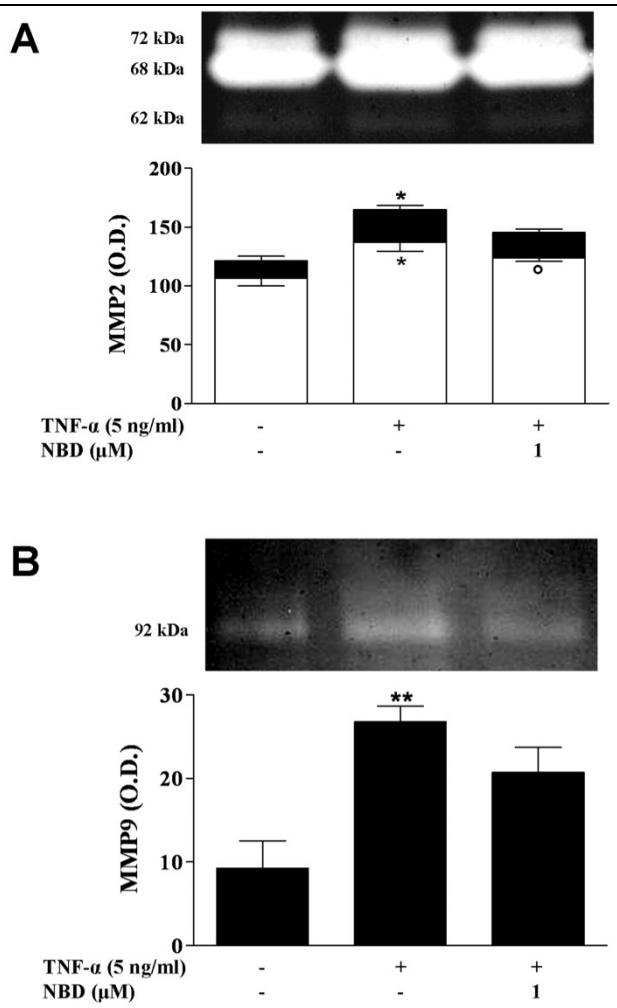

Figure 2.6

(A) Representative gel zymography of conditioned medium from SMCs and relative densitometric analysis showing the effect of the NBD peptide on both MMP2 latent (white columns) and activated (black columns) forms. Results are expressed as mean±SEM of 4 experiments. **P*<0.05 *vs* unstimulated cells; °*P*<0.05 *vs* TNF-α stimulated cells. (B) Representative gel zymography of conditioned medium from SMCs and relative densitometric analysis showing the effect of the NBD peptide on MMP9 activated form. Results are expressed as mean±SEM of 4 experiments. ***P*<0.01 *vs* unstimulated cells.

2.2.5 Effect of the NBD peptide on MCP-1 production

MCP-1 production by cultured rat SMCs was determined in cell supernatants by ELISA. As shown in Figure 2.7, stimulation of SMCs with TNF-α (5 ng/mL) caused an increased release of MCP-1 compared to that observed in unstimulated cells. In the presence of the NBD peptide (0.01-1 μM) a concentration-related inhibition of MCP-1 production was observed. Interestingly, the NBD peptide, at higher concentrations totally abolished TNF-α-induced MCP-1 production. The NBD peptide alone (1 μM) did not affect basal MCP-1 production (Fig. 2.7).

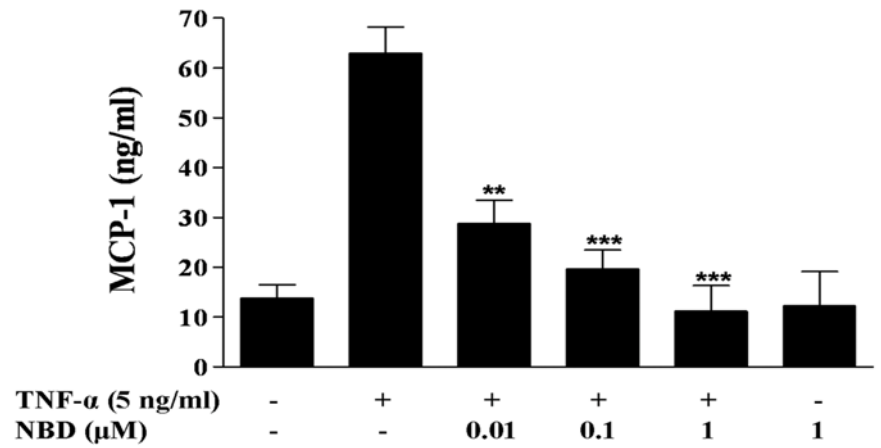

Figure 2.7

Effect of the NBD peptide on MCP-1 production evaluated by ELISA on SMCs. Results are expressed as mean±SEM of 3 experiments run in triplicate. ***P*<0.01 and *** *P*<0.001 *vs* TNF-α-stimulated cells.

2.2.6 Effect of the NBD peptide on neointimal formation in rat injured carotid arteries

Rats were treated with either the NBD peptide, the mut-NBD peptide (300 μg/site), or an equal volume of pluronic gel (100 μL, control group) immediately after balloon injury. A reduction of proliferating cells was demonstrated in the carotid arteries of the NBD peptide-treated rats 7 days after injury (*P*<0.01, n=5) (Fig. 2.8A). Moreover, the NBD peptide treatment caused a significant inhibition of neointimal formation by 54% (*P*<0.01, n=10) at day 14 compared with the control group (Fig. 2.8B). The local application of the mut-NBD peptide (300 μg/site) did not

affect neointimal formation (n=5; Fig. 8B). In addition, the NBD peptide significantly (*P*<0.01) increased the lumen area and decreased neointima/media ratio (Table 2.1).

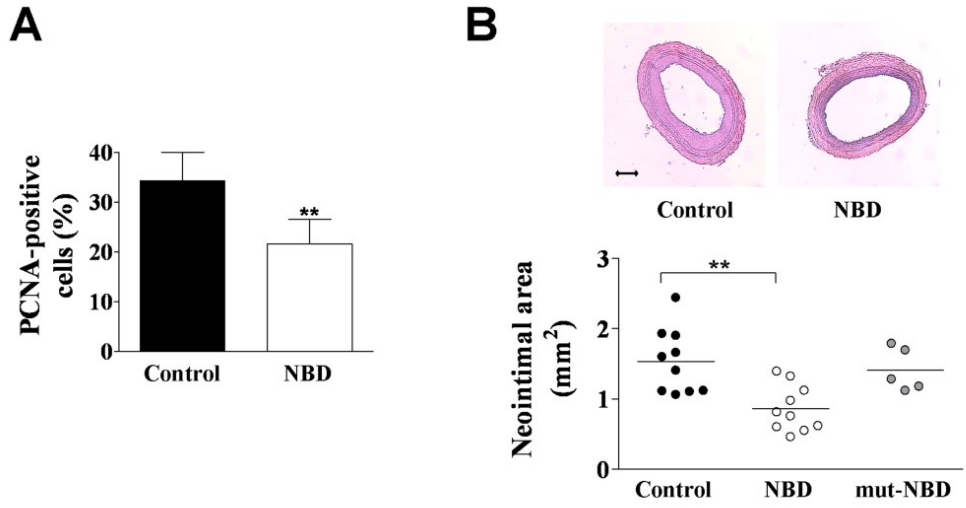

Figure 2.8

(A) Percentage of total medial and neointimal cells positive for PCNA 7 days after vascular injury. Results are expressed as mean±SEM (n=5). ***P*<0.01 *vs* control group. (B) Representative microphotograph showing the effect of local administration of the NBD peptide (300 µg/site; n=10) or the mut-NBD peptide (300 µg/site; n=5) on the neointimal area in rat carotid artery, 14 days after injury. Control animals (n=10) received pluronic gel only as described in Methods. ***P*<0.01 *vs* control group. Scale bar=200 µm.

Table 2.1 Morphometric analysis of rat carotid arteries 14 days after angioplasty

	Control	NBD	Mut-NBD
Vessel area (mm^2)	0.457 ± 0.020	0.464 ± 0.019	0.451 ± 0.008
Media area (mm^2)	0.139 ± 0.018	0.132 ± 0.005	0.143 ± 0.006
Lumen area (mm^2)	0.108 ± 0.020	0.216 ± 0.024 **	0.104 ± 0.027
Neointimal area (mm^2)	0.210 ± 0.060	0.116 ± 0.059 **	0.202 ± 0.056
Neointima/Media ratio	1.532 ± 0.146	0.858 ± 0.104 **	1.410 ± 0.138

The results are expressed as mean ± SEM (n=10 for control and NBD group; n=5 for mut-NBD group). Control animals received pluronic gel only. ***P*<0.01 *vs* control group.

2.2.7 Effect of the NBD peptide on NF-kB activation in rat Injured carotid arteries

To support the hypothesis that the reduction of neointimal thickness correlated with NF-κB inhibition, the NF-κB/DNA binding activity was evaluated on extracts from carotidarteries by EMSA. The NBD peptide, but not the mut-NBD peptide, significantly (n=3, *P*<0.001) reduced balloon-induced NF-κB activation in injured arteries 3 and 14 days after injury. A low level of NF-κB/DNA binding activity was detected in total protein extracts from carotid arteries of sham-operated rats (Fig. 2.9A, B).

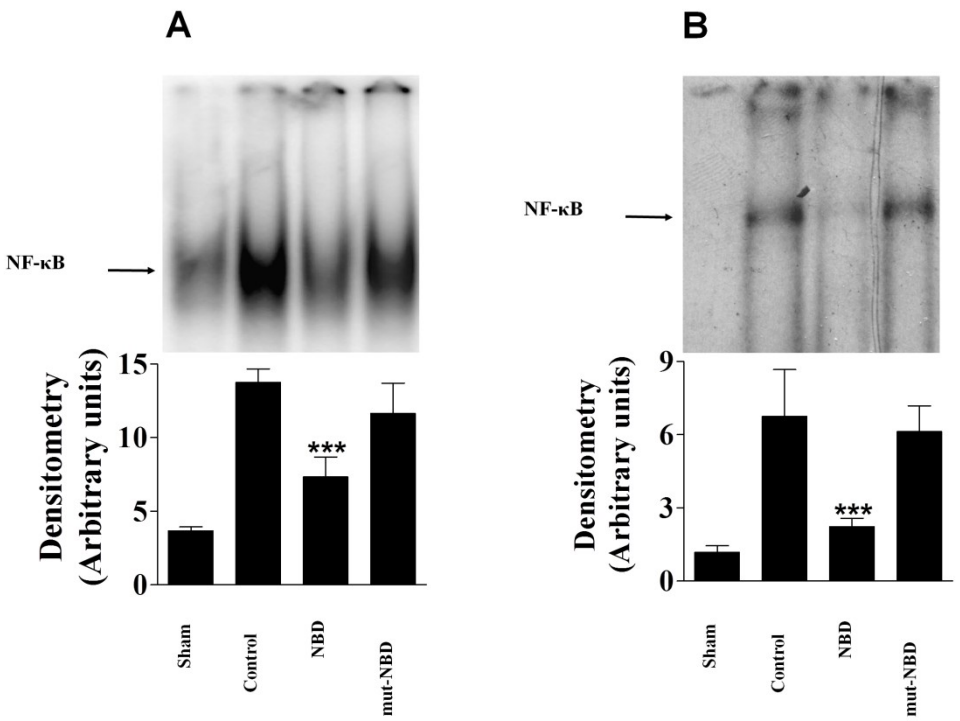

Figure 2.9

Representative EMSA and relative densitometric analysis showing the effect of the NBD peptide (300 µg/site; n=3) or the mut-NBD peptide (300 µg/site; n=3) on NF-κB activation in rat carotid arteries 3 (A) and 14 (B) days after angioplasty. Results are expressed as mean±SEM of 3 separate experiments. ****P*<0.001 *vs* control group.

2.2.8 Effect of the NBD peptide on MCP-1 production in rat carotid arteries

The NBD peptide was able to significantly inhibit MCP-1 protein production, evaluated by ELISA as described above, 7 and 14 days after injury. (Fig. 2.10).

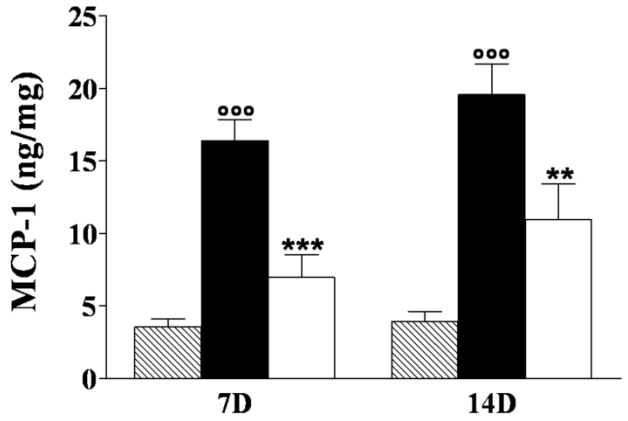

Figure 2.10

Effect of the NBD peptide (300 µg/site) on MCP-1 expression in rat carotid arteries 7 and 14 days after balloon injury evaluated by ELISA. Results are expressed as mean±SEM of MCP-1 levels normalized with protein concentrations, where n=3. ***P*<0.01 and ****P*<0.001 *vs* control group; °°°*P*<0.001 *vs* sham-operated animals. Sham (grey columns), Control (black columns), NBD (white columns).

2.2.9 Effect of the NBD peptide on neointimal formation in apoE$^{-/-}$ mice

Carotid endothelial denudation was performed in apoE$^{-/-}$ mice fed an atherogenic diet. Twenty-eight days after injury, the neointimal area was reduced by 46% (*P*<0.01) in apoE$^{-/-}$ mice treated with the NBD peptide compared with mut-NBD-treated mice (Fig. 2.11). The NBD peptide significantly increased the lumen area (*P*<0.01) and decreased the neointima/media ratio (*P*<0.05) (Table 2.2).

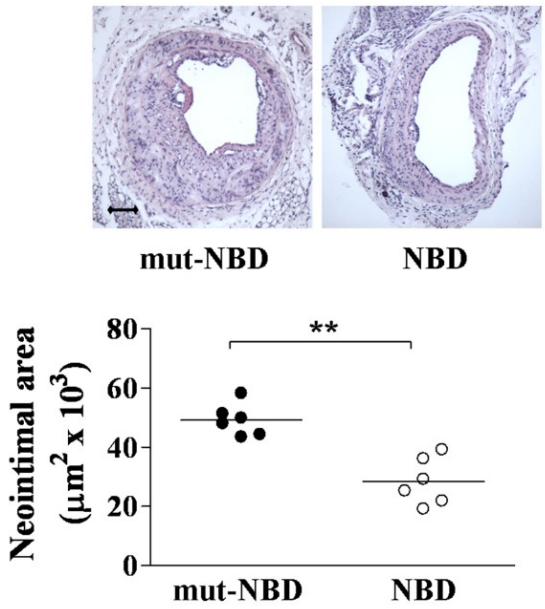

Figure 2.11

Effect of local administration of the NBD peptide (150 µg/site; n=6) on neointimal area in apoE$^{-/-}$ mouse carotid artery, 28 days after injury. ***P*<0.01 *vs* mut-NBD treated group (n=6). Scale bar=100 µm.

Table 2.2 Morphometric analysis of apoE$^{-/-}$ carotid arteries 28 days after injury

	NBD	Mut-NBD
Vessel area (µm^2 x 10^3)	137.25 ± 11.97	165.99 ± 8.92
Media area (µm^2 x 10^3)	32.84 ± 5.66	31.58 ± 3.19
Lumen area (µm^2 x 10^3)	55.25 ± 6.81	105.99 ± 9.40 **
Neointimal area (µm^2 x 10^3)	49.15 ± 2.19	28.42 ± 3.23 **
Neointima/Media ratio	1.88 ± 0.23	1.23 ± 0.15 *

The results are expressed as mean ± SEM (n=6). ***P*<0.01; **P*<0.05 *vs* mut-NBD treated group.

2.10 *In vivo* localization of the bio-NBD peptide

No positive staining was found in non injured arteries or pluronic gel-treated carotids 14 days after angioplasty. In contrast, the bio-NBD peptide was detectable in the adventitia and media of injured vessels 3 days following injury. The bio-NBD peptide was also detectable in the media and the neointima at days 7 and 14 (Fig. 2.12).

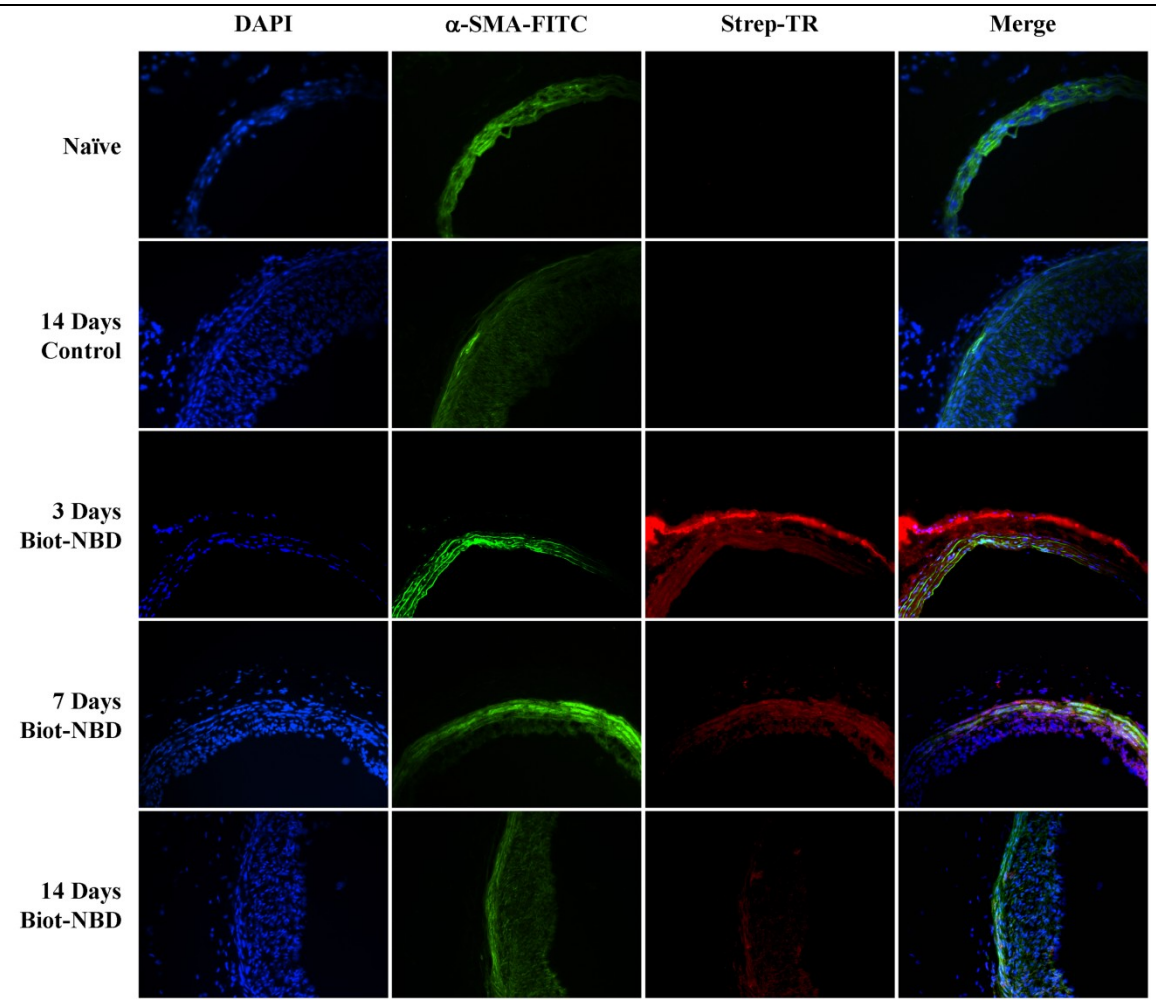

Figure 2.12

Immunofluorescence visualization of α-SMA (green) and bio-NBD peptide (red) in rat carotid arteries 3, 7, and 14 days after balloon angioplasty. Dapi (blue) was used to locate nuclei. In the control group was used the pluronic gel only.

2.3 Discussion

The results obtained in this study show that the local administration of the NBD peptide, a selective inhibitor of IKK activation, reduces neointimal formation in rodent models of vascular injury mainly by inhibiting SMC activation. Increased SMC proliferation and acquisition of a proinflammatory phenotype are central features associated with the development of neointimal lesions (Dzau et al., 2002). The NBD peptide showed both *in vivo* and *in vitro* antiproliferative activity. Treatment with the NBD peptide diminished the number of PCNA-positive proliferating cells in the rat vessel wall 7 days after balloon injury, concomitant with the beginning of neointimal formation. Furthermore, the NBD peptide inhibited *in vitro* TNF-α- and PDGF-BB-induced rat SMC proliferation and migration, effects associated with the inhibition of NF-κB activation. On the contrary, the NBD peptide showed no effect on FGF-2-induced SMC proliferation/migration. This discrepancy could be explained by the facts that FGF-2 induces IkB degradation and NF-κB activation through a pathway distinct from TNF-α (Hoshi et al., 2000) and that p38 and p42/p44 MAPKs are also involved in FGF-2-induced SMC activation (Skaletz-Rorowski et al., 2005). Interestingly, although the NBD peptide significantly reduced rat SMC invasion through the Matrigel barrier, it was able to inhibit only the latent form of MMP2 without significantly affecting the activated forms of both MMP2 and MMP9, which are known to be required for SMC proliferation and migration into the intimal area of vascular wall (Newby and Zaltsman, 2000; Bendeck et al., 1994). These results suggest that other proteases may cooperate with gelatinases in the TNF-α-induced cell invasion process. Activated NF-κB mediates the expression of several proinflammatory genes in SMCs, among which MCP-1 has been demonstrated to play a pivotal role in SMC proliferation/migration (Parenti et al., 2004) and neointimal formation in several animal models (Schober and Zernecke, 2007). Interestingly, treatment with the NBD peptide significantly inhibited MCP-1 production, both in vitro and *in vivo*. Moreover, the total inhibition of MCP-1 production and SMC proliferation observed at the highest concentration (1 μM) suggests that NF-κB triggers the autocrine/paracrine loop mechanism involved in the amplification of the inflammatory vascular response. Recent findings support the concept of NF-κB as a regional regulator of SMC survival rather than a direct promoter of proliferation of these cells (Mehrhof et al., 2005). In our experiments,

the highest concentration of the NBD peptide showed no effect on SMC apoptosis, either when used alone or when used with TNF-α. These results are in contrast with previous data obtained by Obara et al (Obara et al., 2000), showing increased apoptosis rate in TNF-α-stimulated SMCs overexpressing a truncated IkBα. Our results could be justified, at least in part, by the use of a selective inhibitor of the IKK complex formation. It is known that under physiological conditions, NF-κB is partially activated and involved in cell survival (Mehrhof et al., 2005). The NBD peptide inhibits only the inflammatory-induced NF-κB activation without modifying the amount constitutively activated (May et al., 2000; Baima et al., 2010). To confirm this point, we observed that the use of the NBD peptide, at higher concentrations, did not reduce the basal level of MCP-1 production compared with resting cells, most likely reflecting the fact that the NBD peptide does not affect basal NF-κB activity. In the last 10 years, NF-κB has been investigated as a novel therapeutic target to prevent restenosis. However, the potential for developing effective therapeutic strategies based on NF-κB blockade remains to be determined. Several studies have targeted NF-κB activation in the control of vascular injury (Ohtani et al., 2006) and a phase I/IIa open-label multicenter study to assess the inhibitory effects of an NF-κB ODN decoy on in-stent coronary restenosis (INDOR Study) has reported the clinical safety of such approach in humans (Egashira et al., 2008). In contrast to other therapeutic principles, the inhibition of the NF-κB system represents a broad-spectrum, multipurpose weapon that can interfere with several fundamntal pathophysiological mechanisms in the development of neointimal formation, targeting both proliferation and inflammation. In our study, the use of a peptide that selectively inhibits the IKK complex represents a novel and interesting approach. Compared with other NF-κB inhibitors tested to inhibit neointimal formation, the NBD peptide has the advantage of inhibiting the induction of NF-κB activation without inhibiting basal NF-κB activity that may be involved in fundamental cellular processes (May et al., 2000; Baima et al., 2010). Notably, the continuous administration of the peptide for >45 days did not lead to overt toxicity in mice (Jimi et al., 2004). Importantly, the Pluronic F-127 gel has been shown to be absorbed *in vivo* at 3 days. Such a short-term local administration of traditional NF-κB inhibitors (eg, pyrrolidine dithiocarbamate) has been shown to inhibit NF-κB activation in the injured vessels at day 3, without

affecting intimal formation at day 14. (Bu et al., 2005) Intriguingly, using the same delivery approach, we have clearly shown the presence of the biotinylated peptide in the rat media and neointima up to 14 days after injury. Importantly, the NBD peptide efficacy was also confirmed in the hyperlipidemic mouse model, demonstrating the efficacy of the peptide under circumstances of increased vascular inflammation (Maffia et al. 2007). Neither rodent model is a reliable experimental model of human angioplasty, and as such, the present study has some limitations. It would be desirable to explore the efficacy and therapeutic potential of the NBD peptide in larger preclinical animal models. However, our results demonstrate the involvement of NF-κB as a regulator in the formation of neointima in mouse and rat vascular injury models and support the use of specific IKK inhibitors to reduce neointimal hyperplasia.

3. THE ANTI-INFLAMMATORY AGENT BINDARIT INHIBITS NEOINTIMAL FORMATION IN BOTH RATS AND HYPERLIPIDAEMIC MICE

Bindarit is an original indazolic derivative able to inhibit MCP-1/CCL2, MCP-2/CCL8 and MCP-3/CCL7 synthesis (Mirolo et al., 2008) (Fig. 3.1). Although it shows neither immunosuppressive effects nor activity on arachidonic acid metabolism, it has a potent anti-inflammatory activity in a number of experimental models including nephritis, arthritis, pancreatitis and colitis (Zoja et al., 1998; Guglielmotti et al., 2002; Bhatia et al., 2005; Bhatia et al., 2008) as well as in reducing myocardial and renal dysfunction in swine renovascular hypertension (Lin et al., 2009; Zhu et al., 2009). Phase II clinical trials have shown that bindarit is well tolerated and significantly reduced urinary MCP-1 and albumin excretion in kidney disease (Perico et al.,2008; Guglielmotti et al.,2009).

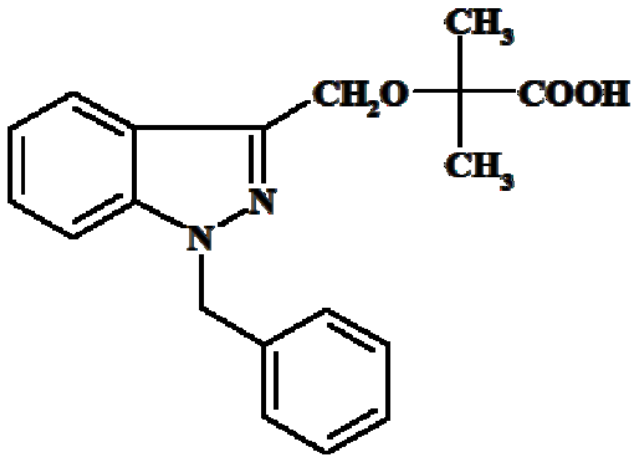

Figure 3.1

2-Methyl-2-[[1-(phenylmethyl)-1H-indazol-3yl]methoxy]propanoic acid (bindarit)

As described above, chemokines have been implicated in the response of the arterial wall to injury. Among pro-inflammatory CC chemokines, MCP-1 is one of the most interesting in this sence. Elevated circulating levels of MCP-1 were observed

in patients with restenosis after coronary angioplasty (Cipollone et al., 2001). Moreover blocking MCP-1 pathway decreases neointimal hyperplasia in preclinical models of vascular injury (Furukawa et al., 1999; Egashira et al.,2007; Nakano et al.,2007). These data suggest that an anti-inflammatory treatment based on the inhibition of MCP-1 may be an appropriate and reasonable approach for the prevention of neointimal formation.

Here, we investigated the effect of bindarit on neointimal formation *in vivo* using the carotid artery balloon angioplasty model in rats and the wire-induced carotid injury model in apoE$^{-/-}$ mice. In addition, the effects of bindarit on SMC proliferation and migration *in vitro* were also examined.

3.1 Methods

3.1.1 Treatments

Bindarit, 2-methyl-2-[[1-(phenylmethyl)-1H-indazol-3-yl]methoxy] propanoic acid (MW 324.38), was synthesized by Angelini (Angelini Research Center—ACRAF, Italy). Pharmacokinetic studies in rodents show that bindarit is well absorbed when administered by oral route, and it has a mean half-life of ~9 h and, at dose regimen used in this study, reaches plasma levels in the range of 150–450 μM (Product data sheet, Angelini Research Center). Animals were treated with bindarit, suspended in 0.5% methylcellulose aqueous solution, at the dose of 100 mg/kg given orally, by gastric gavage, twice a day (Bhatia et al., 2008). Rats were treated with bindarit from 2 days before angioplasty up to 14 days after, whereas apoE$^{-/-}$ mice were treated from 1 week before endothelial denudation up to 28 days after. In each experiment, control animals received an equal volume of methylcellulose (0.5 mL/100 g in rats; 0.1 mL/10 g in mice). The concentrations of bindarit used for *in vitro* experiments have been found previously to be effective at inhibiting MCP-1 synthesis in human monocytes and umbilical vein endothelial cells (Mirolo et al., 2008).

3.1.2 Cell culture

Primary aortic SMCs isolated from aorta of rats or apoE$^{-/-}$ mice were used as described above (chapter 2, section 2.1.1)

3.1.3 Enzyme-linked immunosorbent assay (ELISA) for MCP-1 protein

Cells were used after the induction of quiescence in 24-well plastic culture plates at a density of 1.5 × 10^4 cells/well. The cells were stimulated with platelet derived growth factor-BB (PDGF-BB; 10 ng/mL; R&D Systems) in the presence or absence of bindarit (10–300 μM). After 6, 12, 24, and 48 h, media were collected, centrifuged at 2000 *g* for 15 min at 4°C, and supernatants were used for enzyme-linked immunosorbent assay (ELISA) (OptEIA™, Biosciences).

3.1.4 Proliferation assay

The cell proliferation assay was carried out using the MTT assay. SMCs were plated on 24-well plastic culture plates at the density of 1.5 × 10^4 cells/well and then incubated with DMEM containing PDGF-BB (10 ng/mL) for 48 h in the presence or absence of bindarit (10–300 μM). The absorbance values were obtained with an ELISA assay reader (630 nm).

3.1.5 Chemotactic migration and invasion

SMC migration was evaluated using a modified Boyden chamber (Corning 24 mm Transwell with 8.0 μm pore polycarbonate membrane insert) coated with rat-tail collagen I (Sigma-Aldrich). Biocoat Matrigel invasion chambers (with 8.0 μm pore) were used according to the manufacturer's instructions for invasion studies (Becton–Dickinson). Briefly, starved SMCs were trypsinized and pre-treated or not with bindarit (10–300 μM) for 2 h. 5 × 10^5 cells were plated in the upper chamber in 150 μL of 1% FBS medium with or without bindarit (10–300 μM) and the lower chamber was filled with 600 μL of 1% FBS medium in the absence (untreated cells) or presence of PDGF-BB 10 ng/mL. After 6 h for migration assay or 48 h for invasion assay, the migrated cells were fixed and stained with haematoxylin. The number of migrated cells was counted in eight randomly chosen fields per insert.

3.1.6 Animals

The investigation conforms to the Guide for the Care and Use of Laboratory Animals published by the US National Institutes of Health (NIH Publication No. 85-23, revised 1996), and Italian ministerial authorization (DL 116/92) was obtained to carry out the experimentation. Male Wistar rats (Harlan Laboratories) weighing 250 g and 8-week-old female apoE$^{-/-}$ mice (Charles River) were used for the present study. Animals were housed at the Department of Experimental Pharmacology, University of Naples Federico II.

3.1.7 Rat carotid balloon angioplasty

Balloon-induced carotid injury in rats was performed as described above (chapter 2, section 2.1.11). Blood and carotid arteries were collected and processed as described below.

3.1.8 Atherogenic murine model of vascular injury

Wire-induced carotid injury in apoE$^{-/-}$ mice was performed as described above (chapter 2, section 2.1.12). Blood and carotid arteries were collected 7 and 28 days after wire injury and processed as described below.

3.1.9 Evaluation of neointimal formation

Carotid arteries from rats or apoE$^{-/-}$ mice were fixed by perfusion with phosphate-buffered saline (PBS; pH 7.2) followed by PBS containing 4% formaldehyde through a cannula placed in the left ventricle. Paraffin-embedded sections were cut (6 μm thick) from the approximate middle portion of the artery and stained with haematoxylin and eosin to demarcate cell types. Ten sections from each carotid artery were reviewed and scored under blind conditions. The cross-sectional areas of media and neointima were determined by a computerized analysis system (LAS, Leica).

3.1.10 Proliferating cell nuclear antigen analysis in injured rat carotid arteries

Proliferating cell nuclear antigen (PCNA) analysis was used to quantify the proliferative activity of cells at the injury sites and was performed using monoclonal

mouse anti-PCNA Ab (1:250, PC10, Sigma) and biotinylated anti-mouse secondary Ab (1:400, DakoCytomation). Slides were treated with streptavidin–HRP (DakoCytomation) and exposed to diaminobenzidine chromogen (DakoCytomation) with haematoxylin counterstain. The proliferating cell number in the rat carotid arteries was scored in 10 fields for each section, six sections from each carotid artery, and expressed as the percentage of total medial and neointimal cells positive for PCNA 7 days after angioplasty. The proliferating cell number in the mouse apoE$^{-/-}$ carotid arteries was scored in 10 sections from each carotid artery and expressed as the percentage of positive cells 7 days after wire injury.

3.1.11 MCP-1 immunohistochemistry

Rat carotid arteries (1, 7, and 14 days after angioplasty, or naive) were snap-frozen in liquid nitrogen in OCT embedding medium (Tissue Tek, Sakura Finetek). Ten cross-sections were cut (6 μm) from the approximate middle portion of the artery and used for MCP-1 detection. Sections were incubated with polyclonal goat anti-MCP-1 Ab (1:50, R-17, Santa Cruz) diluted in blocking buffer/0.3% Triton X-100 (MP Biomedicals) in PBS overnight before being washed in TNT wash buffer (Tris–HCl, pH 7.5, 0.15 M NaCl, and 0.05% Tween 20; Sigma). Sections incubated with goat non-immune serum were used as negative controls. Subsequently, sections were incubated with biotinylated anti-goat secondary Ab (1:400, DakoCytomation) diluted in blocking buffer/0.3% Triton X-100, washed in TNT wash buffer, treated with streptavidin–HRP, and exposed to diaminobenzidine chromogen with haematoxylin counterstain. The sections were photographed and the images were stored in the image analysis system (LAS, Leica).

3.1.12 Enzyme-linked immunosorbent assay (ELISA)

Rat carotid arteries were crushed into powder and resuspended in 100 μL of lysis buffer (20 mM HEPES, 0.4 mM NaCl, 1.5 mM $MgCl_2$, 1 mM EGTA, 1 mM EDTA, 1% Triton X-100, and 20% glycerol) with protease inhibitors (1 mM DTT, 0.5 mM PMSF, 15 μg/mL Try-inhibitor, 3 μg/mL pepstatin-A, 2 μg/mL leupeptin, and 40 μM benzamidine). After centrifugation at 13 000 ***g*** at 4°C for 30 min, MCP-1 in the supernatant was quantified using an ELISA kit (OptEIA™, Biosciences). All measurements were performed in duplicate. The values were corrected by protein

concentrations measured by the Bio-Rad protein assay kit (Bio-Rad). Serum MCP-1 levels (1, 7, and 14 days after angioplasty) were also measured in the same animals used above by ELISA (OptEIA™, Biosciences). The results are expressed as nanograms per millilitre.

3.1.13 Western blot analysis

The levels of CD68 were evaluated in total extracts prepared from two pooled rat carotid arteries. The extraction procedure was performed as described above. Protein concentration was determined by the Bio-Rad protein assay kit (Bio-Rad). Equivalent amounts of protein (50 µg) from each sample were electrophoresed in an 8% discontinuous polyacrylamide minigel. The proteins were transferred onto nitrocellulose membranes according to the manufacturer's instructions (Bio-Rad). The membranes were saturated by incubation with 10% non-fat dry milk in PBS/0.1% Triton X-100 for 3 h at room temperature and then incubated with anti-CD68 mouse Ab (1:1000; Serotec) or anti-β-actin (1:5000; Sigma) mouse Ab overnight at 4°C. The membranes were washed three times with 0.1% Tween 20 in PBS and then incubated with anti-mouse immunoglobulins coupled to peroxidase (1:1000; DakoCytomation) for 1 h at room temperature. The immune complexes were visualized by enhanced chemiluminescence (Amersham). Subsequently, the relative intensities of the bands were quantified by densitometric scanning of the X-ray films with a GS-800 Imaging Densitometer (Bio-Rad) and the computer program ‘Quantity One’ (Bio-Rad). Results are expressed as arbitrary units of CD68 protein levels, normalized to protein levels of the housekeeping protein β-actin.

3.1.14 Evaluation of re-endothelialisation in injured rat carotid arteries

Re-endothelialisation was assessed 2 weeks after balloon injury by staining with Evans Blue dye (0.5 mL of 0.5% Evans Blue dye iv; Sigma) as described previously (Asahara et al., 1996). Planimetric analysis with an image analysis program (LAS, Leica) was performed. Re-endothelialisation was expressed as the percentage of re-endothelialised area *vs* the total denuded area. To verify that the Evans Blue stain accurately depicted the presence or absence of endothelium, sections of completely or partially re-endothelialised carotid arteries (based on

Evans Blue appearance) were stained with Ab to von Willebrand factor (vWF, Cytomation Dako) as described previously (Yue et al., 2000).

3.1.15 Immunohistochemisty analysis in injured apoE$^{-/-}$ mouse carotid arteries

Carotid arteries were snap-frozen in liquid nitrogen in OCT embedding medium. Fifteen cross-sections were cut (6 µm) from the approximate middle portion of the artery and used for MCP-1, α-smooth muscle actin (α-SMA), and macrophage detection by immunofluorescence. For staining, the sections were processed as described above and incubated with polyclonal goat anti-mouse MCP-1 Ab (1:50, M-18, Santa Cruz) or rat anti-F4/80 monoclonal Ab (1:50, clone BM8, Abcam) diluted in blocking buffer/0.3% Triton X-100 (MP Biomedicals) in PBS overnight before being washed in TNT wash buffer. Sections incubated with non-immune goat serum or an isotype-matched control Ab were used as negative controls. Subsequently, the sections were incubated with 1:75 Texas Red-donkey anti-goat IgG (Jackson ImmunoResearch Laboratories) or with 1:200 biotinylated anti-rat secondary Ab (DakoCytomation), amplified with Tyramide Signal Amplification Systems (PerkinElmer), and revealed with streptavidin–FITC (1:50, DakoCytomation). Monoclonal anti-α-SMA FITC (1:250, clone 1A4, Sigma) was added in blocking buffer for 1 h before washing as described above. DAPI was used to identify nuclei. Images were taken using an AxioCam HRc video-camera (Zeiss) connected to an Axioplan fluorescence microscope (Zeiss) using the AxioVision 3.1 software. The neointimal areas stained for F4/80 were determined in digitized images (five sections per mouse), and positive areas for specific immunostaining were quantified (NIH Imaging; http://rsb.info.nih.gov/ij). Data are expressed as the percentage of the immunostained area per total neointimal area. Serial carotid paraffin-embedded sections were cut (5 µm) and used for detection of calponin (1:100, clone hCP, Sigma). Ten sections from each carotid artery were reviewed and scored under blind conditions. The number of calponin-positive cells in neointima was counted.

3.1.16 Evaluation of MCP-1, total cholesterol, and triglyceride serum levels in apoE$^{-/-}$ mice

The concentrations of serum MCP-1, triglycerides, and cholesterol were determined using enzymatic immunoassays according to the manufacturer's instructions (OptEIA™, Biosciences; Serum Triglyceride Kit, Sigma; Cholesterol Assay Kit, Cayman Chemical).

3.1.17 Statistical analysis

Results are expressed as mean±SEM of n animals for *in vivo* experiments and mean±SEM of multiple experiments for *in vitro* assays. Student's *t*-test was used to compare two groups and ANOVA (two-tailed *P*-value) was used with the Dunnett *post hoc* test for multiple groups using Graph Pad Instat 3 software (San Diego). The level of statistical significance was 0.05 per test.

3.2 Results

3.2.1 Effect of bindarit on rat SMC proliferation and migration

As shown in Figure 3.2A, bindarit at 100 and 300 μM significantly inhibited PDGF-BB-induced rat SMC proliferation by 27% ($P<0.05$, n=3) and 42% ($P<0.01$, n=3), respectively. Another key mechanism of neointimal formation is mitogen-mediated migration of SMCs. Therefore, we evaluated the effects of bindarit on PDGF-BB-induced rat SMC chemotaxis. Bindarit inhibited significantly ($P<0.01$, n=3) chemotactic migration at 100 and 300 μM by 45 and 50%, respectively (Fig. 3.2B). Moreover, bindarit (100 μM) also significantly reduced rat SMC invasion (by 30%, $P<0.01$, n=3, Fig. 3.2C) through the Matrigel barrier which mimics extracellular matrix.

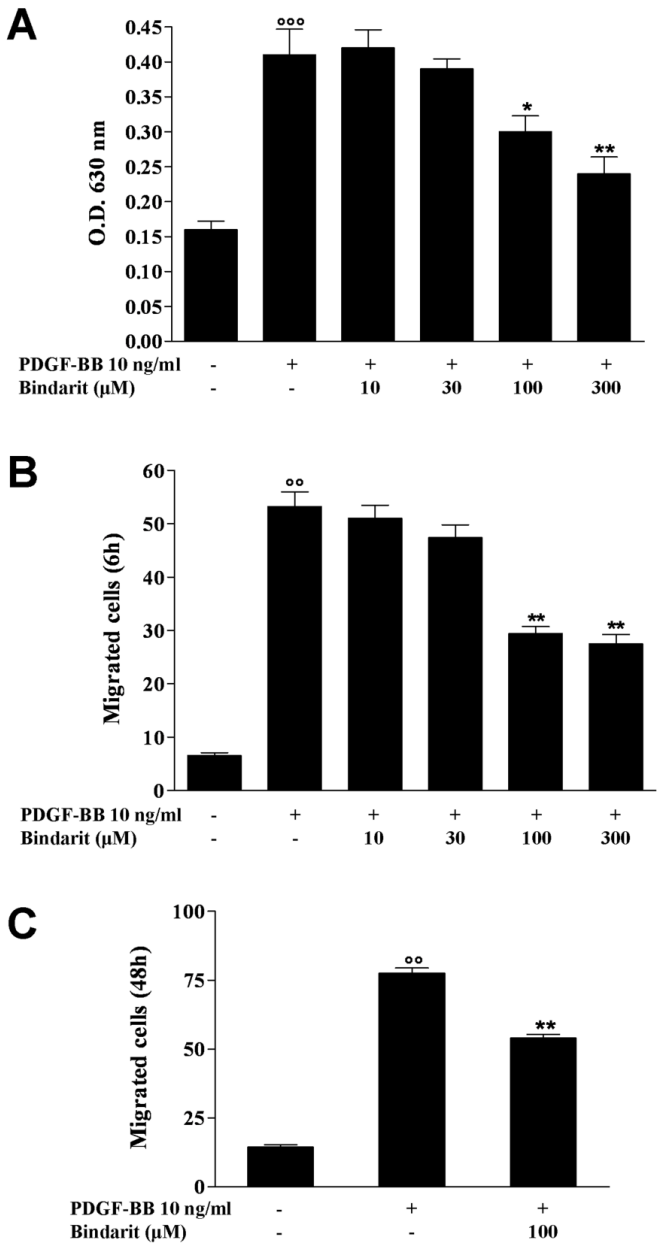

Figure 3.2

(A) Effect of bindarit (10–300 µM) on rat SMC proliferation, (*B*) migration, and (*C*) invasion performed as described in Section 2. Results are expressed as mean±SEM from three separate experiments. **P*<0.05, ***P*<0.01 *vs* platelet derived growth factor-BB (PDGF-BB); °°*P*<0.01, °°°*P*<0.001 *vs* unstimulated cells.

3.2.2 Effect of bindarit on MCP-1 production

To determine whether the anti-proliferative and anti-migratory effects of bindarit were associated with MCP-1 inhibition, protein concentration of MCP-1 in the supernatant of cultured rat SMCs was determined by ELISA. As shown in Table

3.1, stimulation of SMCs with PDGF-BB (10 ng/mL) caused a time-dependent increased release of MCP-1 compared with that observed in unstimulated cells. When rat SMCs were stimulated with PDGF-BB in the presence of bindarit (10–300 μM), a concentration-related inhibition of MCP-1 production was observed.

Table 3.1 Effect of bindarit on MCP-1 production by PDGF-BB-stimulated SMCs

	MCP-1 (ng/mL)			
	6h	12h	24h	48h
Unstimulated cells	0.32±0.02	3.2±0.21	18.5±0.9	34.1±1.4
PDGF-BB 10 ng/mL	3.1±0.1°°	20.8±1.58°°	59.6±0.4°°	142.6±2.8°°
PDGF-BB 10 ng/mL + bindarit 10 μM	3.0±0.2	18.3±1.2	50.9±1.2**	128.0±3.7**
PDGF-BB 10 ng/mL + bindarit 30 μM	1.5±0.1**	13.7±0.5**	42.8±0.6**	87.3±1.7**
PDGF-BB 10 ng/mL + bindarit 100 μM	1.3±0.2**	11.9±0.4**	34.0±1.0**	80.1±1.8**
PDGF-BB 10 ng/mL + bindarit 300 μM	0.8±0.1**	4.8±0.5**	29.3±1.1**	72.1±1.3**

Results are expressed as mean±SEM of three separate experiments run in triplicate.
°° $P<0.01$ *vs* unstimulated cells; ** $P<0.01$ *vs* PDGF-BB

3.2.3 Effect of bindarit on neointimal formation in rat carotid arteries

To determine the efficacy of a systemic treatment with bindarit for the limitation of neointimal hyperplasia, a rat carotid arterial injury model was used. A remarkable increase in the number of PCNA-positive cells was demonstrated in both the media and neointima 7 days after injury in control rats, which was significantly reduced ($P<0.001$, n=9) in the bindarit-treated group (200 mg/kg/day) by 54 and 30%, respectively (Fig. 3.3A). Bindarit caused a significant inhibition of neointimal formation by 39% ($P<0.01$, n=19) at day 14 compared with the control animals (Fig. 3.3B). Medial area (0.124±0.003 mm^2 in the sham group) was not affected by both vascular injury and bindarit.

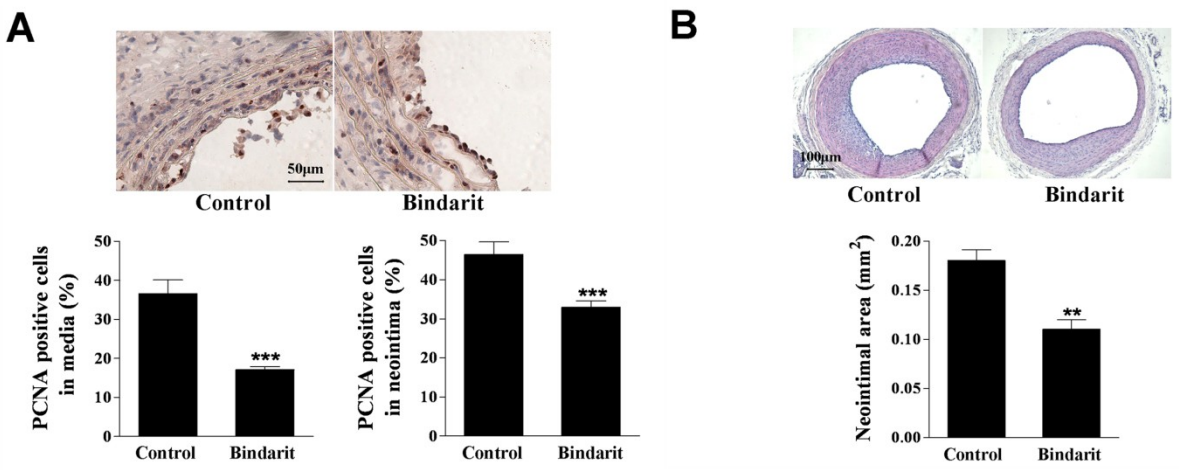

Figure 3.3

(A) Photomicrographs showing the effect of bindarit (200 mg/kg/day) on PCNA-positive cells in rat carotid arteries at day 7 after injury (magnification x 400). Results are expressed as mean+SEM of the percentage of total medial and neointimal cells positive for PCNA as described in Section 2, where n=9 rats for each group. ****P*<0.001 *vs* control group. (B) Photomicrographs showing the effect of bindarit (200 mg/kg/day) on neointimal formation in rat carotid arteries 14 days after balloon injury (magnification x 100). Results are expressed as mean+SEM, where n=15–19 rats. ***P*<0.01 *vs* control group.

3.2.4 Effect of bindarit on monocytes/macrophages infiltration in rat carotid arteries

Western blot analysis was performed to examine the effect of bindarit on the carotid monocyte/macrophage content. Monocyte/macrophage marker CD68 was highly expressed in carotid arteries 14 days after angioplasty when compared with that of sham-operated animals (Fig. 3.4). Bindarit significantly reduced CD68 levels as shown by relative densitometric analysis.

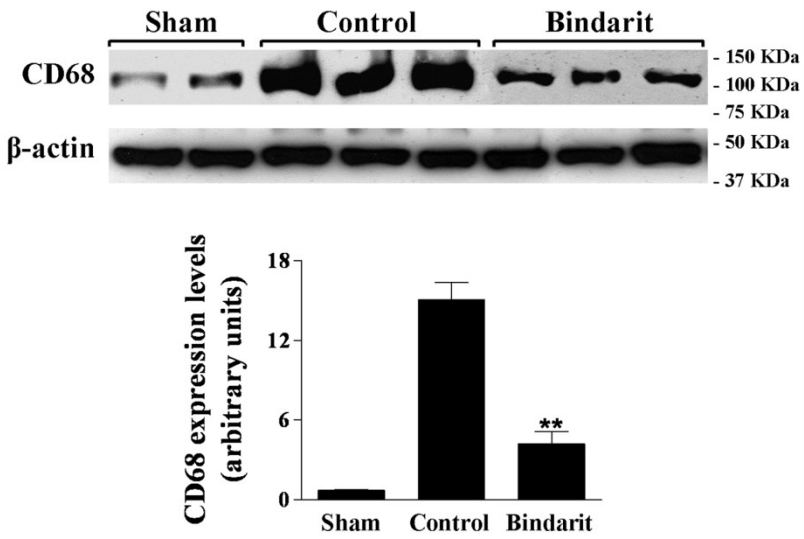

Figure 3.4

Effect of bindarit (200 mg/kg/day) on monocyte/macrophage marker CD68 protein expression in carotid arteries 14 days after angioplasty. Equal loading was confirmed by b-acting staining. Results are expressed as mean+SEM of three separate experiments. ***P*<0.01 *vs* control group.

3.2.5 Effect of bindarit on MCP-1 production in rat carotid arteries

We observed a significant time-dependent increase in MCP-1 production in the injured arteries at 1, 7, and 14 days after angioplasty when compared with that of sham-operated animals (Fig. 3.5). Bindarit was able to inhibit the MCP-1 protein expression throughout the time course considered, by 31% (*P*<0.05; n=5), 38% (*P*<0.05; n=5), and 49% (*P*<0.001; n=5) at 1, 7, and 14 days after injury, respectively. In carotid arteries from naive animals, the levels of MCP-1 measured were 0.74±0.34 ng/mg (n=5).

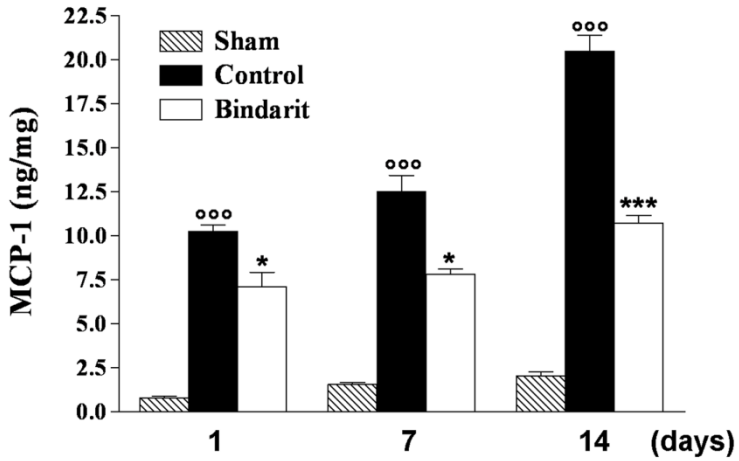

Figure 3.5

Effect of bindarit (200 mg/kg/day) on MCP-1 expression in rat carotid arteries 1, 7, and 14 days after balloon injury evaluated by ELISA. Results are expressed as mean+SEM of MCP-1 levels normalized with protein concentrations, where n=5. **P*<0.05; ****P*<0.001 *vs* control group; °°°*P*<0.001 *vs* sham-operated animals.

3.2.6 Effect of bindarit on MCP-1 localization in rat carotid arteries

Non-injured carotid arteries lacked immunoreactivity for MCP-1, whereas injured arteries stained strongly for MCP-1 (Fig. 3.6). Negative controls showed no signal. MCP-1-positive staining was detectable in media of injured vessel from days 1 up to 14 and in neointimal cells at days 7 and 14. MCP-1 localization was not modified by bindarit, whereas the drug treatment resulted in a lower MCP-1 expression in both media and neointima (Fig. 3.6).

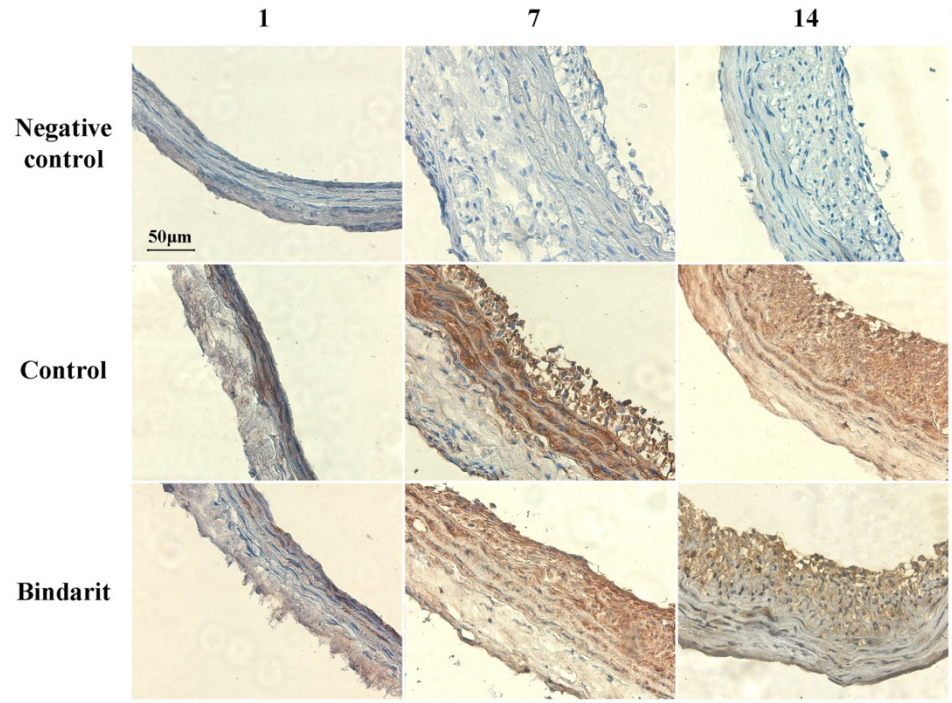

Figure 3.6

Immohistochemical localization of MCP-1 expression in rat carotid arteries 1, 7, and 14 days after angioplasty.

3.2.7 Effect of bindarit on re-endothelialisation in rat carotid arteries

Evans Blue staining identifies segments of injured carotid arteries that have not been re-endothelialised. As shown in Figure 3.7, the presence of intact endothelium in the carotid artery of naive rats was demonstrated by the absence of Evans Blue staining. Immunohistochemical staining with Ab to vWF verified the presence of endothelium. In contrast, the entire area of the artery harvested 1 day after injury was stained by Evans Blue. The absence of positive staining with Ab to vWF confirmed the observation. Analysis of samples at 2 weeks from angioplasty showed that bindarit treatment did not affect re-endothelialisation of arteries when compared with control animals.

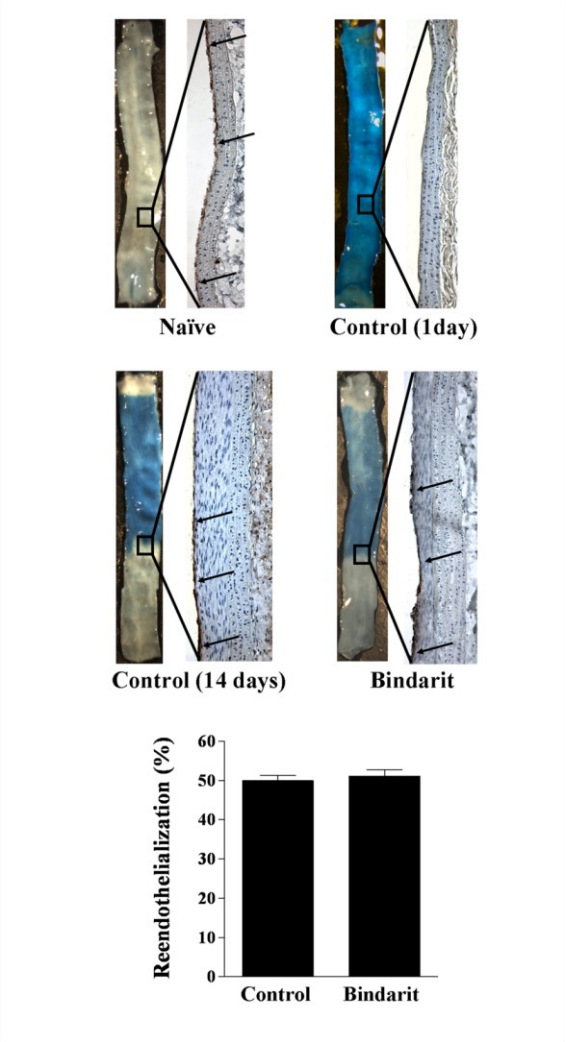

Figure 3.7

Extent of re-endothelialisation in injured carotid arteries evaluated by Evans Blue staining. Representative arteries harvested from naïve animals, as well as 1 and 14 days after carotid injury in vehicle- or bindarit treated rats. Evans Blue staining identifies segments of each artery that have not been recovered by endothelium. Immunohistochemical staining with Ab to vWF verified the presence of endothelium. Re-endothelialisation was expressed as the percentage of re-endothelialised area *vs* the total denuded area (bottom panel) (n=5).

3.2.8 Effect of bindarit on MCP-1 serum levels

A time-dependent increase in MCP-1 serum concentration was observed in rats subjected to angioplasty (Table *3.2*). Bindarit caused a significant inhibition of MCP-1 serum levels at day 1 by 20% ($P<0.05$, n=10) and at days 7 and 14 by 30% ($P<0.001$, n=10) compared with their respective control groups. In naive animals, the MCP-1 serum level was 29.4±3.0 ng/mL (n=5).

Table 3.2 Effect of bindarit on MCP-1 serum levels in rats

Group	MCP-1 (ng/mL)		
	1-day	7-day	14-day
sham-operated	37.1±2.4	35.4±1.2	32.8±2.7
Control	69.2±3.5°°	51.4±2.2°°	53.7±3.9°°
bindarit (200 mg/kg/day)	55.6±3.0*	36.2±2.4***	37.2±2.1***

Results are expressed as mean±SEM where n=5-10 rats per each time point considered.
°°P<0.01 *vs* sham-operated animals; * P<0.05; *** P<0.001 *vs* control group.

3.2.9 Effect of bindarit on neointimal formation in apoE$^{-/-}$ mice

To evaluate the effect of bindarit after arterial injury in hyperlipidaemic animals, carotid endothelial denudation was performed in apoE$^{-/-}$ mice fed an atherogenic diet. Seven days after injury, the number of PCNA-positive cells was significantly reduced (42%; P<0.05, n=10) by treatment with bindarit (200 mg/kg/day) compared with control mice (Fig. 3.8A). Neointimal area was reduced by 47% in apoE$^{-/-}$ mice treated with bindarit compared with control mice 28 days after injury (Fig. 3.8B). Moreover, the apoE$^{-/-}$mice receiving bindarit showed a 66% reduction in the relative content of F4/80-positive macrophages and a 30% reduction in the number of SMCs in neointimal lesion (Fig. 3.8 C and D).

Injured carotid arteries stained strongly for MCP-1 detectable in media and neointima 28 days after injury. Co-localization of MCP-1 and α-actin was evident in both media and neointima. MCP-1 localization was not modified by bindarit, but again the drug reduced both medial and neointimal MCP-1 expression (Fig. 3.9).

Total cholesterol levels did not differ between groups (1036±38 mg/dL in bindarit-treated group, n=10 *vs* 1167±50 mg/dL in control group, n=10), whereas triglyceride levels were significantly lower (P<0.05) in bindarit-treated animals (191.6±21.3 mg/dL, n=10) than in the control group (260.7±20.6 mg/dL, n=10). Moreover, bindarit caused a significant inhibition (P<0.01) of MCP-1 serum levels by 42% (131.0±15.6 pg/mL in bindarit-treated group, n=10 *vs* 224.8±28.3 pg/mL in control group, n=10; P<0.01).

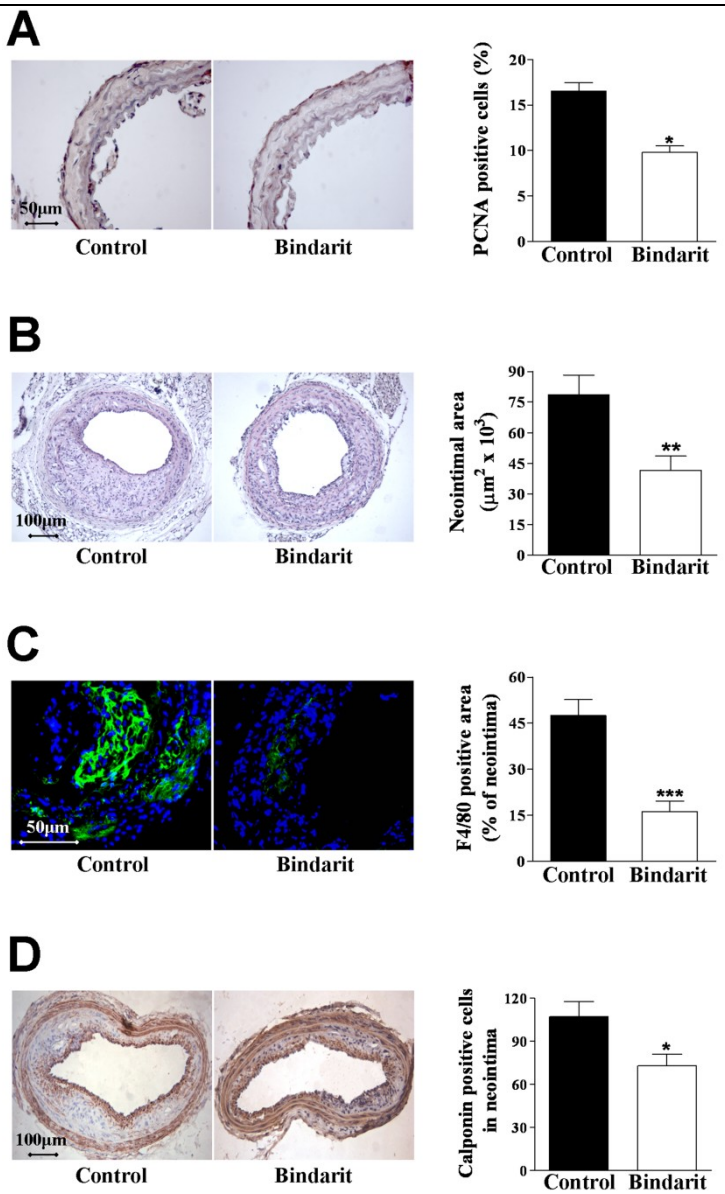

Figure 3.8

(A) Photomicrographs showing the effect of bindarit (200 mg/kg/day) on PCNA-positive cells in apoE$^{-/-}$ mice 7 days after injury (magnification x400). Results are expressed as mean+SEM of the percentage of total PCNA-positive cells as described in Section 2, where n=10 rats for each group. **P*<0.05 *vs* control group. (B) Photomicrographs showing the effect of bindarit (200 mg/kg/day) on neointimal formation in apoE$^{-/-}$ mice 28 days after carotid injury (magnification x100). Results are expressed as mean+SEM, where n=10 for each group; ***P*<0.01 *vs* control group. (C) Photomicrographs showing the effect of bindarit (200 mg/kg/day) on macrophage content in carotid arteries 28 days after injury (magnification x400). Results are expressed as mean+SEM of the percentage of F4/80 immunostained area per total neointimal area, where n=10 for each group; ****P*<0.001 *vs* control group. (D) Photomicrographs showing the effect of bindarit (200 mg/kg/day) on neointimal SMC content in carotid arteries 28 days after injury (magnification x 100). Results are expressed as mean+SEM of the calponin-immunostained cell number, where n=10 for each group; **P*<0.05 *vs* control group.

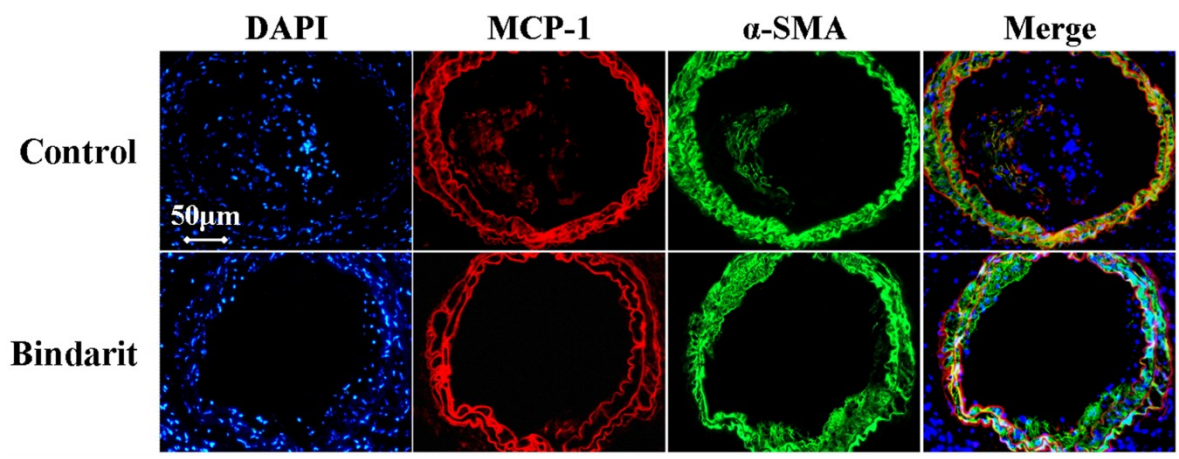

Figure 3.9

Immunofluorescence visualization of α-SMA (green) and MCP-1 (red) in mouse carotid arteries 28 days after injury. DAPI (blue) was used to locate nuclei. Co-localization of MCP-1 and α-actin (yellow) was evident in some cells in both media and neointima (magnification x 200).

3.3 Discussion

The results provided in this study show that bindarit given systemically significantly reduced neointimal formation in animal models of arterial injury by inhibiting SMC proliferation/migration, and macrophage infiltration; these effects correlated with a reduction in MCP-1 synthesis. Bindarit is an original compound selected by screening a series of indazolic derivatives endowed with peculiar antiinflammatory activity associated with a selective inhibition of a subfamily of CC inflammatory chemokines, including MCP-1/CCL2, MCP-3/CCL7, and MCP-2/CCL8, showing no effect on other CC and CXC chemokines such as MIP-1a/CCL3, MIP-1b/CCL4, MIP-3/CCL23, RANTES/CCL5, and IL8/CXCL8 (Zoja et al., 1998; Guglielmotti et al., 2002; Bhatia et al., 2005; Bhatia et al., 2008; Mirolo et al., 2008). After vascular damage, the rat carotid artery develops neointimal formation, mainly due to proliferation and migration of SMCs, that causes a clear narrowing of the vessel lumen. Neointimal formation contributes to the development of restenosis after coronary artery angioplasty, with or without stenting, in which a pivotal mechanism is represented by the loss of differentiation of SMCs that were able to proliferate and migrate (Owens et al., 2004). It is well known that among pro-inflammatory CC chemokines, MCP-1 is implicated in all these processes and the

source of this chemokine is likely to include the major cells in injured arteries, such as endothelial cells, SMCs, and macrophages (Charo and Taubman, 2004). In injured carotid arteries from animals treated with bindarit, a significant inhibition of neointimal formation associated with a reduced MCP-1 production was observed. Bindarit did not modify MCP-1 localization but reduced MCP-1 expression in both media and neointima. Moreover, bindarit caused a significant inhibition of MCP-1 serum levels. Increased levels of circulating MCP-1 in animals subjected to vascular injury are in keeping with an active role for this chemokine in tissue pathogenesis and correlate with epidemiological evidence showing higher MCP-1 plasma levels associated with human restenosis (Cipollone et al., 2001; Martinovic et al., 2005). Bindarit showed both *in vivo* and *in vitro* antiproliferative effects. For example, bindarit diminished the number of PCNA-positive proliferating cells in the media and intima 7 days after angioplasty, concomitantly with the beginning of neointimal formation, without affecting re-endothelialisation evaluated 14 days after injury. *In vitro* studies further demonstrated inhibitory effects of bindarit on PDGF-BB-stimulated rat SMC proliferation and migration. These effects were associated with a significant and concentration-related inhibition of MCP-1 amounts measured in the supernatants of stimulated cells treated with bindarit. It is well known that MCP-1 activity is in part due to recruitment of monocytes/macrophages that are responsible for local production of cytokines, but MCP-1 may also directly induce SMC proliferation and migration through cell cycle proteins and intracellular proliferative signals (Selzmam et al., 2002; Parenti et al., 2004). Our results also showed that bindarit reduced monocytes/ macrophages recruitment in injured rat carotid arteries. The rat balloon angioplasty model could be considered ideal to study the proliferation of SMCs *in vivo*; however, it is not an ideal model for the study of monocytes/macrophages recruitment, considering the injury is performed in a non-atherosclerotic arterial bed. (Reidy et al., 1992; Roque et al., 2000). It is well known that hypercholesterolaemia, a potent trigger of vessel wall inflammation in atherosclerosis, induces MCP-1 expression in SMCs and upregulates CCR2 in human monocytes, enhancing monocyte recruitment after arterial injury and thus mediates the exacerbation of neointimal growth (Yu et al., 1992; Han et al., 1998; Oguchi et al., 2000). In our experiments, no clear atherosclerotic lesions were detectable in the aortic root of mice 28 days after injury. However, we and others

have demonstrated that lymphocytes already reside into the adventitia of arterial wall of apoE$^{-/-}$ mice even before the onset atherosclerosis (Galkina et al., 2006; Maffia et al., 2007). In this light, the hyperlipidaemic mice tool represents a step forward to the rat balloon angioplasty model, allowing us to study the effect of bindarit in the contest of increased vascular inflammation. Our results clearly demonstrated that bindarit reduced neointimal formation by reducing proliferating rate and macrophage infiltration, effects associated with a reduced expression of MCP-1 in injured vessels. In hypercholesterolaemic rabbits, gene transfer of a plasmid coding for a mutant form of MCP-1 appeared to reduce neointimal formation after balloon injury, mainly inhibiting macrophage infiltration to the injured vessels. Similarly, in hypercholesterolaemic apoE$^{-/-}$ mice also deficient in CCR2, neointimal lesions after wire injury of the carotid artery were diminished and showed a marked reduction in macrophage content compared with apoE$^{-/-}$/CCR2$^{+/+}$ mice (Schober et al., 2004). In conclusion, this study demonstrates that bindarit is effective in reducing neointimal formation both in a nonhyperlipidaemic animal model of vascular injury, mainly by a direct effect on SMC proliferation/migration, and in hyperlipidaemic animals by reducing macrophage infiltration. The exploitation of the chemokine system as a drug target in vascular pathology has relied mainly on the development of receptor antagonists and blocking antibodies (Charo and Taubman, 2004). However, the attempt to block chemokines and their receptors in humans is more complex (Perico et al., 2008). Here, we report the use of bindarit, an inhibitor of MCP-1 synthesis, as a potentially viable approach to control neointimal formation even if the clinical effects cannot be immediately predicted and further experiments, as well as clinical trials, will be necessary

4. MONOCYTE CHEMOTACTIC PROTEIN-3 INDUCES HUMAN CORONARY SMOOTH MUSCLE CELL PROLIFERATION

Monocyte chemotactic protein-3 (MCP-3), also known as CCL7, belongs to the monocyte chemotactic protein (MCP) subfamily of CC chemokines. MCP-3 plays a critical role in regulating the mobilization and recruitment of monocytes and macrophages to inflammatory sites (Tsou et al., 2007). It has potent eosinophil chemoattractant properties (Shang et al., 2002) and is involved in the bone marrow homing of human multiple myeloma cells (Broek et al., 2003). Several studies suggest that MCP-3 may also be involved in vascular pathologies such as atherosclerosis and restenosis. Oxidised low-density lipoprotein (LDL) induced expression of MCP-3 in human atherosclerotic plaques (Jang et al., 2004). MCP-3 mRNA expression has also been induced in the carotid artery after balloon angioplasty and in cultured rat vascular smooth muscle cells (SMCs) by various stimuli, such as TNF-α (Wang et al., 2000). Furthermore, mouse aortic SMCs were found to participate in the formation of tertiary lymphoid tissue in atherosclerosis through an increase in chemokine mRNA levels, including MCP-3 (Lötzer et al., 2010). SMCs express receptors for CC chemokines such as chemokine receptor 1 (CCR1), CCR2, CCR3, and CCR5 (Hayes et al., 1998; Kodali et al., 2004). MCP-3 acts through interaction with CCR1, CCR2, and CCR3, but appears to be an antagonist for CCR5 (Rollins, 1997; Blanpain et al., 1999). Interestingly, CCR2 is known to be shared with MCP-1 (Hayes et al., 1998), which directly induces SMC proliferation (Selzman et al., 2002). Although all these data suggest the possibility that SMCs react to MCP-3, the effect of MCP-3 on SMC activation has not yet been investigated.

The aim of the current study was to evaluate the direct influence of MCP-3 on human coronary artery SMC (CASMC) proliferation, which plays a critical role in neointimal formation during vascular injury. Furthermore we analysed the intracellular signalling pathways involved in MCP-3 induced CASMC proliferation .

4.1. Methods

4.1.1 Cell culture

Human CASMCs (lots 7F3272 and 16737; Lonza) were grown in Smooth Muscle Basal Medium (SmBM; Lonza) supplemented with 0.5 mg/mL hEGF, 5 mg/mL insulin, 1 mg/mL hFGF, 50 mg/mL gentamicin/amphotericin-B, and 5% FBS, and used between passages 4 and 8 for all experiments. Before initiation of assays, to achieve cell quiescence, CASMCs in exponential growth were switched into SmBM supplemented with 0.1% FBS in the absence of growth factors for 48 h.

4.1.2 Cell proliferation studies

Cell proliferation was analysed via measurement of DNA synthesis by a colorimetric bromodeoxyuridine (BrdU) enzyme linked immunosorbent assay (ELISA) kit (Roche) according to the manufacturer's instructions. Briefly, CASMCs were seeded in 96 multi-well plates at a density of 5×10^3 cells/well. After quiescence induction, cells were stimulated with human MCP-3 (0.001–30 ng/mL; PeproTech) for 24 h and then incubated with 10 μM BrdU 16 h prior to analysis. Human TNF-α (30 ng/mL; R&D Systems) was used as the positive control. In some experiments, BrdU uptake in CASMCs stimulated with MCP-3 (0.3 ng/mL) was measured in the presence of anti-MCP-3 Ab (20 ng/mL, PeproTech), RS 102895 (CCR2 antagonist, 0.06–6 μM, Sigma–Aldrich), U0126 (MEK1/2 inhibitor, 1 μM, Santa Cruz Biotechnology), or LY-294002 (phosphotidylinositol 3 kinase, IP3K inhibitor, 5 μM, Santa Cruz Biotechnology). BrdU uptake was also evaluated in TNF-α (30 ng/mL), IL-1β (1 ng/mL, PeproTtech), FBS (5%), or PDGF-BB (10 ng/mL, R&D Systems)-stimulated cells, respectively, with or without anti-MCP-3 Ab (20 ng/mL). In a separate set of experiments, CASMC proliferation was also evaluated by directly counting the cell number using the trypan blue method. Briefly, CASMCs (1×10^5) were seeded in 25 cm^2 cell culture flasks. After quiescence induction, cells were stimulated with MCP-3 (0.3 ng/mL) or TNF-α (30 ng/mL) for 96 h. Cells were trypsinized, stained with trypan blue solution (0.4%, Sigma–Aldrich), and counted by an independent observer blinded to the experiment.

4.1.3 Cytotoxicity assay

The cytotoxicity assay was carried out using the MTT method. Briefly, CASMCs were plated in 48 multi-well plates at a density of 1.5×10^4 cells/well. After quiescence induction, cells were treated with RS 102895 (0.06–6 μM), U0126 (1–100 μM), or LY-294002 (5–50 μM) for 24 h. The absorbance values were obtained with an ELISA assay reader (630 nm).

4.1.4 Total cellular extracts

CASMCs were cultured in 24 multi-well plates until 90% confluence. After quiescence induction, cells were stimulated with MCP-3 (0.3 ng/mL) or TNF-α (30 ng/mL). At different time points, cells were washed twice with ice cold PBS after which 30 μL/well of lysis buffer (50 mM Tris–HCl, 1% Triton, 1 mM Na_3VO_4, 1 mM ethylenediaminetetraacetic acid (EDTA), 0.2 mM phenylmethylsulfonyl fluoride (PMSF), 25 μg/mL Leupeptin, 10 μg/mL Aprotinin, 10 mM NaF, 150 mM NaCl, 10 mM β-glycerophosphate, 5 mM pyrophosphate, and H_2O) were added. Protein concentration was determined using a Bio-Rad protein assay kit (Bio-Rad).

4.1.5 Western blot analysis

Total cell lysates (20 μg) were separated by sodium dodecyl sulfate polyacrylamide gel electrophoresis (SDS-PAGE) and transferred to nitrocellulose membranes (Millipore). Membranes from 3 experiments were incubated with anti-p-ERK1/2 Ab (phosphorylated at Thr 202/Tyr 204, 1:2000, Cell Signaling), followed by stripping and reprobing with anti-ERK1/2 Ab (1:2000, Cell Signaling). Different membranes (n=3) were incubated with either (1) anti-p-AKT Ab (phosphorylated at Ser 473, 1:1000, Cell Signaling), followed by stripping and reprobing with anti-AKT Ab (1:1000, Cell Signaling); (2) anti-p-p70 S6K Ab (phosphorylated at Ser 411, 1:1000, Santa Cruz Biotechnology), followed by stripping and reprobing with anti-β-actin Ab (1:5000, Sigma–Aldrich); or (3) anti-IκB-α Ab (1:1000, Santa Cruz Biotechnology), followed by stripping and reprobing with anti-β-actin Ab (1:5000, Sigma–Aldrich). The membranes were washed three times with 0.5% Triton in PBS and then incubated with anti-rabbit or anti-mouse immunoglobulins coupled to peroxidase (1:1000, DAKO). The immunocomplexes were visualised by the ECL chemiluminescence method. ERK 1/2 activity is expressed as the ratio of

phosphorylated ERK 1/2 to total ERK 1/2; AKT as the ratio of phosphorylated AKT to total AKT; p70 S6K as the ratio of phosphorylated p70 S6K to β-actin; and IκB-α as the ratio of IκB-α to β-actin.

4.1.6 Electrophoretic mobility shift assay (EMSA)

Double stranded nuclear factor (NF)-κB consensus oligonucleotide probe (5′ AGC TTC AGA GGG GAC TTT CCG AGA GG 3′) was end-labeled with [^{32}P]γ-ATP. Cellular extracts (5 µg protein per sample) were incubated for 30 min with radiolabeled oligonucleotides (2.5–5.0 × 10^4 cpm) in 20 µL reaction buffer containing 3 µg poly dI-dC, 10 mM Tris–HCl (pH 7.5), 100 mM NaCl, 1 mM EDTA, 1 mM dithiothreitol, 1 µg/µL bovine serum albumin, and 10% (v/v) glycerol. Protein–oligonucleotide complexes were resolved by electrophoresis on a 6% non-denaturing polyacrylamide gel in 1× Tris–borate/EDTA at 180 V for 2 h at 4 °C. The gels were dried and autoradiographed with intensifying screens at −80 °C for 24 h.

4.1.7 Enzyme linked immunosorbent assay (ELISA)

CASMCs were seeded in 48 multi-well plates at a density of 1.5 × 10^4 cells/well. After quiescence induction, cells were stimulated with TNF-α (30 ng/mL), IL-1β (1 ng/mL), PDGF-BB (10 ng/mL), or FBS (5%). After 12, 24, and 48 h, media were collected and centrifuged at 5000 × *g* for 15 min at 4 °C. The supernatants extracted were immediately frozen at −80 °C until use. MCP-3 levels in the cell supernatants were evaluated by ELISA according to the manufacturer's instructions (R&D Systems).

4.1.8 Statistical analysis

Results are expressed as mean±SEM of n experiments run in triplicate. The results were statistically analysed by the *t* test or ANOVA (Two-Tail *P* value) and the Bonferroni *post hoc* test. The level of statistical significance was 0.05 per test.

4.2 Results

4.2.1 Effect of MCP-3 on coronary artery smooth muscle cell (CASMC) proliferation

To assess the effect of MCP-3 on CASMC proliferation we performed, concentration–response experiments using BrdU uptake as a marker of DNA synthesis. TNF-α (30 ng/mL) was chosen as the positive control owing to its well-known mitogenic effect on SMCs. When CASMCs were stimulated with increasing concentrations of MCP-3 (0.001–0.3 ng/mL), a concentration-dependent proliferation was observed (Fig. 4.1A). MCP-3, which was ineffective at 0.001 ng/mL, showed moderate increase of CASMC proliferation at 0.01 and 0.03 ng/mL of 12% (n=7) and 24% (n=7), respectively, and significant increase of CASMC proliferation at 0.1 ng/mL of 36% (P<0.05, n=7). The maximum stimulating effect, which was observed at 0.3 ng/mL, was 55% (P<0.001, n=7) compared to unstimulated cells. CASMC proliferation induced by 1 ng/mL MCP-3 showed a slight decrease compared to 0.3 ng/mL (38%,P<0.05, n=7). MCP-3 at concentrations ranging from 3 to 30 ng/mL induced no significant changes in CASMC proliferation (Fig. 4.1A). TNF-α (30 ng/mL) significantly increased CASMC proliferation by 62% (P<0.001, n=7) (Fig. 4.1A). We also evaluated CASMC proliferation by directly counting the cells in 25 cm^2 flasks (Fig. 4.1B). The CASMC number significantly increased at 96 h after stimulation with MCP-3 (0.3 ng/mL) ($20.6 \times 10^4 \pm 2 \times 10^4$, P<0.05, n=3) when compared to unstimulated cells ($13.8 \times 10^4 \pm 1 \times 10^4$, n=3). The number of CASMCs counted 96 h after stimulation with 30 ng/mL TNF-α was $21.0 \times 10^4 \pm 1.1 \times 10^4$ (n=3).

To demonstrate the specificity of the MCP-3 stimulation, BrdU uptake was measured in the presence of anti-MCP-3 Ab (20 ng/mL), which completely inhibited the proliferation induced by MCP-3 (0.3 ng/mL, P<0.001, n=5) (Fig. 4. 1C).

BrdU uptake was also measured in the presence of RS 102895, a specific antagonist of the CCR2 receptor (Ma et al., 2007), to investigate its involvement in MCP-3-induced CASMC proliferation. As shown in Figure 4.1D, RS 102895 at 0.06 μM moderately reduced MCP-3 (0.3 ng/mL)-induced CASMC proliferation by 38% (n=4), whereas at 0.6 and 6 μM induced significant inhibition of cell proliferation by 64% (P<0.05, n=4) and 88% (P<0.01, n=4), respectively. RS

102895 alone, at the concentrations used, did not affect CASMC proliferation (Fig. 4.1D).

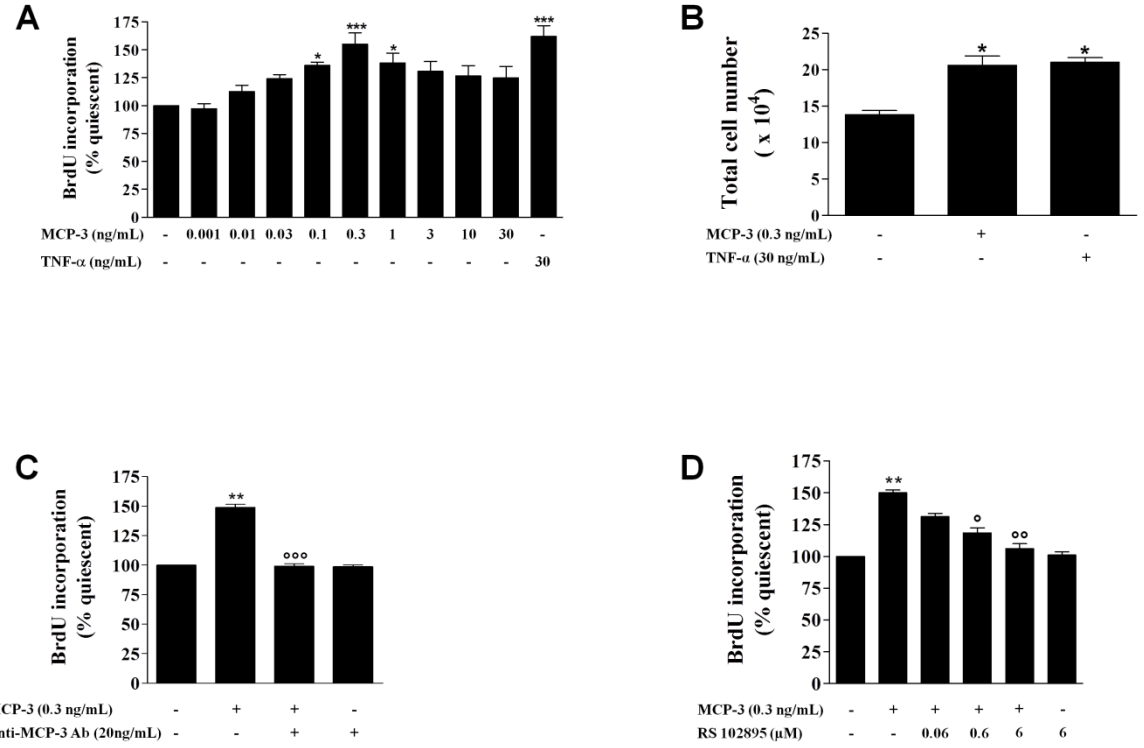

Figure 4.1.

Effect of MCP-3 (0.001-30 ng/mL) on CASMC proliferation assessed by BrdU incorporation (A) and by cell counting expressed as total cells number (B). Effects of neutralizing anti-MCP-3 Ab (20 ng/mL), and RS 102895 (0.06-6 μM) on MCP-3-induced CASMC proliferation (C, D). TNF-α (30 ng/mL) was used as positive control. Results are expressed as mean±SEM of three to seven separate experiments run in triplicate. **P*<0.05, ***P*<0.01, ****P*<0.001 *vs* unstimulated cells; °*P*<0.05, °°*P*<0.01, °°°*P*<0.001 *vs* MCP-3-stimulated cells.

4.2.2 Effect of MCP-3 on ERK1/2 and AKT/p70 S6K activation in coronary artery smooth muscle cells (CASMCs)

We tested the hypothesis that MCP-3-induced CASMC proliferation is associated with ERK1/2 and AKT–mTOR-p70 activation since these two signalling pathways are the major regulators of cell growth and proliferation (Peppel et al., 2005; Duan et al., 2000; Stabile et al., 2003; Brito et al., 2009). CASMCs were stimulated with MCP-3 (0.3 ng/mL) or TNF-α (30 ng/mL), used as the positive

control. Western blot analysis shows that ERK activation, visible as an increase of phosphorylation of p44 and p42 proteins, occurred in MCP-3-stimulated CASMCs within 5 min (32% *vs* unstimulated cells) and returned to basal levels after 15 min (Fig. 4.2A). As shown in Figure 4.2B and 4.2C, MCP-3 also enhanced AKT and p70 S6K phosphorylation. In both cases the peak of phosphorylation was observed within 5 min (40% and 53% *vs* unstimulated cells, respectively).

4.2.3 Effect of MCP-3 on NF-κB activation in coronary artery smooth muscle cells (CASMCs)

Since the NF-κB pathway is also involved in SMC proliferation, we investigated NF-κB activation in CASMCs stimulated with MCP-3 (0.3 ng/mL) or TNF-α (30 ng/mL), used as the positive control. TNF-α, as expected, induced significant and time-dependent IκB-α degradation (Fig. 4.3A) and strong NF-κB activation as evaluated by EMSA at 4 h after stimulation (Fig. 4.3B). In contrast, MCP-3 showed no effect on NF-κB activation (Fig. 4.3A and B).

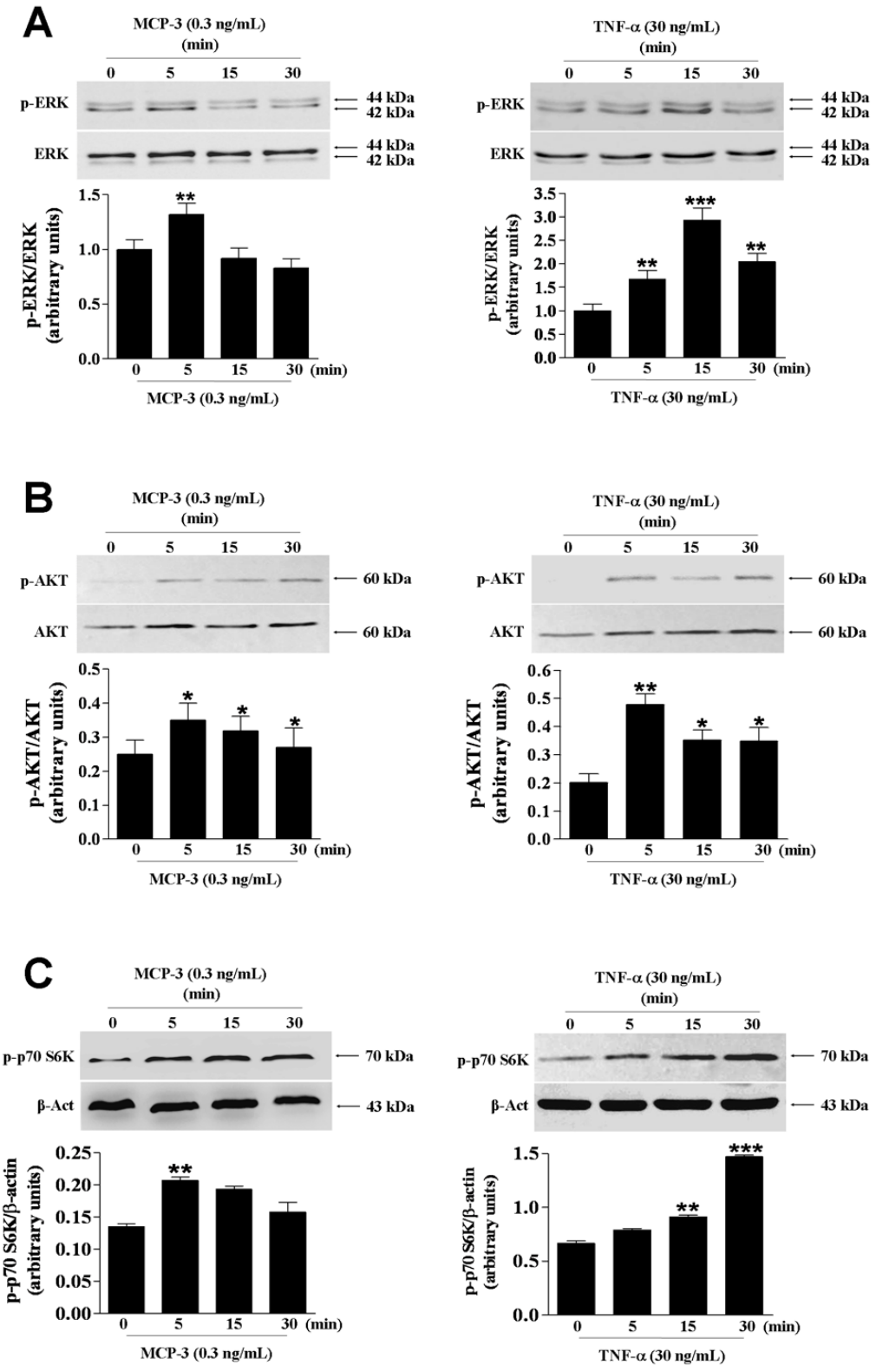

Figure 4.2.

Representative Western Blot and relative densitometric analysis showing the effects of MCP-3 (0.3 ng/mL) and TNF-α (30 ng/mL), used as positive control, on ERK 1/2 (A), AKT (B) and p70 S6K (C) activation in CASMCs. Results are expressed as mean±SEM from three separate experiments. **P*<0.05, ***P*<0.01, ****P*<0.001 *vs* unstimulated cells.

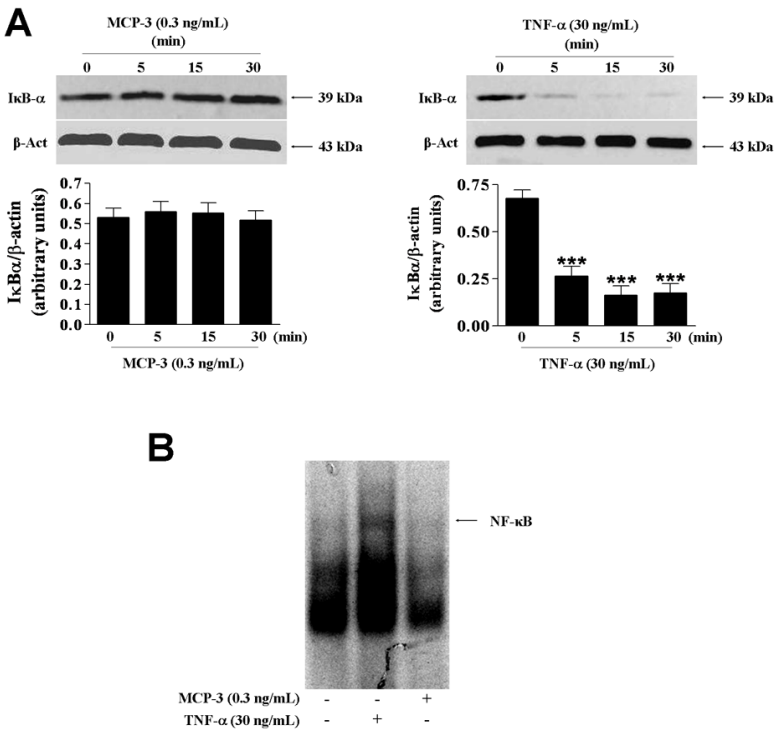

Figure 4.3.

Representative Western Blot and relative densitometric analysis showing the effect of MCP-3 (0.3 ng/mL) and TNF-α (30 ng/mL), used as positive control, on IκBα degradation in CASMCs (A). Representative EMSA showing the effect of MCP-3 (0.3 ng/mL) and TNF-α (30 ng/mL), on NF-κB activation (B). Results are expressed as mean±SEM of three separate experiments. ***P<0.001 *vs* unstimulated cells.

4.2.4 Effect of inhibition of ERK 1/2 and IP3K activation on MCP-3-induced coronary artery smooth muscle cell (CASMC) proliferation

To confirm the involvement of the ERK 1/2 and IP3K signalling pathways in MCP-3-induced CASMC proliferation, cells were stimulated with MCP-3 (0.3 ng/mL) in the presence of U0126, an inhibitor of MEK 1/2 (MAPK of ERK kinases) (Yao et al., 2008) or LY-294002, a selective inhibitor of IP3K (Walcher, et al., 2006), followed by BrdU uptake measurement. As shown in Figure 4.4, U0126 (1 μM) and LY-294002 (5 μM) significantly reduced MCP-3-induced CASMC proliferation by 36% (P<0.05, n=3) and 64% (P<0.01, n=3), respectively. Neither U0126 nor LY-294002 alone affected CASMC proliferation (Fig. 4.4).

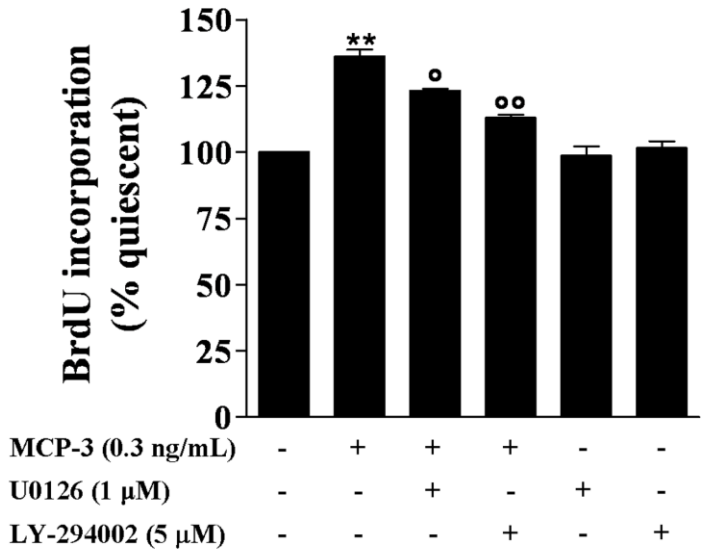

Figure 4.4.

Effect of U0126 (1 µM) and LY-294002 (5 µM) on MCP-3 (0.3 ng/mL)-induced CASMC proliferation. Results are expressed as mean±SEM from three separate experiments run in triplicate. ***P*<0.01 *vs* unstimulated cells; °*P*<0.05 and °°*P*<0.01 *vs* MCP-3-stimulated cells.

4.2.5 Evaluation of MCP-3 production by coronary artery smooth muscle cells (CASMCs)

To investigate the pathophysiological role of MCP-3, CASMCs were stimulated with different stimuli such as TNF-α (30 ng/mL), IL-1β (1 ng/mL), PDGF-BB (10 ng/mL), or FBS (5%). MCP-3 protein concentration in the supernatants of cultured CASMCs was determined by ELISA. As shown in Table 4.1, stimulation of CASMCs with TNF-α (30 ng/mL) or IL-1β (1 ng/mL) caused a time-dependent increased release of MCP-3 compared to that observed in unstimulated cells. In contrast, neither PDGF-BB (10 ng/mL) nor FBS (5%) affected MCP-3 production.

Table 4.1 MCP-3 production by stimulated CASMCs

	MCP-3 (pg/mL)		
	12h	24h	48h
Unstimulated cells	384±35	602±25	971±77
TNF-α 30 ng/mL	1077±54°°°	1805±167°°°	3636±235°°°
IL-1β 1 ng/mL	850±82°	1157±47°	2702±283°°°
PDGF-BB 10 ng/mL	581±133	716±75	1171±56
5% FBS	391±37	731±141	1469±112

Results are expressed as mean±SEM of three separate experiments run in triplicate. °P<0.05, °°°P<0.001 *vs* unstimulated cells.

4.2.6 Effect of MCP-3 neutralization on coronary artery smooth muscle cell (CASMC) proliferation

To further investigate the pathophysiological role of MCP-3 production by CASMCs, we also evaluated the effect of MCP-3 neutralization on cell proliferation induced by TNF-α (30 ng/mL), IL-1β (1 ng/mL), PDGF-BB (10 ng/mL), and FBS (5%), respectively. Treatment with anti-MCP-3 Ab (20 ng/mL) significantly reduced the proliferation induced by TNF-α (79% *vs* unstimulated cells) and IL-1β (58% *vs* unstimulated cells) by about 12% (P<0.01, n=3) and 14% (P<0.05, n=3), respectively, while no effect was observed in PDGF-BB- or FBS-stimulated CASMCs (Fig. 4.5).

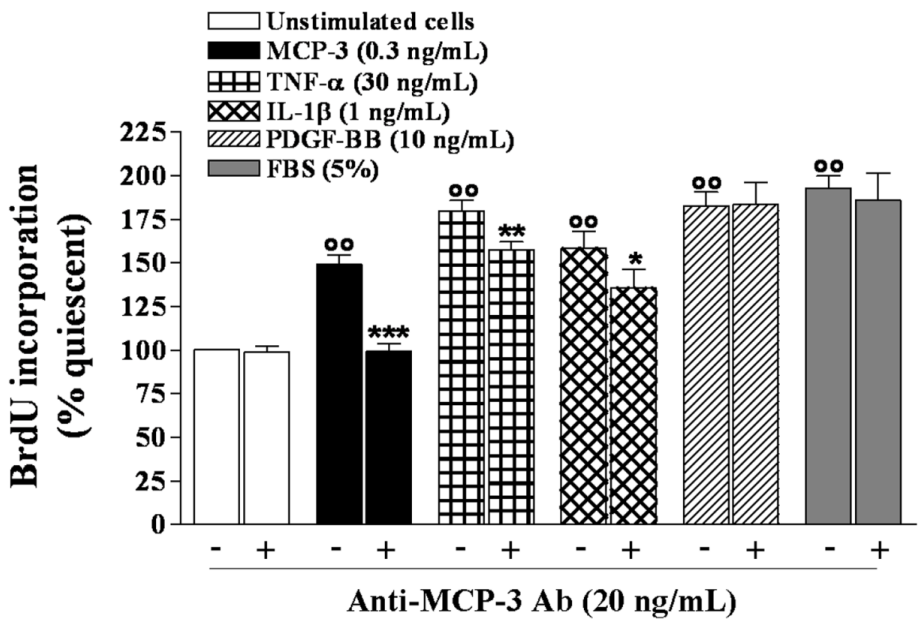

Figure 4.5

Effect of anti-MCP-3 neutralizing Ab on CASMC proliferation induced by TNF-α (30 ng/mL), IL-1β (1 ng/mL), PDGF-BB (10 ng/mL) and FBS (5%). Results are expressed as mean±SEM from five separate experiments run in triplicate. °° P<0.01 *vs* unstimulated cells, ** P<0.01 *vs* TNF-α-stimulated cells, * P<0.05 *vs* IL-1β-stimulated cells.

4.3 Discussion

MCP-3 exhibits biological activity in various cell types (Tsou et al., 2007; Shang et al., 2002; Broek et al., 2003), however, previously nothing was known about its direct influence on SMC activation and the intracellular signalling pathways involved. In the present study, we demonstrate that human MCP-3 directly promotes *in vitro* proliferation of human CASMCs, at least in part, through the activation of the ERK1/2 MAPK and PI3K signalling pathways. We also demonstrate that MCP-3 is produced by CASMCs, and that its inhibition by anti-MCP-3 Ab reduces cell proliferation induced by both TNF-α and IL-1β.

To better identify the proliferative activity of MCP-3, we analysed a large concentration–response range. Our results show that MCP-3 induced concentration-dependent CASMC proliferation up to 0.3 ng/mL, while higher concentrations of MCP-3 (3–30 ng/mL) did not cause any significant increase of cell proliferation. This bimodal proliferative response of MCP-3-stimulated CASMCs was similar to that observed by Selzman et al. (Selzman et al., 2002) for MCP-1 in

human thoracic SMCs, and is a typical finding for a chemotactic response to CC chemokines (Haque et al., 2004). A possible explanation for this is that activation of more than one receptor could be involved in the proliferation process. Indeed, MCP-3 exhibits a promiscuous nature of receptor recognition, being an agonist on CCR1, CCR2, and CCR3, while an antagonist for CCR5 (Rollins, 1997; Blanpain et al., 1999).

We studied a number of different mechanisms for MCP-3-induced CASMC proliferation. The involvement of the ERK1/2 MAPK cascade and PI3K/AKT signalling pathway in SMC proliferation has previously been demonstrated (Peppel et al., 2005; Duan et al., 2000; Stabile et al., 2003). It has also been shown that the ERK1/2 pathway is involved in MCP-3-mediated chemotaxis of peripheral blood mononuclear cells (Wain et al., 2001), and that ERK1/2 inactivation prevents intimal hyperplasia after balloon angioplasty of rat carotid artery (Izumi et al., 2001), a well-known animal model for studying proliferation of SMCs *in vivo*. In previous studies, it was shown that SMC proliferation is also regulated by PI3K/AKT signalling (Duan et al., 2000; Stabile et al., 2003). The activation of this pathway in different cell types, such as fibroblasts, is induced by MCP-3 stimulation (Ong et al., 2009). Results from the present study show an increase of ERK1/2 and AKT phosphorylation in MCP-3-stimulated CASMCs. Moreover, the selective inhibition of MEK1/2 (MAPK of ERK kinases) by U0126 and the inhibition of PI3K by LY-294002 significantly reduced MCP-3-induced CASMC proliferation. It is well established that SMC proliferation is also influenced by NF-κB activation. However, our results show that MCP-3 affects neither IκB-α degradation nor NF-κB activation. These data, taken together, clearly demonstrate that MCP-3-induced CASMC proliferation is partially dependent on ERK1/2 and PI3K activation, without direct involvement of the NF-κB pathway.

The induction of cultured human SMC proliferation by MCP-3, demonstrated here, and the increased MCP-3 mRNA expression in rat carotid artery after balloon angioplasty (Wang et al., 2000) suggest a potential role of this chemokine in intimal hyperplasia. To better clarify this point, we measured the MCP-3 production in CASMCs stimulated with TNF-α, IL-1β, or PDGF-BB, which are known to be involved in intimal hyperplasia (Peppel et al., 2005; Isoda et al., 2003). We observed time-dependent increase of MCP-3 production in the IL-1β- and TNF-α-

stimulated CASMCs. Moreover, treatment with anti-MCP-3 Ab significantly reduced the proliferation induced by these mediators. Our results demonstrate that *in vitro* MCP-3 can act in a paracrine/autocrine way, promoting SMC proliferation. Jang et al. (Jang et al., 2004) observed expression of MCP-3 in foam cells but not in SMCs in human atherosclerotic plaques. This lack of MCP-3 production in SMCs could be due to the different experimental approaches. Nevertheless, MCP-3 produced in the vessel wall by macrophages and/or SMCs could be a potential mediator for inflammatory and proliferative cellular responses. To elucidate the role of MCP-3 in intimal hyperplasia, future investigations *in vivo* are necessary.

The initiation and development of atherosclerosis and intimal hyperplasia after vascular injury is regulated by the MCP-1/CCR2 pathway (Boring et al., 1998; Egashira et al., 2002). There is strong evidence that MCP-1/CCR2 plays an important role in SMC proliferation and migration (Selzman et al., 2002). The CCR2 receptor is known to be shared with MCP-3 and is expressed on human SMCs (Hayes et al., 1998). Our results show that the proliferative effect of MCP-3 is due to its interaction with CCR2, as demonstrated by the reduction of the effect when using the selective antagonist RS 102895. It is interesting to note that $CCR2^{-/-}$ mice have a ≈60% decrease in intimal hyperplasia and medial DNA synthesis in response to femoral arterial injury while $MCP\text{-}1^{-/-}$ mice show a ≈30% reduction in intimal hyperplasia, which is not associated with diminished medial DNA synthesis (Kim et al., 2003), suggesting that MCP-1 and CCR2 deficiencies have distinct and separate effects on arterial injury. Therefore, it is possible that the results obtained with $CCR2^{-/-}$ mice may not be solely mediated by MCP-1 but also by other chemokines such as MCP-3.

In conclusion, our results demonstrate that MCP-3 is produced by human CASMCs and directly induces SMC proliferation *in vitro via* ERK and PIK3 activation. Therefore, MCP-3 could play a role in the molecular cascades leading to neointimal hyperplasia.

5. MURINE VASCULAR SMOOTH MUSCLE CELLS DO NOT PRESENT ANTIGEN AND LACK ESSENTIAL COSTIMULATORY MOLECULES

Inflammation and immunity are essential components of the pathogenesis of cardiovascular diseases (Libby, 2002; Hansson et al., 2002), participating in every phase during the development of atherosclerosis (Hansson and Libby, 2006).

Activation of SMCs has a critical role in intimal thickening resulting from atherosclerosis or arterial injury (Owens et al., 2004) and, during the past 20 years, the hypothesis that SMCs could play a proimmunogenic role in cardiovascular disease has been explored. Indeed, SMCs participate in the formation of vascular tertiary lymphoid tissue in atherosclerosis (Lötzer et al., 2010) and express class II major histocompatibility complex molecules (MHC II) in the human atherosclerotic plaque (Hansson et al., 1986). Expression of MHC II has also been shown *in vivo* after ballon-induced rat arterial injury and *in vitro* after stimulation of aortic SMCs with IFN-γ (Hansson and Jonasson, 2009).

It is well known that T cells, resident in normal arteries or infiltrating diseased arteries, recognize antigens as a complex formed by antigenic peptides bound to self allelic forms of MHC molecules expressed on the surface of antigen-presenting cells (APC). The possibility that SMCs can act as APC and, consequently, activate T cell response is now disputed. It has been demonstrated that brain microvessel SMCs treated with OVA antigen are able to activate A2.2E10 cells, an OVA-specific T cell hybridoma (Fabry et al., 1990). However, human SMCs from saphenous vein do not activate allogeneic memory T cells and fail to effectively support T-cell proliferation to the polyclonal activator, phytohemagglutinin. This inability results from a defect in costimulation function, particularly the lack of essential costimulators such as OX40 ligand (OX40L) (Zhan et al., 2010). Up to now the effective ability of SMCs in capturing, processing and presenting the antigen in the context of MHC II has not yet been demonstrated.

The aim of the present study was to investigate the contribution of SMCs in antigen presentation to better understand their role in vascular immunity. These experiments were performed in the Institute of Infection, Immunity and Inflammation University of Glasgow, UK.

5.1 Methods

5.1.1 Cell culture

Murine primary SMCs were derived from the thoracic aorta of C57BL/6 mice as previously described (Choi et al., 2004) and grown in DMEM (Cambrex Bio Sciences), supplemented with L-glutamine (Cambrex Bio Sciences), 10% fetal bovine serum (FBS, Cambrex Bio Sciences), 100 U/mL penicillin, and 100 µg/mL streptomycin. Before initiation of assay the cells were characterized by immunofluorescence microscopy using FITC labeled anti-smooth muscle α-actin (α-SMA) monoclonal Ab (Sigma). Studies were performed with cells at passages 3-6. Dendritic cells (DCs) were obtained by flushing the bone marrow of C57BL/6 mice and grown in complete RPMI (Cambrex Bio Sciences) containing 10% Granulocyte-Macrophage Colony Stimulating Factor (GM-CSF) for 7 days. All cells used were kept in a humidified incubator at 37°C in 5% CO_2.

5.1.2 MHC II and costimulatory molecules expression

Murine SMCs were cultured in 6 multi-well plates until 80% confluence and stimulated with IFN-γ (100 ng/ml, R&D Systems). After 72 h of stimulation cells were collected for flow cytometric analysis.

5.1.3 Ealpha-GFP preparation

To assess the ability of murine SMCs to act as APC, we employed the Ealpha (Eα)-GFP/Y-Ae system as previously described (Itano et al., 2003). The peptide was prepared as follows: bacterial E.Coli culture, that espressed the Eα-GFP gene, were used. Protein production was induced with 1 mM Isopropil β-D-1-tiogalattopiranoside (IPTG) overnight, and the Eα-GFP fusion protein was purified from the bacterial lysates using HisPur Cobalt Spin Columns (Thermo Scientific). The endotoxin was removed from protein preparation using Detoxi-Gel Endotoxin Removing Columns (Thermo Scientific).

5.1.4 Ealpha-GFP treatment

Murine SMCs were cultured in 6 multi-well plates, as described above, stimulated with IFN-γ (100 ng/ml) for 72 h, then treated with Eα-GFP (100 μg/mL). After 24 h of treatment cells were collected for flow cytometric analysis.

5.1.5 Flow Cytometry

Aliquots of cells were washed and resuspended in Fc block (2.4G2 hybridoma supernatant) for 25 mins at 4°C to block Fc receptors. Subsequently, cells were incubated with Abs (in PBS containing 2% FBS) for 30 mins at 4°C, washed twice and then, where necessary, incubated with Streptavidin for additional 20 mins at 4°C. Following washing, cells were analysed on a FACScalibur using the CellQuest-Pro software (BD Biosciences), or on a MACSQuant Analyzer® using the MACSQuantify™ Software (Miltenyi Biotec). Fluorescence signals were accumulated as two-parameter fluorescence histograms with the percent positive cells being recorded and data analysis was performed using 6 FlowJo (Tree Star Inc.).

Murine SMCs were stained with the following primary mouse (m) Abs: Y-Ae-Bio (specific for I-Eα 52-68 of I-Ed presented on I-Ab; ebioY-Ae), anti-MHC II (I-A/I-E)-APC, anti-CD54-PE, anti-CD44-FITC, anti-OX40L-Bio followed by streptavidin-PerCP. Dendritic cells were stained with anti-CD11c-APC mAb. Isotype-matched Abs were used as a negative control. Y-Ae Ab was from eBioscience, Streptavidin-Pacific Blue was from Invitrogen, all other Abs were from BD Biosciences.

5.1.6 Statistical analysis

Results are expressed as mean±SEM of 3 experiments run in triplicate. The results were statistically analysed by ANOVA (Two-Tail P value) and the Bonferroni *post hoc* test. The level of statistical significance was 0.05 per test.

5.2 Results

5.2.1 Effect of IFN-γ stimulation on MHC II and costimulatory molecules expression in murine SMCs

We examined the MHC II and some costimulatory molecules expression in murine SMCs at baseline and after IFN-γ (100 ng/mL) stimulation for 72 h.

As shown in Figure 5.1, the percentage of MHC II positive unstimulated SMCs was about 2%. The stimulation with IFN-γ significantly caused a 7 to 8 fold increase in this percentage ($P<0.01$). SMCs expressed CD54 (ICAM-1) and CD44 (30% and 87% positive cells, respectively) at the basal conditions. The stimulation with IFN-γ significantly caused a 2 fold increase in the percentage of ICAM-1 ($P<0.01$) positive cells while it did not affect the expression of CD44 (Fig. 5.1). In contrast, low levels of OX40L expression were detectable in unstimulated SMCs. IFN-γ stimulation did not increase the percentage of SMCs positive to this molecule (Fig. 5.1).

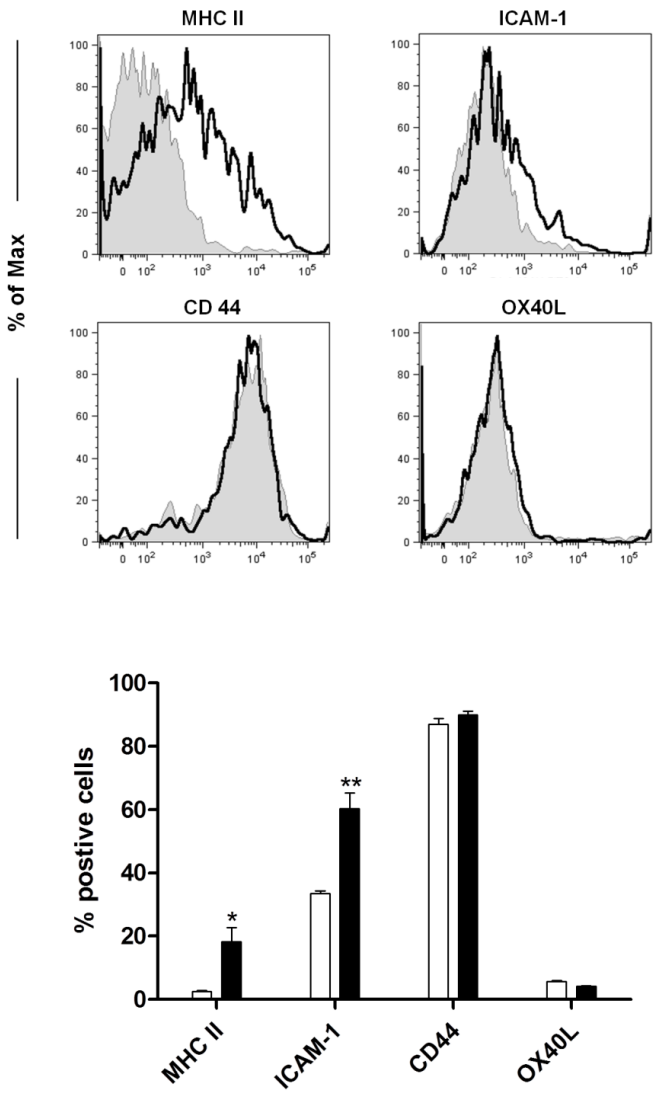

Figure 5.1

Representative flow cytometry histograms and relative graph showing the effect of IFN-γ (100 ng/mL) on costimulatory molecules expression in murine SMCs. Black empty histograms or black columns (IFN-γ-stimulated cells) *vs* gray filled histograms or white columns (unstimulated cells). Results are expressed as mean±SEM from three separate experiments. **P*<0.05, ***P*<0.01, *vs* unstimulated cells.

5.2.2 Assessment of antigen presentation by SMCs using the Eα-GFP/Y-Ae system

Recent investigations suggest that SMCs can induce T cell activation *in vitro*. However, it is not known if vascular SMCs can function as antigen presenting cells. We utilized the Eα-GFP/Y-Ae model, recently established in Prof. Garside's group (University of Glasgow, UK), that allows visualisation of antigen uptake, as the Eα is GFP labelled, and tracking of antigen presentation using the Y-Ae Ab. The Eα-GFP

peptide is internalised, processed by APCs to generate the antigenic peptide for presentation on MHC II. The monoclonal Ab Y-Ae detects Eα when bound to MHC II molecules in I-E-/I-Ab+ mouse strains (e.g. C57BL/6).

The stimulation with IFN-γ (100 ng/mL) for 72 h significantly caused a 5 to 6 fold increase in the percentage of MHC II positive SMCs compared with unstimulated cells (P<0.01, Fig. 5.2A). Similar results were observed in IFN-γ-stimulated SMCs treated with Eα peptide (100 μg/mL) for 24 h (P<0.05, Fig. 5.2A). As shown in Figure 5.2 B, SMC treatment with Eα peptide induced an increase in the percentage of GFP positive cells, both in presence or absence of IFN-γ-stimulation, being indicative of antigen uptake. No significant changes were observed in the percentage of Y-Ae positive SMCs after IFN-γ-stimulation and/or treatment with Eα peptide (Fig. 5.2C), suggesting that, although SMCs internalize the antigen, they are not able to present the Eα peptide in the context of MHC II molecules. The results obtained with dendritic cells, used as positive control, showed that the treatment with Eα peptide for 24 h significantly caused a 50 to 60 fold increase in the percentage of both GFP and Y-Ae positive cells (data not shown).

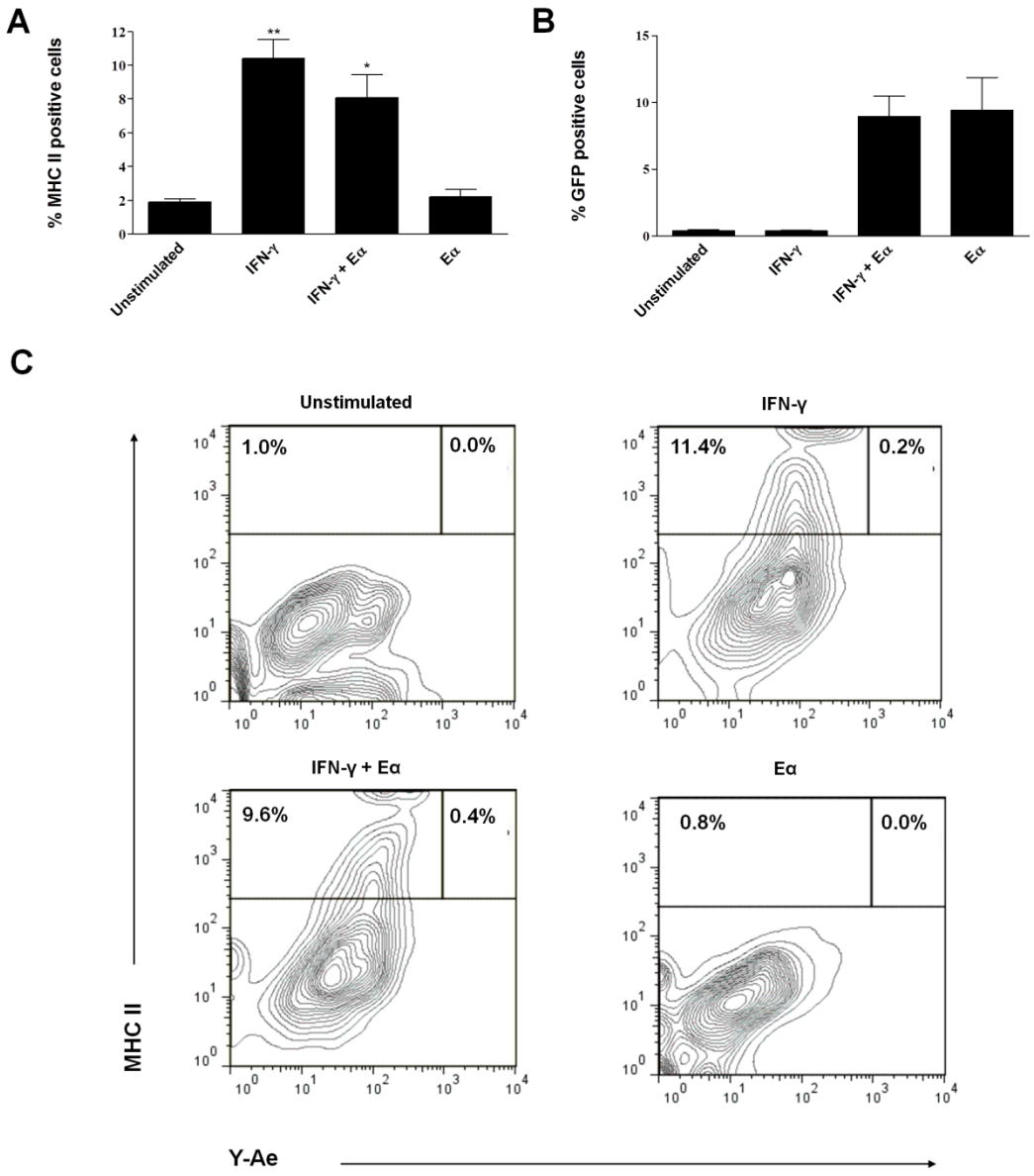

Figure 5.2

Evaluation of antigen presentation by murine SMCs. Cells were stimulated with IFN-γ (100 ng/mL) for 72 h and treated with Eα-GFP peptide (100 µg/mL) for 24 h. (A) MHC II expression. (B) GFP expression. (C) Representative flow cytometry plots showing no positivity of SMCs to Y-Ae Ab. Results are expressed as mean±SEM from three separate experiments. **P*<0.05, ***P*<0.01, *vs* unstimulated cells.

5.3 Discussion

The finding of this study is that cultured primary murine SMCs express MHC II molecules after stimulation with IFN-γ but are not able to present the antigen in the context of MHC II.

It is now generally accepted that atherosclerosis is an inflammatory process with an immune component. The first findings that SMCs espress MHC II molecules both during atherosclerosis (Hansson et al., 1986) and arterial response to injury (Jonasson et al., 1988) suggested their active role in cellular immunity. Previous studies have reported that human SMCs, do not activate allogeneic CD4 T cells in co-culture although once T cells are activated by endothelial cells, they are capable of responding to SMCs from the same donor (Murray et al., 1995). Zhang et al demonstrated that lack of costimulation function of human SMCs contributes to their immunologic ignorance (Zhang et al., 2010) but they hypothesized that their conclusions may not apply to rodents, as it has been reported that brain murine SMCs activate CD4 T-cell cytokine production and proliferation (Fabry et al., 1993; Swanson et al., 2003). Although SMCs in certain experimental condition can activate T cells, it has not been directly demonstrated that SMCs can act as APC.

Here we investigated the costimulatory molecules expression in murine aortic SMCs and the capability of SMCs in antigen presentation, using a direct and specific method: the Eα-GFP/Y-Ae system. In agreement with the data obtained on human SMCs by Zhang et al (Zhang et al., 2010), our results show that murine SMCs do not express OX40L, usually present on APC enabling T cell activation (Maizels and Yazdanbakhsh, 2003) neither in absence nor in presence of IFN-γ. The failure of SMCs to respond to IFN-γ in our assays is selective for the costimulatory molecule because the percentage of MHC II and ICAM-1 positive cells increases after IFN-γ stimulation under the same conditions. In this study we also demonstrate that after 24 h of treatment with the Eα peptide, SMCs internalize the antigen without presenting it.

The data obtained in this study must be considered preliminary, since it could be possible that SMCs require a more long period of treatment to be able in processing/presenting the peptide, thus a time course of the potential antigen presentation by SMCs should be examined. Moreover, the expression of other costimulatory molecules will be analysed.

Although our data suggest that SMCs are not able to present the antigen, they could have other critical roles in T cell activation. In order to investigate this issue we will co-culture SMCs, treated with different antigens, with specific T cell lines, some of them can be activated by APC without any requirement for co-stimulation, and T cell activation/proliferation will be evaluated.

6. CONCLUSIONS

Restenosis is the most problematic complication of percutaneous coronary intervention. Evidences from experimental and clinical studies suggest that at the base of this process there is an immune/inflammatory response going with a hyperplastic reaction involving SMC migration/proliferation and remodelling of the arterial wall leading finally to the reocclusion of the enlarged artery (Welt and Rogers, 2002). Many of the cellular and molecular elements responsible for inflammation and/or SMC activation have been elucidated, providing potential therapeutic targets for the treatment of restenosis.

It is well known that the transcriptional factor NF-κB plays a critical role in the vascular response to injury (Yamasaki et al., 2003) regulating both inflammatory response and proliferation-apoptosis balance in the vessel wall (De Winther et al., 2005). The identification and characterization of the NBD peptide, which blocks the IKK complex, essential for NF-κB pathway activation, have provided an opportunity to selectively abrogate the inflammation-induced activation of NF-κB. In this study we demonstrated that the NBD peptide reduces neointimal formation and SMC proliferation/migration, both effects associated with the inhibition of NF-κB activation and with the decrease of MCP-1 production, which role in vascular disease has been well described. Our results confirm the involvement of NF-κB as a regulator in the formation of neointima and support the use of specific IKK inhibitors to reduce neointimal hyperplasia.

The increasing appreciation of the importance of inflammation in vascular disease has focused attention on the molecules that direct the migration of leukocytes from the blood stream to the vessel wall. Recently particular attention has been received by chemokines, a family of proteins which genes are under the control of NF-κB (Landry et al., 1997). Chemokines selectively recruit monocytes, neutrophils, and lymphocytes to sites of vascular injury, inflammation or atherosclerosis and some of them seem also to be involved in SMC activation (Schober, 2008). MCP-1, acting through its receptor CCR2, appears to play an important role in the formation of intimal hyperplasia after arterial injury, being involved in both leukocyte recruitment and SMC activation (Charo and Taubman, 2004). Studies in different animal models suggest that an anti-inflammatory

treatment, based on the inhibition of MCP-1, may be an appropriate and reasonable approach for the prevention of neointimal formation (Furukawa et al., 1999; Egashira et al., 2007; Nakano et al., 2007). Nevertheless, the possibility to use an oral inhibitor of MCP-1 pathway, has not yet been investigated. Here we evaluated the effect of bindarit, a selective inhibitor of the MCPs subfamily (including MCP-1, MCP-2 and MCP-3) in neointimal formation in both non-hyperlipidaemic and hyperlipidaemic animal models of vascular injury. The results provided in this study demostrate that bindarit is effective in reducing neointimal formation through a direct effect on SMC proliferation and migration and macrophage recruitment, thus supporting its beneficial effect on the inflammatory/proliferative processes leading to neointimal formation.

During the past few years we have witnessed a rapid increase in our understanding of the role of chemokines and their receptors in cardiovascular pathologies. Nevertheless, the precise mechanism of the chemokine pathways involved in the response of the arterial wall to injury is not fully elucidated. As told above, it is known that chemokines have a great impact on initiating and progressing neointimal formation by controlling each step of the vascular obstructive remodelling process. Indeed, they can direct inflammatory cell recruitment, endothelial regeneration as well as SMC accumulation (Schober, 2008). Several studies suggest that, apart MCP-1, other chemokines, belonging to the same family, may be involved in vascular pathology (Wang et al., 2000). Our attention has been focused on MCP-3, that we consider very interesting since it acts through interaction with the receptors CCR1, CCR2 and CCR3 (Rollins, 1997; Blanpain et al., 1999), all expressed by vascular SMCs (Hayes et al., 1998; Kodali et al., 2004). It is known that CCR2 is shared with MCP-1, thus MCP-3 could have a role in SMC activation just like MCP-1 (Selzman et al., 2002). Here we demonstrate that MCP-3 is produced by human coronary SMCs and directly induces cell proliferation *in vitro*, suggesting a potential role for this chemokine in vascular pathology and supporting the potential benefit of antichemokine strategies in this sense.

The exploitation of the chemokine system as a drug target in vascular pathology has relied mainly on the development of receptor antagonists and blocking antibodies (Charo and Taubman, 2004). In addition, other antichemokine strategies may be feasible by locally confined delivery: blockers of signal

transduction, siRNAs or transcription factor inhibitors. As shown in this study, these approaches could be used to reduce chemokine activity or expression, combining the decreased inflammation with the lowered SMC activation, in an effort to control the neointimal hyperplasia. It is clear that further studies are needed before transcription factor- or chemokine-based therapies can be applied in clinical practice: valuable prognostic and therapeutic information must be acquired to be incorporated into the development of antirestenotic therapy.

In the drug-eluting stent era it is interesting to note that some of immunosuppressive agents, currently used in therapy, have known inhibitory effect on regulatory elements of the cell cycle as well as on chemokines production. For example, in a porcine model of stent injury, sirolimus coated stents, are associated with reduced vessel wall protein expression of MCP-1 (Welt and Rogers, 2002). Anyway, the benefits of immunosuppressive current therapy are to be well elucidated, since the role of immunity in vascular response to injury remains still unclear.

Recently it has been explored the hypothesis that SMCs could play a proimmunogenic role in cardiovascular disease (Murray et al.,1995; Swanson et al.,2003). The understanding of this issue could open the perspective to identify drugs having effect on both immunological and proliferative processes regarding SMC activation. Working in this direction, we investigate the contribution of SMCs in antigen presentation *in vitro*. Our results suggest that murine SMCs express MHC II molecules after stimulation with IFN-γ but they do not present the antigen in the context of MHC II. Because MHC II are usually expressed on APC, however, we hypothesize that SMCs could have other roles in T cell activation. Further investigations will be carry on to understand if SMCs are capable of participating in, and/or initiating an immune response during vascular pathology.

Our findings and the evolving understanding of the pathogenesis of restenosis motivate major efforts on multiple fronts to fight cardiovascular disease, with the desirable goals of prevention as well as improved therapy.

7. REFERENCES

1. Apostolakis S, Papadakis EG, Krambovitis E et al. *Chemokines in vascular pathology (review).* Int J Mol Med. 2006;17:691-701.
2. Asahara T, Chen D, Tsurumi Y et al. *Acceleratedrestitution of endothelial integrity and endothelium-dependent function after phVEGF165 gene transfer.* Circulation 1996;94:3291–3302.
3. Baima ET, Guzova JA, Mathialagan S et al. *Novel insights into the cellular mechanisms of the anti-inflammatory effects of NF-kB essential modulator binding domain peptides*. J Biol Chem. 2010;285:13498–13506.
4. Bakkar N and Guttridge DC. *NF-κB Signaling: A Tale of Two Pathways in Skeletal Myogenesis.* Physiol Rev 2010; 90:495-511.
5. Bendeck MP, Zempo N, Clowes AW et al. *Smooth muscle cell migration and matrix metalloproteinase expression after arterialinjury in the rat.* Circ Res. 1994;75:539 –545.
6. Bhatia M, Landolfi C, Basta F et al. *Treatment with bindarit, an inhibitor of MCP-1 synthesis, protects mice against trinitrobenzene sulfonic acid-induced colitis.* Inflamm Res 2008;57:1–8.
7. Bhatia M, Ramnath RD, Chevali L et al. *Treatment with bindarit, a blocker of MCP-1 synthesis, protects mice against acute pancreatitis.* Am J Physiol Gastrointest Liver Physiol 2005;288:G1259–G1265.
8. Blanpain C, Migeotte I, Lee B et al. *CCR5 binds multiple CC-chemokines: MCP-3 acts as a natural antagonist.* Blood 1999;94:1899–1905.
9. Bochaton-Piallat ML, Ropraz P, Gabbiani F et al. *Phenotypic heterogeneity of rat arterial smooth muscle cell clones. Implications for the development of experimental intimal thickening.* Arterioscler Thromb Vasc Biol. 1996; 16 :815-820.
10. Boring L, Gosling J, Cleary M et al. *Decreased lesion formation in CCR2−/− mice reveals a role for chemokines in the initiation of atherosclerosis.* Nature 1998;394:894–7.
11. Brand K, Page S, Rogler G et al. *Brand K, Page S, Rogler G, Bartsch A, Brandl Activated transcription factor nuclear factor-kappa B is present in the atherosclerotic lesion.* J Clin Invest. 1996; 97: 1715-1722.
12. Breuss JM, Cejna M, Bergmeister H et al. *Activation of nuclear factor-kB significantly contributes to lumen loss in a rabbit iliac artery balloon angioplasty model.* Circulation. 2002;105:633–638.
13. Brito PM, Devillard R, Nègre-Salvayre A et al. *Resveratrol inhibits them TOR mitogenic signaling evoked by oxidized LDL in smooth muscle cells.* Atherosclerosis 2009;205:126–3.
14. Bu DX, Erl W, De Martin R et al *IKKβ-dependent NF-kB pathway controls vascular inflammation and intimal hyperplasia*. FASEB J. 2005;19:1293–1295.
15. Charo IF and Taubman MB. *Chemokines in the pathogenesis of vascular disease.* Circ Res. 2004;95:858-66.
16. Choi ET, Khan MF, Leidenfrost JE et al. *Beta3-integrin mediates smooth muscle cell accumulation in neointima aftercarotid ligation in mice.* Circulation. 2004;109:1564-9.
17. Cipollone F, Marini M, Fazia M et al. *Elevated circulating levels of monocyte chemoattractant protein-1 in patients with restenosis after coronary angioplasty.* Arterioscler Thromb Vasc Biol. 2001;21:327-34.
18. Cogswell PC, Kashatus DF , Keifer JA et al. *NF-kappa B and I kappa B alpha are found in the mitochondria. Evidence for regulation of mitochondrial gene expression by NF-kappa B.* J Biol Chem 2003; 278: 2963-2968.
19. Collins T and Cybulsky MI. *NF-kappaB: pivotal mediator or innocent bystander in atherogenesis?* J Clin Invest. 2001;107:255-64.
20. Costa MA and Simon DI. *Molecular basisofrestenosisanddrug-eluting stents.* Circulation 2005;111:2257-2273.
21. D'Acquisto F, May MJ and Ghosh S. *Inhibition of nuclear factor kappa B (NF-κB): an emerging theme in anti-*

inflammatory therapies. Mol Interv. 2002;2: 22-35.

22. Davé SH, Tilstra JS, Matsuoka K et al. *Amelioration of chronic murine colitis by peptide-mediated transduction of the IkappaB kinase inhibitor NEMO binding domain peptide.* J Immunol. 2007; 179: 7852-9.
23. De Winther MP, Kanters E, Kraal G. *Nuclear factor kappaB signaling in atherogenesis.* Arterioscler Thromb Vasc Biol. 2005; 25: 904-914.
24. Di Meglio P, Ianaro A and Ghosh S. *Amelioration of acute inflammation by systemic administration of a cell-permeable peptide inhibitor of NF-kappaB activation.* Arthritis Rheum. 2005;52:951-8.
25. Dimayuga P, Cercek B, Oguchi S et al. *Inhibitory effect on arterial injury-induced neointimal formation by adoptive B-cell transfer in Rag-1 knockout mice.* Arterioscler Thromb Vasc Biol. 2002;22:644-9.
26. Dimayuga PC, Chyu KJ and Cercek B. *Immune responses regulating the response to vascular injury.* Current Opinion in Lipidology 2010;21:416–421.
27. Dimayuga PC, Li H, Chyu KJ. *T cell modulation of intimal thickening after vascular injury: the bimodal role of IFN-gamma in immune deficiency.* Arterioscler Thromb Vasc Biol. 2005;25:2528-2534.
28. Duan C, Bauchat JR and Hsieh T. *Phosphatidylinositol 3-kinase is required for insulin-like growth factor-I-induced vascular smooth muscle cell proliferation and migration.* Circ Res 2000;86:15–23.
29. Dzau VJ, Braun-Dullaeus RC and Sedding DG. *Vascular proliferation and atherosclerosis: new perspectives and therapeutic strategies.* Nat Med.2002;8:1249 –1256.
30. Egashira K, Nakano K, Ohtani F et al. *Local delivery of anti-monocyte chemoattractant protein-1 by gene-eluting stents attenuates in-stent stenosis in rabbits and monkeys.* Arterioscler Thromb Vasc Biol 2007;27:2563–2568.
31. Egashira K, Suzuki J, Ito H et al. *Long-term follow up of initial clinical cases with NF-kB decoy oligodeoxynucleotide transfection at the site of coronary stenting*. J Gene Med. 2008;10:805–809.
32. Egashira K, Zhao Q, Kataoka C et al. *Importance of monocyte chemoattractant protein-1 pathway in neointimal hyperplasia after periarterial injury in mice.* CircRes 2002;90:1167–72.
33. Elezi S, Kastrati A, Neumann FJ et al. *Vessel size and long-term outcome after coronary stent placement.* Circulation 1998;98:1875– 80.
34. Fabry Z, Sandor M, Gajewski TF et al. *Differential activation of Th1 and Th2 CD4+ cells by murine brain microvessel endothelial cells and smooth muscle/pericytes.* J Immunol. 1993;151:38–47.
35. Fabry Z, Waldschmidt MM, Moore SA et al. *Antigen presentation by brain microvessel smooth muscle and endothelium.* Journal of Neuroimmunology 1990;28:63-71.
36. Furukawa Y, Matsumori A, Ohashi N et al. *Anti-monocyte chemoattractant protein-1/monocyte chemotactic and activating factor antibody inhibits neointimal hyperplasia in injured rat carotid arteries.* Circ Res. 1999;84:306-14.
37. Galis ZS and Khatri JJ. *Matrix metalloproteinases in vascular remodelling and atherogenesis: the good, the bad and the ugly.* Circ Res. 2002;90:251-262.
38. Galis ZS, Sukhova GK, Lark MW et al. *Increased expression of matrix metalloproteinases and matrix degrading activity in vulnerable regions of human atherosclerotic plaques.* J Clin Invest. 1994;94:2493-503.
39. Galkina E, Kadl A, Sanders J et al. *Lynphocyte recruitment into the aortic wall before and during development of atherosclerosis is partially L-selectin dependent.* J Exp Med 2006;203:1273–1282.
40. Guglielmotti A, D'Onofrio E, Coletta I et al. *Amelioration of rat adjuvant arthritis by therapeutic treatment with bindarit, an inhibitor of MCP-1 and TNF-alpha production.* Inflamm Res. 2002;51:252-8.
41. Guglielmotti A, Orticelli G, Di Loreto G et al. *Bindarit decreases monocyte chemoattractant protein-1 urinary*

excretion in humans. A pilot study in active lupus nephritis patients. Inflammation Res. 2009;58:S169. (Abstract).

42. Han JW, Shimada K, Ma-Krupa W et al. *Vessel wall-embedded dendritic cells induce T-cell autoreactivity and initiate vascular inflammation.* Circ Res. 2008;102:546-553.

43. Han KH, Tangirala RK, Green SR et al. *Chemokine receptor CCR2 expression and monocyte chemoattractant protein-1-mediated chemotaxis in human monocytes.* Arterioscl Thromb Vasc Biol 1998;18:1983–1991.

44. Hansson GK and Jonasson L. *The Discovery of Cellular Immunity in the Atherosclerotic Plaque.* Arterioscler Thromb Vasc Biol. 2009;29:1714-1717.

45. Hansson GK and Libby P. *The immune response in atherosclerosis: a double-edged sword.* Nat Rev Immunol. 2006;6:508-19.

46. Hansson GK, Holm J, Holm S et al. *T lymphocytes inhibit the vascular response to injury.* Proc Natl Acad Sci U S A. 1991;88:10530-4.

47. Hansson GK, Jonasson L, Holm J et al. *Class II MHC antigen expression in the atherosclerotic plaque: smooth muscle cells express HLA-DR, HLA-DQ and the invariant gamma chain.* Clin Exp Immunol. 1986;64:261–268.

48. Hansson GK, Libby P, Schonbeck U et al. *Innate and adaptive immunity in the pathogenesis of atherosclerosis.* Circ. Res. 2002;91:281-291.

49. HaqueNS, Fallon JT, Pan JJ et al. *Chemokine receptor-8 (CCR8) mediates human vascular smooth muscle cell chemotaxis and metalloproteinase-2 secretion.* Blood 2004;103:1296–1304.

50. Hayden MS and Ghosh S. *Shared principles in NF-kappaB signaling.* Cell. 2008;132:344-62.

51. Hayes IM, Jordan NJ, Towers S et al. *Human vascular smooth muscle cells express receptors for CC chemokines.* Arterioscler Thromb Vasc Biol 1998;18:397–403.

52. Hoshi S, Goto M, Koyama N et al. *Regulation of vascular smooth muscle cell proliferation by nuclear factor-kB and its inhibitor, I-kB.*J Biol Chem. 2000;275:883– 889.

53. Ianaro A, Maffia P, Cuzzocrea S et al. *2-Cyclopenten-1-one and prostaglandin J2 reduce restenosis after balloon angioplasty in rats: role of NF-kB.* FEBS Lett. 2003;553:21–27.

54. Indolfi C, Coppola C, Torella D et al. *Gene therapy for restenosis after balloon angioplasty and stenting.* Cardiol Rev. 1999;7: 324-331.

55. Isoda K, Shiigai M, Ishigami N et al. *Deficiency of interleukin-1 receptor antagonist promotes neointimal formation after injury.* Circulation 2003;108:516–518.

56. Itano AA, McSorley SJ, Reinhardt RL et al. *Distinct dendritic cell populations sequentially present antigen to CD4 T cells and stimulate different aspects of cell-mediated immunity.* Immunity. 2003;19:47-57.

57. Izumi Y, Kim S, Namba M et al. *Gene transfer of dominant negative mutants of extracellular signal-regulated kinase and c-Jun NH2-terminal kinase prevents neointimal formation in balloon-injured rat artery.* Circ Res 2001;88:1120–1126.

58. Jang MK, Kim JY, Jeoung NH et al. *Oxidized low-density lipoproteins may induce expression of monocyte chemotactic protein-3 in atherosclerotic plaques.* Biochem Biophys Res Commun 2004,323:898–905.

59. Jimi E, Aoki K, Saito H et al. *Selective inhibition of NF-kB blocks osteoclastogenesis and prevents inflammatory bone destruction in vivo.* Nat Med. 2004;10:617– 624.

60. Jonasson L, Holm J and Hansson GK. *Smooth muscle cells express Ia antigens during arterial response to injury.* Lab Invest. 1988;58:310-5.

61. Karin M. *Nuclear factor-kappaB in cancer development and progression.* Nature. 2006; 441: 431-6.

62. Karin M, Yamamoto Y and Wang QM. *The IKK NF-kappa B system: a treasure trove for drug development.* Nat Rev Drug Discov. 2004; 3:17-26.

63. Kim WJ, Chereshnev I, Gazdoiu M et al. *Taubman, MCP-1 deficiency is associated with reduced intimal*

hyperplasia after arterial injury. Biochem Biophys Res Commun 2003;310:936–942.

64. Kodali RB, Kim WJ, Galaria II et al. *CCL11 (Eotaxin) induces CCR3-dependent smooth muscle cell migration.* Arterioscler Thromb Vasc Biol. 2004;24:1211-1216.

65. Landry DB, Couper LR, Bryant SR et al. *Activation of the NF-κB and IκB system in smooth muscle cells after rat arterial injury: induction of vascular cell adhesion molecule-1 and monocyte chemotactic protein-1.* Am J Pathol 1997;151:1085-1095.

66. Lawrence T, Bebien M, Liu GY et al. *IKKalpha limits macrophage NF-kappaB activation and contributes to the resolution of inflammation.* Nature. 2005;434:1138-1143.

67. Li ZM, Chu W, Hu Y et al. *The IKKbeta subunit of IkappaB kinase (IKK) is essential for nuclear factor kappaB activation and prevention of apoptosis.* J Exp Med. 1999;189:1839-1845.

68. Libby P. *Inflammation in atherosclerosis.* Nature. 2002;420:868-874.

69. Lin J, Zhu X, Chade AR et al. *Monocyte chemoattractant proteins mediate myocardial microvascular dysfunction in swine renovascular hypertension.* Arterioscler Thromb Vasc Biol. 2009; 29:1810-6.

70. Lincoff AM, Topol EJ and Ellis SG. *Local drug delivery for the prevention of restenosis. Fact, fancy, and future.* Circulation. 1994;90:2070-2084.

71. Lindner V, Fingerle J and Reidy MA. *Mouse model of arterial injury.* Circ Res 1993;73:792–796.

72. Lötzer K, Döpping S, Connert S et al. *Mouse aorta smooth muscle cells differentiate into lymphoid tissue organizer-like cells on combined tumor necrosis factor receptor-1/lymphotoxin beta-receptor NF-kappaB signaling.* Arterioscler Thromb Vasc Biol 2010;30:395-402.

73. Maffia P, Grassia G, Di Meglio P et al. *Neutralization of interleukin-18 inhibits neointimal formation in a rat model of vascular injury.* Circulation. 2006;114:430–437.

74. Maffia P, Zinselmeyer BH, Ialenti A. *Images in cardiovascular medicine. Multiphoton microscopy for 3-dimensional imaging of lymphocyte recruitment intoapolipoprotein-E-deficient mouse carotid artery.* Circulation. 2007;115:e326–e328.

75. Maizels RM and Yazdanbakhsh M. *Immune regulation by helminth parasites: cellular and molecular mechanisms.* Nat Rev Immunol. 2003;3:733-44.

76. Ma J, Wang Q, Fei T et al. *MCP-1 mediates TGF-beta-induced angiogenesis by stimulating vascular smooth muscle cell migration.* Blood 2007;109:987–94.

77. Martinovic I, Abegunewardene N, Seul M et al. *Elevated monocyte chemoattractant protein-1 serum levels in patients at risk for coronary artery disease.* Circ J 2005;69:1484–1489.

78. Massberg s, Vogt f, Dickfeld t et al. *Activated platelets trigger an inflammatory response and enhance migration of aortic smooth muscle cells.* Thromb Res. 2003;110:187-94.

79. May MJ, D'Acquisto F, Madge LA et al. *Selective inhibition of NF-kappaB activation by a peptide that blocks the interaction of NEMO with the IkappaB kinase complex.* Science. 2000;289:1550-4.

80. Mehrhof FB, Schmidt-Ullrich R, Dietz R et al. *Regulation of vascular smooth muscle cell proliferation: role of NF-kB revisited.* Circ Res. 2005;96:958 –964.

81. Mirolo F, Fabbri M, Sironi M et al. *Impact of the anti-inflammatory agent bindarit on the chemokinome: selective inhibition of the monocyte chemotactic proteins.* Eur Cytokine Netw 2008;19:119–122.

82. Murray AG, Libby P and Pober JS. *Human vascular smooth muscle cells poorly co-stimulate and actively inhibit allogeneic CD4+ T cell proliferation in vitro.* J Immunol. 1995;154:151–161.

83. Nakano K, Egashira K, Ohtani K et al. *Catheter-based adenovirus-mediated anti-monocyte chemoattractant.* Atherosclerosis 2007;194:309–316.

84. Newby AC and Zaltsman AB. *Molecular mechanisms in intimal hyperplasia.* J Pathol. 2000;190:300 –309.

85. Obara H, Takayanagi A, Hirahashi J et al. *Overexpression of truncated IkBα induces TNF-α-dependent apoptosis in human vascular smooth muscle cells.* Arterioscler Thromb Vasc Biol. 2000;20:2198–2204.

86. Oguchi S, Dimayuga P, Zhu J et al. *Monoclonal antibody against vascular cell adhesion molecule-1 inhibits neointimal formation after periadventitial carotid artery injury in geneticallyhypercholesterolemic mice.* Arterioscl Thromb Vasc Biol 2000;20:1729–1736.

87. Ohtani K, Egashira K, Nakano K et al. *Stent-based local delivery of nuclear factor-kappaB decoy attenuates in-stent restenosis in hypercholesterolemic rabbits.* Circulation 2006;114:2773-2779.

88. Ong VH, Carulli MT, Xu S et al. *Cross-talk between MCP-3 and TGFbeta promotes fibroblast collagen biosynthesis.* Exp Cell Res 2009;315:151–161.

89. Owens GK, Kumar MS and Wamhoff BR. *Molecular regulation of vascular smooth muscle cell differentiation in development and disease.* Physiol Rev. 2004;84:767-801.

90. Parenti A, Bellik L, Brogelli L et al. *Endogenous VEGF-A is responsible for mitogenic effects of MCP-1 on vascular smooth muscle cells.* Am J Physiol Heart Circ Physiol. 2004;286:H1978–H1984.

91. Peppel K, Zhang L, Orman ES et al. *Activation of vascular smooth muscle cells by TNF and PDGF: overlapping and complementary signal transduction mechanisms.* Cardiovasc Res 2005;65:674–682.

92. Perico N, Benigni A and Remuzzi G. *Present and future drug treatments for chronic kidney diseases: evolving targets in renoprotection.* Nat Rev Drug Discov. 2008;7:936-853.

93. Post MJ, De Smet BJ, Van Der Helm Y et al. *Arterial Remodeling After Balloon Angioplasty or Stenting in an Atherosclerotic Experimental Model.* Circulation. 1997;96:996-1003.

94. Reidy MA, Fingerle J and Lindner V. *Factors controlling the development of arterial lesions after injury.* Circulation 1992;86:III-43–III-46.

95. Remskar M, Li H, Chyu KY et al. *Absence of CD40 signaling is associated with an increase in intimal thickening after arterial injury.* Circ Res. 2001;88:390-4.

96. Rollins BJ. *Chemokines.* Blood 1997;90:909–928.

97. Roque M, Fallon JT, Badimon JJ et al. *Mouse model of femoral artery denudation injury associated with the rapid accumulation of adhesion molecules on the luminal surface and recruitment of neutrophils.* Arterioscler Thromb Vasc Biol 2000;20:335–342.

98. Rostène W, Kitabgi P and Parsadaniantz SM. *Chemokines: a new class of neuromodulator?* Nat Rev Neurosci. 2007;8:895-903. Review.

99. Schober A. *Chemokines in vascular dysfunction and remodeling.* Arterioscler Thromb Vasc Biol. 2008;28:1950-1959.

100. Schober A and Zernecke A. *Chemokines in vascular remodeling.* Thromb Haemost. 2007;97:730 –737.

101. Schober A, Zernecke A, and Liehn EA et al. *Crucial role of the CCL2/CCR2 axis in neointimal hyperplasia hyperplasia after arterial injury in hyperlipidemic mice involves early monocyte recruitment and CCL2 presentation on platelets.* Circ Res 2004;95:1125–1133.

102. Selzman CH, Miller SA, Zimmerman MA. *Monocyte chemotactic protein-1 directly induces human vascular smooth muscle proliferation.* Am J Physiol Heart Circ Physiol 2002;283:H1455–H1461.

103. Shang XZ, Chiu BC, Stolberg V. *Eosinophil recruitment in type-2 hypersensitivity pulmonary granulomas: source and contribution of monocyte chemotactic protein-3 (CCL7).* Am J Pathol 2002;61: 257–266.

104. Sherr CJ and Roberts JM. *CDK inhibitors: Positive and negative regulators of G1-phase progression.* Genes and Dev. 1999;13:1501-1512.

105. Skaletz-Rorowski A, Eschert H, Leng J et al. *PKC delta-induced activation of MAPK pathway is required for bFGF-stimulated proliferation of coronary smooth muscle cells* Cardiovasc Res. 2005;67:142–150.

106. Stabile E, Zhou YF, Saji M et al. *Akt controls vascular smooth muscle cell proliferation in vitro and in vivo by delaying G1/S exit.* Circ Re 2003;93:1059–1065.

107. Strickland I and Ghosh S. *Use of cell permeable NBD peptides for suppression of inflammation.* Ann Rheum Dis. 2006; Suppl 3:iii75-82.

108. Suzuki J, Tezuka D, Morishita R et al. *An initial case of suppressed restenosis with nuclear factor-kappa B decoy transfection after percutaneous coronary intervention.* J Gene Med. 2009;11:89-91.

109. Swanson BJ, Baiu DC, Sandor M et al. *A small population of vasculitogenic T cells expands and has skewed T cell receptor usage after culture with syngeneic smooth muscle cells.* J Autoimmun. 2003;20:125–133.

110. Topol EJ and Serruys PW. *Frontiers in interventional cardiology.* Circulation. 1998;98:1802-1820.

111. Toutouzas K, Colombo A and Stefanadis C. *Inflammation and restenosis after percutaneous coronary interventions.* Eur Heart J. 2004;25:1679-87. Review.

112. Tsou CL, Peters W, Si Y et al. *Critical roles for CCR2 and MCP-3 in monocyte mobilization from bone marrow and recruitment to inflammatory sites.* J Clin Invest 2007;117:902–909.

113. Vande Broek I, Asosingh K, Vanderkerken K et al. *Chemokine receptor CCR2 is expressed by human multiple myeloma cells and mediates migration to bone marrow stromal cell-produced monocyte chemotactic proteins MCP-1, -2 and -3.* Br J Cancer 2003,88:855–862.

114. Wain JH, Kirby JA and Ali S. *Leucocyte chemotaxis: examination of mitogen-activated protein kinase and phosphoinositide 3-kinase activation by monocyte chemoattractant proteins-1, -2, -3 and -4.* Clin Exp Immunol 2001;127:436–444.

115. Walcher D, Babiak C, Poletek P et al. *C-Peptide induces vascular smooth muscle cell proliferation:involvement of SRC-kinase, phosphatidyl inositol 3-kinase, and extracellular signal-regulated kinase1/2.* CircRes 2006;99:1181–7.

116. Wang X, Li X, Yue TL et al. *Expression of monocyte chemotactic protein-3 mRNA in rat vascular smooth muscle cells and in carotid artery after balloon angioplasty.* Biochim Biophys Acta 2000,1500:41–48.

117. Welt FGP and Rogers C. *Inflammation and restenosis in the stent era.* Arterioscler Thromb Vasc Biol. 2002;22:1769-76.

118. Whan Lee C, Kim SH, Suh J et al. *Long-term clinical outcomes after sirolimus-eluting stent implantation for treatment of restenosis within bare-metal versus drug-eluting stents.* Catheter Cardiovasc Interv. 2008;71:594-8.

119. Yamasaki k, Asai T, Shimizu M et al. *Inhibition of NFκB activation using cis-element 'decoy' of NFκB binding site reduces neointimal formation in porcine balloon-injured coronary artery model.* Gene Therapy. 2003;10:356–364.

120. Yan BP, Duffy SJ, Clark DJ et al. *Melbourne Interventional Group. Rates of Stent Thrombosis in Bare-Metal Versus Drug-Eluting Stents (from a Large Australian Multicenter Registry).* Am J Cardiol. 2008;101:1716-22.

121. Yao EH, Fukuda N, Ueno T et al. *Complement 3 activates the KLF5 gene in rat vascular smooth muscle cells.* Biochem Biophys Res Commun 2008;367:468–73.

122. Yoshida T and Owens GK. *Molecular determinants of vascular smooth muscle cell diversity.* Circ Res. 2005;96:280-291.

123. Yu X, Dluz S, Graves DT et al. *Elevatated expression of monocyte chemoattractant protein 1 by vascularsmooth muscle cells in hypercholesterolemic primates.* Proc Natl Acad Sci USA 1992;89:6953–6957.

124. Yue TL, Vickery-Clark L, Louden CS et al. *Selective estrogen receptor modulator idoxifene inhibits smooth muscle cell proliferation, enhances reendothelialization, and inhibits neointimal formation in vivo after vascular injury.* Circulation 2000;102:III281–III288.

125. Zeiffer U, Schober A, Lietz M et al. *Zeiffer U, Schober A, Lietz M, LiehnNeointimal smooth muscle cells display a proinflammatory phenotype resulting in increased leukocyte recruitment*

mediated by P-selectin and chemokines. Circ Res. 2004;94:776-784.

126. Zhang P, Manes TD, Pober JS et al. *Human Vascular Smooth Muscle Cells Lack Essential.* Arterioscler, Thromb Vasc Biol. 2010;30:1795-1801.

127. Zhu XY, Chade AR, Krier JD et al. *The chemokine monocyte chemoattractant protein-1 contributes to renal dysfunction in swine renovascular hypertension.* J Hypertens. 2009;27:2063-73.

128. Zoja C, Corna D, Benedetti G et al. *Bindarit retards renal disease and prolongs survival in murine lupus autoimmune disease.* Kidney Int. 1998;53:726-34.